Experimental Studies on Performance, Exhaust Emission and Combustion Characteristics of Acetylene-Diesel Fuelled Stationary Single Cylinder C.I. Engine

Ph.D. Thesis

ANMESH KUMAR SRIVASTAVA
ID. No. 2012RME9038

DEPARTMENT OF MECHANICAL ENGINEERING
MALAVIYA NATIONAL INSTITUTE OF TECHNOLOGY JAIPUR

April 2018

Experimental Studies on Performance, Exhaust Emission and Combustion Characteristics of Acetylene-Diesel Fuelled Stationary Single Cylinder C.I. Engine

Submitted in

fulfillment of the requirements for the degree of

Doctor of Philosophy

by

ANMESH KUMAR SRIVASTAVA

ID: 2012RME9038

Under the Supervision of

Prof. S.L. Soni

Prof. Dilip Sharma

DEPARTMENT OF MECHANICAL ENGINEERING

MALAVIYA NATIONAL INSTITUTE OF TECHNOLOGY JAIPUR

April 2018

I dedicate this Thesis to the loving memory of my revered father. His constant motivation, visionary thoughts, support and sacrifice has inspired me to achieve the doctorate.

I also dedicate this Thesis to my mother. Her endless love, prayers and blessings always encouraged me to complete this work.

CERTIFICATE

This is to certify that the thesis entitled **'Experimental Studies on Performance, Exhaust Emission and Combustion Characteristics of Acetylene-Diesel Fuelled Stationary Single Cylinder C.I. Engine'** being submitted by **Mr. Anmesh Kumar Srivastava (2012RME9038)**, is a bonafide research work carried out under my supervision and guidance in fulfillment of the requirement for the award of the degree of **Doctor of Philosophy** in the Department of Mechanical Engineering, Malaviya National Institute of Technology Jaipur, India. The matter embodied in this thesis is original and has not been submitted to any other University or Institute for the award of any other degree.

(Dr. S. L. Soni)
Professor
Department of Mechanical Engineering
Malaviya National Institute of Technology Jaipur

(Dr. Dilip Sharma)
Professor
Department of Mechanical Engineering
Malaviya National Institute of Technology Jaipur

Place: Jaipur
Date:

DECLARATION

I, Anmesh Kumar Srivastava, declare that this thesis titled, "**Experimental Studies on Performance, Exhaust Emission and Combustion Characteristics of Acetylene-Diesel Fuelled Stationary Single Cylinder C.I. Engine**" and the work presented in it, are my own. I confirm that:

- This work was done wholly or mainly while in candidature for a research degree at this university.
- Where any part of this thesis has previously been submitted for a degree or any other qualification at this university or any other institution, this has been clearly stated.
- Where I have consulted the published work of others, this is always clearly attributed.
- Where I have quoted from the work of others, the source is always given.
  With the exception of such quotations, this thesis is entirely my own work.
- I have acknowledged all main sources of help.
- Where the thesis is based on work done by myself, jointly with others, I have made clear exactly what was done by others and what I have contributed myself.

Date: April 18, 2018

Anmesh Kumar Srivastava

(2012 RME 9038)

ACKNOWLEDGEMENT

I wish to express my deep regards and profound sense of gratitude to my revered and learned supervisors **Prof. S. L. Soni** and **Prof. Dilip Sharma** of Department of Mechanical Engineering, Malaviya National Institute of Technology Jaipur, who through their excellent guidance have enabled me to accomplish this work. They have been a great source of inspiration to me, all through. I am very grateful to them for guiding me on how to conduct the research and how to effectively present the work in a well-articulated manner.

I am grateful to **Prof. Udaykumar Yaragatti**, Director, MNIT Jaipur, **Prof. I K Bhat**, ex-Director, MNIT Jaipur and **Prof. G. S. Dangayach**, Head, Mechanical Engineering Department, MNIT Jaipur for granting permission to do this research and for various approvals and funding for the same. I extend my sincere thanks to my Departmental Research Evaluation Committee (DREC) members, **Dr. G.D. Agrawal** and **Dr. N. Rohatgi**, for their valuable suggestions and encouragement throughout the course of study. My sincere thanks to **Mr. N.S. Yadav**, Associate Professor, Department of Mechanical Engineering, Malaviya National Institute of Technology Jaipur for his constant encouragement.

I would like to thank **Mr. Pradeep Kumar Gupta** and **Mr. Pushpendra Kumar Sharma** Research Scholars, Mechanical Engineering Department from the deep of my heart, for their continuous help during the experimental work, writing research papers and for the preparation of this report.

I am also grateful to **Mr. Dheeraj Kishor Johar, Mr. Amit Jhalani, Mr. Hemant Raj Singh, Mr. Narayan Lal Jain, Mr. Jitendra Singh Singhasan, Mr. Deepanshu Arora**, **Mr. Umardaraj**, **Mr. Sumit Sharma** and **Mr. Sheetal Kumar Jain,** Research Scholars at MNIT Jaipur for their useful support from time to time during this research. I am thankful to **Mr. Ramesh Chand Meena,** Sr. Lab. Technician, for helping me in conducting the experiments and would like to thank **Mr. Mahaveer**, Technician, **Mr. Kolahal Prashad**, Lab Attendant and other technical staff members of Mechanical Engineering Department, MNIT Jaipur for their help in documentations, procurement of equipment, experimental work, etc. Thanks to **Mr. Bhupesh Kumar Yadav, Mr. Narender Kumar, Mr. Digambar Singh, Ms. Deepika Kumari** and **Mr. Vineet Kumar Sharma**, M.Tech. (Thermal Engineering) students of MNIT Jaipur for their support in my research work.

I thank **Mr. Deepak Maheshwari**, Assistant Registrar (Accounts), for his timely and appropriate help during procurement process of my experimental set up.

I am thankful to **Mr. D.K. Garg** and **Mr. N.K. Garg** of M/s. International Industrial Gases Ltd., Howrah for their guidance on the conduct of the experimental work and for arranging the equipment for the experimental work.

Words will never be adequate to express the sense of reverence, veneration and gratitude to my father, who always wished to see me completing my doctorate. Unfortunately, he left for his heavenly abode before the completion of this work. My heartfelt thanks to my mother **Smt. Kiran Srivastava,** for her blessings and good wishes to complete this work.My sincere thanks to my brothers, **Mr. Rajesh Kumar** and **Mr. Abhishek Kumar,** my sister-in-laws**, Mrs. Roopam Srivastava** and **Mrs. Nandini Srivastava,** my dear nephews, **Ishaan** and **Abhinav** and my adorable nieces, **Aduita Shree** and **Eshita** for their understanding, cooperation, patience and unflinching faith in my potential and for taking care of my parents during my busy years on this research. I would also like to thank my dear **friends and relatives** for their blessings and constant encouragement.

I would like to thank with apology all those, whose names I missed mentioning above inadvertently.

Last but not the least; I would like to say a big thanks to **God, The Almighty**, for making me capable of accomplishing this task.

Place: Jaipur

Date: **(Anmesh Kumar Srivastava)**

ABSTRACT

Energy demand of the world is increasing progressively. The two imperative issues the world currently facing are the depletion of fossil fuels and their environmental impact. Since these fossil fuels are the major source of energy being utilized by the human race, hence the energy demand depends on the availability of fossil fuels. Therefore, increasing demand is endangering the survival and sustainability of life support system. In this regard depletion of fossil fuel reserves, energy scarcity, global warming, and increase in pollutants in atmosphere are matters of great concern today. Internal Combustion (IC) Engines have become a major factor in transforming and organizing social life as these are the prime movers of automobiles and also used in stationary applications such as power generation. IC engines are used either in a form of Compression Ignition (CI) or Spark Ignition (SI) and the commonly used fuels are diesel (CI) and gasoline (SI) for producing power. Both diesel and gasoline are obtained from fossil reserves. So it has become necessary to look for alternate fuels for sustainable development since IC engines will continue to dominate automotive sector and can be used in power generation in near future.

Alternate fuels promise sustainable development, energy conservation, efficiency and environment preservation. Alternate fuels like biodiesels, methyl alcohol, ethyl alcohol, biogas, hydrogen and producer gas have proved themselves as successful fossil fuel substitutes for internal combustion engine. Also, various alternate fuels and polygeneration technologies can be combined, leading to sharp decrease in emission levels in most of the applications in our day today life. Among the new alternate fuels, acetylene has a great potential to act as future alternate fuels for IC engines due to its favorable combustion properties. Hence, in the present research work, the experimental investigation of the performance, emission and combustion characteristics for a diesel-acetylene fuelled, stationary, water-cooled, constant speed, single cylinder, 4-stroke, compression ignition engine was carried out at varying (i) flow rates of acetylene, (ii) compression ratio (CR), (iii) injection pressure (IP) and (iv) injection timing (IT). Constant pressure and constant flow rate acetylene gas generator was used for production of acetylene gas which was utilized as alternate fuel in the present study. To establish the baseline, while running the engine in diesel mode, best performance was obtained at CR 20 with IP 210 bar and IT 23^{o} bTDC and hence, these conditions were taken as baseline for testing in dual fuel mode. Engine was then tested for dual fuel operation to find the optimum flow rate of acetylene. Best results in terms

of performance were obtained at 120 litres per hour (LPH) flow rate of acetylene. In order to find the optimum compression ratio (CR) the engine was operated in dual fuel mode at 120 LPH flow rate of acetylene at varying CRs keeping the IP and IT same as that of baseline. The highest brake thermal efficiency (BTE) was obtained at CR 21 which was considered as optimum CR in dual fuel mode. The engine was further tested in dual fuel mode at 120 LPH flow rate and CR 21 for different injection pressures (IPs) to obtain the optimum injection pressure. Injection pressure (IP) of 200 bar was found to be optimum in case of dual fuel mode. On varying the injection timings (ITs) in dual fuel mode at CR 21, IP 200 bar and 120 LPH, best engine performance was obtained at 23^{o} bTDC IT. Thus, 23^{o} bTDC IT was considered as optimum IT for dual fuel mode.

It was therefore concluded that acetylene can be easily operated in dual fuel mode with better performance at CR 21, IP of 200 bar and IT of 23^{o} bTDC without any major modifications in engine.

CFD analysis using Ansys Fluent software was carried out. Pressure-crank angle diagrams of optimized diesel and optimized dual fuel mode for 100% load were validated with experimental results. Simulations results showed good agreement with the current experimental study.

Hence, using acetylene as alternate fuel in stationary C.I. engine is found feasible with improved performance and reduced emissions except NO_x emissions, which could be controlled by applying emission reduction techniques such as EGR, LNT etc.

Table of contents

LIST OF FIGURES

LIST OF TABLES

NOMENCLATURE

aTDC	After top dead centre
b/d	Barells per day
BMEP	Brake mean effective pressure
BP	Brake Power (kW)
BSEC	Brake specific energy consumption (kJ/s/kW)
BSFC	Brake specific fuel consumption
bTDC	Before top dead centre
BTE	Brake thermal efficiency
BTU	British Thermal unit
CI	Compression Ignition
CNG	Compressed natural gas
CO	Carbon monoxide
CO_2	Carbon dioxide
CR	Compression ratio
DEE	Di ethyl ether
DF	Dual fuel
DI	Direct injection
DIT	Diesel injection timing
DMDF	Diesel methanol dual fuel
DME	Di methyl ether
EGR	Exhaust gas recirculation
EGT	Exhaust gas tempertaure
FEV	Full electric vehicles
HC	Hydrocarbon
HCCI	Homogeneous charge compression ignition
HCNG	Hydrogen-compressed natural gas
HD	Heavy duty
HEV	Hybrid electric vehicle
HRR	Heat release rate
HSD	High speed diesel

IC	Internal combustion
IOP	Injection opening pressure
IP	Injection pressure
IT	Injection timing (^{o})
LPG	Liquefied petroleum gas
LNT	Lean NO_X traps
MHRR	Maximum heat release rate (J/^{o} CA)
NHRR	Net heat release rate (J/^{o} CA)
NO_X	Oxides of nitrogen
NTP	Normal temperature and pressure
O_2	Oxygen
OECD	Organization for economic co-operation and development
PCP	Peak cylinder pressure (bar)
PM	Particulate matter
RPR	Rate of pressure rise (bar/^{o} CA)
SCR	Selective catalytic reduction
SFC	Specific fuel consumption
SI	Spark ignition
SVO	Straight vegetable oil
TDC	Top dead centre
THC	Total hydrocarbon
TMI	Timed manifold injection
TPI	Timed port injection
UHC	Unburnt hydrocarbon
UTO	Used transformer oil
VCR	Variable compression ratio

CHAPTER 1

INTRODUCTION

1.1 Energy demand and crisis

Economic growth of any country is co-related with its energy consumption. Energy demand increases with the advancement in living standard and development of the country. World energy consumption is growing at a fast pace as shown in Fig.1.1 [1].

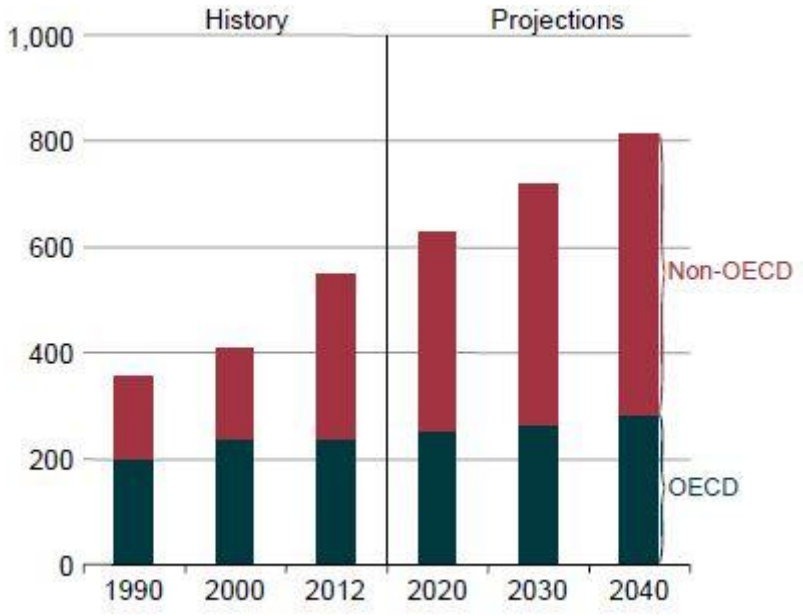

Fig.1.1 Energy consumption of the world for the period 1990–2040 (in quadrillion Btu) [1]

From Fig. 1.1, it is clear that world consumption of marketed energy is likely to increase from 549 quadrillion Btu [579,195 × 10^{15} Joules] (2012) to 815 quadrillion Btu [859,825 × 10^{15} Joules] in 2040 [1]. Along with India and China, Non-OECD Asia account for more than half of universal increase in estimated energy consumption over the period of 2012 to 2040 as is evident from Table 1.1 [1].

Table 1.1 World energy consumption by country / region (in quadrillion Btu) [1]

Year → Region ↓		**2012**	**2020**	**2025**	**2030**	**2035**	**2040**
OECD	America	118	126	128	131	134	138
	Europe	81	85	87	90	93	96
	Asia	39	43	45	46	47	48
NON OECD	Europe	51	52	55	56	58	58
	Asia	175	223	246	270	295	322
	Africa	22	26	30	34	38	44
	Middle East	32	41	45	51	57	62
	America	31	33	37	40	43	47
Total		**549**	**629**	**673**	**718**	**765**	**815**

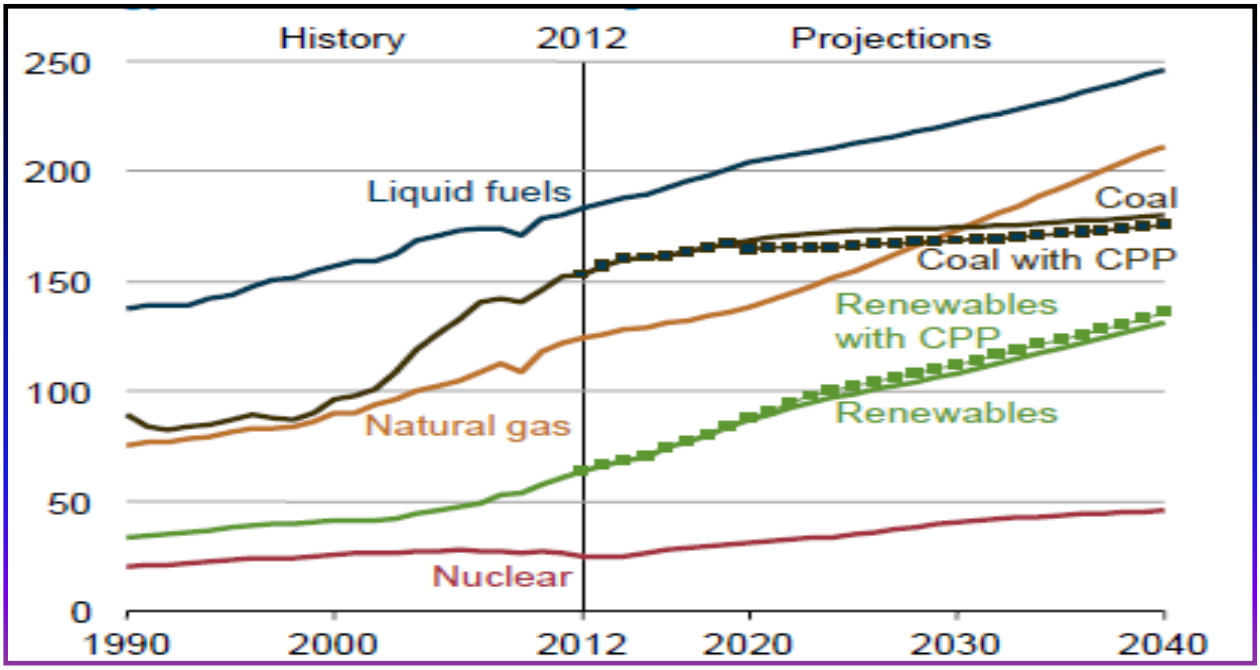

Fig. 1.2 World energy consumption by energy source (in quadrillion Btu) [1]

World projected consumption of marketed energy from most of the fuel sources through 2040 is shown in Fig. 1.2, which shows that liquid fuels (mostly fossil fuels) will continue to be the largest source of world energy supply for many decades to come. Coal will continue to be the second to the largest energy source worldwide after petroleum & other liquids until 2030. For the duration of 2030 to 2040, coal will possibly be the third-largest energy source, after both natural gas and liquid fuels. Worldwide natural gas consumption is projected to increase from

120 Tcf in 2012 or 3.398 trillion cubic metre to 203 Tcf (trillion cubic feet) or 5.748 trillion cubic metre in 2040 i.e. 2.47 % increase per year (taken on straight line) from 2012 to 2040, which is almost 4 times the percentage increase as compared to that of coal.

The transportation sector consumed 25% of total world energy consumption in 2012, and transportation energy use shall increase by 1.4% per year from 2012 till 2040. The industrial sector shares 54% of global delivered energy consumed in 2012, and its energy consumption is estimated to grow by an average of 1.2% a year from 2012 to 2040. Economic growth increases in industrial output, which requires the movement of raw materials to manufacturing sites, as well as transportation of ready to use goods to end users. The key factors for increase in transportation energy demand are growth rates for economic activity, population and trends in vehicle fuel efficiency. In addition, increase in the demand for personal transport facility is a primary contributing factor for increase in energy demand for transportation. Also, urbanization and in increase in income contribute to increase in air travel and vehicle population in the developing non-OECD economies [1].

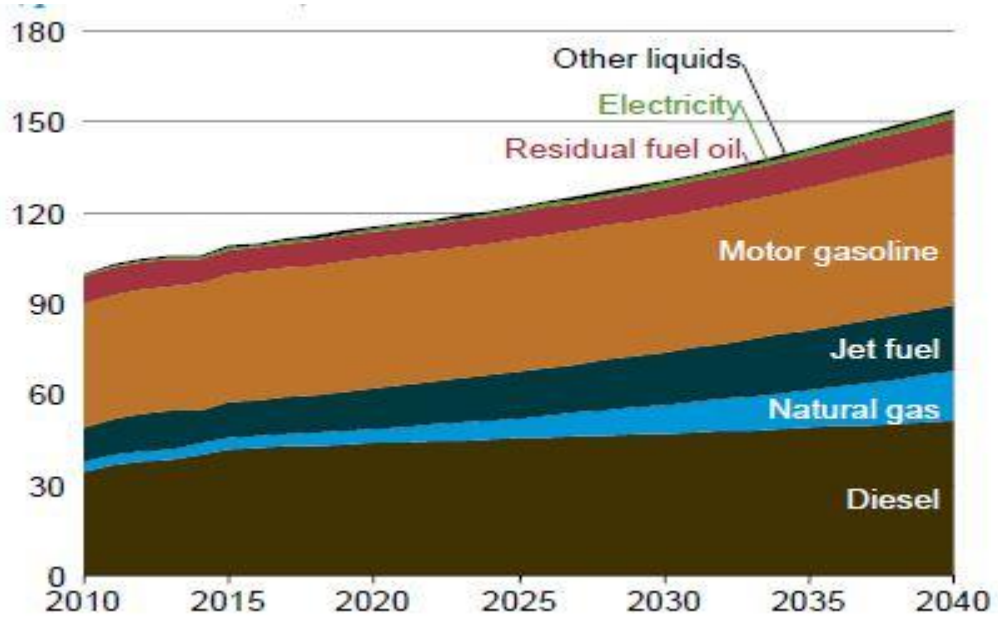

Fig. 1.3 Transportation sector world energy consumption (in quadrillion Btu)[1]

Fig. 1.3 shows the world energy consumption by energy source in transport sector for the period 2010 to 2040 and it is clear for the figure that liquid petroleum fuel constitutes for more than 85% of world energy consumption in transport sector in 2012 and a similar percentage is expected even in 2040.

As seen from Table 1.2, liquid fuels consumption of the world shall increase by approx. 31 million b/d (4929 million litres/d), from 90 million b/d (14310 million litres/d) in 2012 to 121 million b/d in 2040 (19239 million litres/d). Oil prices are estimated to rise as need from the emerging, non-OECD economies increase, especially in the transportation & industrial sectors. Continuous increase in oil prices motivates consumers to swap from liquid fuels to more cost-competitive fuels wherever feasible. A sharp decrease in liquid fuel consumption occurs in the electric power sector where unconventional fuels, nuclear power and natural gas are exchanging liquid fuels at various places of the world.

Table 1.2 Petroleum & other liquid fuel consumption worldwide for the period 1990–2040 (million b/d) [1]

							Average annual percent change	
Region	1990	2000	2012	2020	2030	2040	1990-2012	2012-2040
OECD	42.2	48.7	45.5	45.8	45.5	46.1	0.3	0.0
Americas	20.6	24.3	23.2	24.4	24.3	24.6	0.5	0.2
Europe	14.0	15.6	14.1	13.7	13.7	14.0	0.0	0.0
Asia	7.6	8.8	8.2	7.7	7.5	7.5	0.4	-0.3
Non-OECD	25.0	29.0	44.8	54.5	63.6	74.8	2.7	1.9
Europe and Eurasia	9.3	4.4	5.3	5.8	6.2	6.1	-2.5	0.5
Asia	6.6	12.5	21.5	26.7	32.2	38.9	5.5	2.1
Middle East	3.3	4.5	7.7	10.0	11.3	13.2	3.9	2.0
Africa	2.1	2.5	3.6	4.5	5.5	6.9	2.6	2.4
Americas	3.8	5.0	6.7	7.5	8.5	9.6	2.7	1.3
Total world	67.2	77.7	90.3	100.3	109.1	120.9	1.4	1.0

The alarming situations of energy security, fossil fuel emissions in environment and high oil prices in long term encourage extended use of renewable energy sources, natural gas and nuclear power. In 2040, liquid fuels, coal and natural gas is estimated for about 78% of total world energy supply. Petroleum and other liquid fuels remain the largest source of energy, although their share of total world marketed energy consumption is expected to decline from 33% in 2012 to 30% in 2040[1].

India is in a major transformation phase, fast electrification of villages, digitalization, and enhanced industrialization creating opportunities to its citizens. India has been sharing for almost 10 % of the total increase in world energy need since 2000. India's energy demand is pushing the country's share in global energy demand up to 5.7 % in 2013 from 4.4 % at the beginning of this century. Almost 75% of Indian energy demand is met by fossil fuels. Table 1.3 represents primary energy demand by fuel in India.

Table 1.3 Statistics of India- Primary energy demand of fuel (in Mtoe) [2]

Year → Fuel ↓	**2000**	**2013**	**2020**	**2030**	**2040**
Oil	112	176	229	329	458
Natural Gas	23	45	58	103	149
Coal	146	341	476	690	934
Nuclear	4	9	17	43	70
Renewable	156	204	237	275	297
Total	**441**	**775**	**1018**	**1440**	**1908**

Demand for oil in India is expected to rise from 6.0 mb/d (954 million litres/d) in 2013 to 9.8 mb/d (1558.2 million litres/d) in 2040. Transport sector is the major consumer of petroleum. In India, the current demand in transport sector is 75 Mtoe (i.e. 14 % of total energy consumed in India) and it is expected to reach 240 Mtoe by 2040. Passenger cars' population is expected to rise from 28 million in 2013 to 280 million by 2040 and an additional 30 million more trucks will be on road by 2040 as compared to 2013. 2/3 wheeler population is expected to double by 2040 [3, 2]. Fig. 1.4 shows the expected increase in vehicle population in India and it looks clear that IC engines (gasoline and diesel) will be the main technology in the foreseeable future [4].

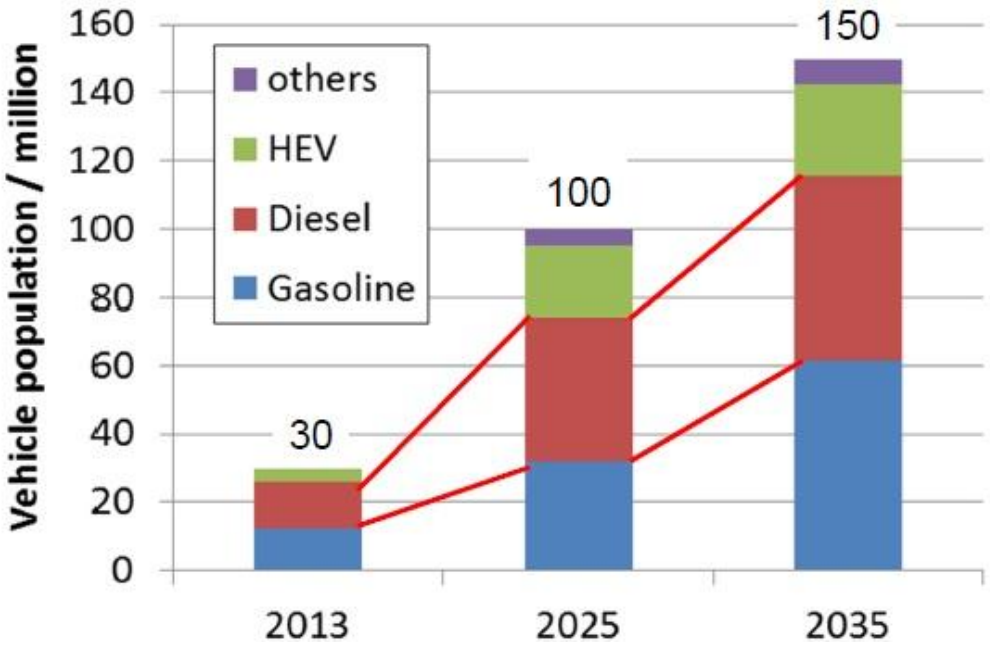

Fig. 1.4 Expected increase of vehicle population in India between 2013 and 2035 [4]

Fig. 1.5 shows the consumption pattern of various petroleum products in India for 2014-15, with diesel having 42% share (much more than triple of motor spirit, i.e. petrol/gasoline and LPG).

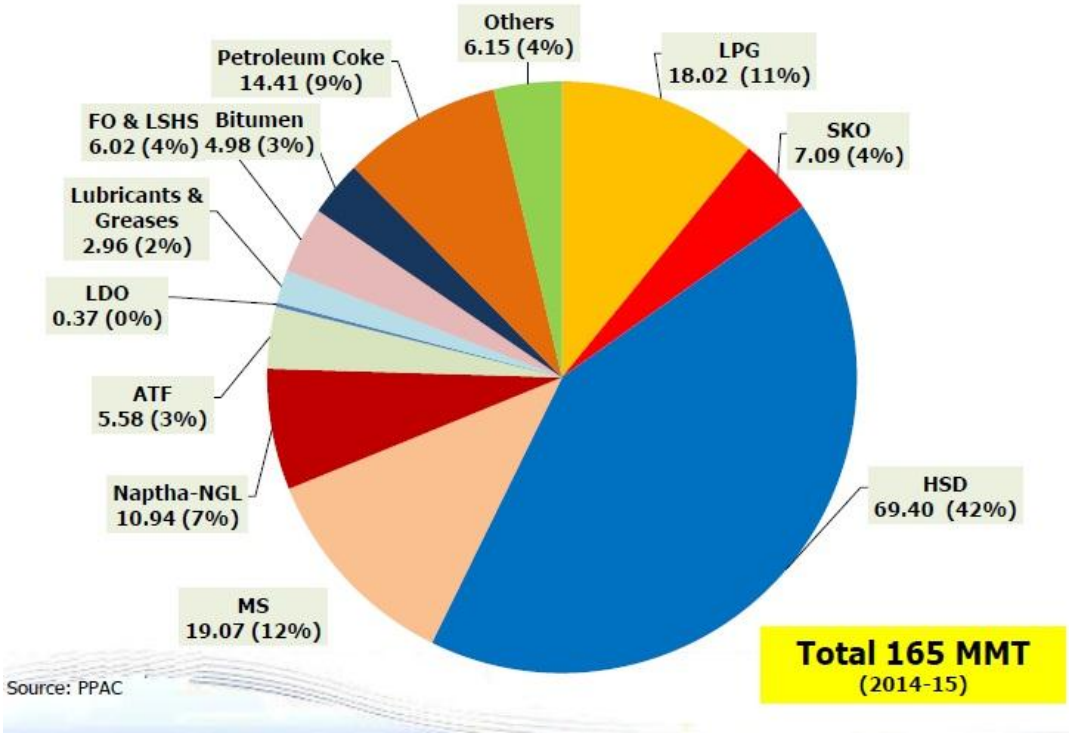

Fig. 1.5 India's consumption pattern of petroleum products in 2014-15 [5]

As seen from the above details, the world is intensely reliant on fossil fuels as primary energy source, and this is particularly evident in all industrialized nations. Some major users of fossil fuels are the utility, industrial, residential, and transportation sectors [6]. These fossil fuels on combustion release greenhouse gases and other pollutants into the atmosphere and become the biggest source of air pollution [7].Exhaust emissions of the diesel engines consists of various toxic and carcinogenic pollutants and greenhouse gases such as CO_2 which are very harmful to the environment. It has been a well-known fact that increased amount of greenhouse gases are key factor to global warming & global climate change. CO_2, NO_x and CH_4 are the three most polluting greenhouse gases which are responsible for lowering the quality environment. Although not a greenhouse gas, particulate matter is also an air pollutant released from exhaust emissions. Ozone gas is a powerful irritant to the human respiratory system which is generated in the atmosphere by the reaction of various gases released from engine. The major health problems due to exhaust emissions (consisting primarily of PM, NO_x and CO_2) are headache, fatigue, respiratory problems, wheezing, cough, cancer, chest

pain, reduced reflexes, etc. Table 1.4 shows the ill effects of various pollutants on health and ecosystem.

Table 1.4 Effect of various air pollutants on health and ecosystem [8]

Air Pollutant	Effects
Criteria pollutants (i.e., CO, SO_2, NO_2, O_3, PM2.5/PM10 and Pb)	Adverse health, ecosystem effects like upper respiratory illnesses such as asthma and emphysema
Light scattering and absorbing PM and gases (e.g., NO_3-, NH_4+, OC, sea salt, soil and NO_2)	Adverse visibility, health and ecosystem effects
Hazardous Air Pollutants (HAPs, or toxics; e.g., persistent organic pollutants [POPs] and metals [e.g. Cr, Cu, Hg, As, Cd, Ni, Pb, Se and Zn])	Carcinogenic health effects (cancer, reproductive or birth defects) Adverse environmental effects (bio-accumulation of Hg in fish and lakes)
Oxidizing pollutants (e.g., H+, SO_4= and O_3)	Destruction of forests, crops and lakes
Depositing pollutants (e.g., SO_2, HNO_3, O_3, soot [BC] and soil dust)	Soiling and degradation of buildings, antiquities, vehicles and clothing
Reduced sulfur compounds and certain VOCs	Unpleasant odors
Climate forcers (e.g., BC, O_3, CO_2, CH_4, and halocarbons [Freon-122])	Alter earth's radiation balance (e.g., absorbing electromagnetic radiation, depleting stratospheric O_3 and changing cloud cover and water vapor)

Diesel engines, despite of their environmental issues, are the popular means of powering heavy-duty trucks, buses, stationary engines and construction vehicles (CV) because they are quite reliable, fuel efficient, durable, relatively lesser inexpensive in operating cost, high-torque (at low speeds) engines. The power and speed of the diesel engine are controlled by varying the amount of fuel injected into the cylinder and hence are called quality governing. Diesel-powered vehicles have shown a 30-40% fuel economical as compare to their gasoline counterparts. This translates to about a 20% reduction in CO_2 emissions [9]. Because of the above features, fuel efficiency and lower CO_2 emissions, diesel engines are popular and significant powertrain for several applications.

1.2 Need for alternate fuels

Fossil fuel reserves are limited and cannot be recycled. Fossil resources suffered from over-exploitation which led to increase in hazardous pollutants also. The uncertainties related to fossil fuels have adversely impacted the developing countries like India, which depend heavily on import of fossil fuels. Energy supplied from fossil fuels is considered to be unsustainable since the energy crisis from early 1970s [10, 11]. Based on the current scenario and energy consumption rate, British Petroleum has estimated that most fossil sources, i.e. crude oil, natural gas and coal, will get depleted quite fast and would be exhausted very soon [10].

Our society relies heavily on IC engines for different purposes viz., transportation, agriculture, power generation, etc. Therefore, research in both gasoline and diesel engines are required for improvement in fuel efficiency and emission reduction. Even a small improvement in fuel efficiency can have a major impact on economy and pollution [12]. Direct injection technology which helps the reduction of environmental pollutants, heavy-duty diesel engines is mandated by federal government regulations. These mandates have provoked the automobile industries to investigate the alternatives for conventional fuel injection systems and have developed interest in the development of "clean" fuels [13].

Hence, for sustainability of energy there is a great demand to identify and explore new and renewable sources of energy, and at the same time invention of new and improved methods or technologies, like alternate fuels, energy storage, cogeneration, trigeneration, waste heat recovery, variable frequency drives, fuel injection systems, etc. to increase energy efficiency, in order to reduce the dependency on primary energy sources.

Alternative fuels promise sustainable development, energy conservation, efficiency and environmental preservation. Various alternate fuels and micro-trigeneration technologies can be combined, leading to sharp decrease in almost all the emissions [14].

1.3 Alternate fuels, engine modifications, HEV, FEV, Fuel cells, etc.

Development of alternative fuels for IC engines has become important for meeting the increasingly stringent exhaust emissions norms being implemented globally. Furthermore, it can be economical, due to the lower costs in process and production of these fuels. Liquefied Petroleum Gas (LPG), Compressed Natural Gas (CNG), Hydrogen-CNG blended fuel

(HCNG), biodiesels, alcohols, etc. are good promising alternative fuels in India. A lot of work for engine sub-parts of the baseline SI/CI engine, such as combustion bowl, CR, the exhaust system, the air-intake system, after treatment device are suitably modified to achieve the target standards. Experience of developing CNG/LPG engines with carburetion and injection kit fuel technologies is available. The charge stratification in the CNG combustion chamber permits extremely lean combustion without high cycle-by-cycle variations with high combustion efficiency. Fuel system parts such as 1st stage reducer, 2nd stage reducer and mixer are also suitably modified & optimized to achieve target specifications. A 6-Cylinder HCNG naturally aspirated engine using the lean burn concept of combustion is being developed. [15].

Fuel cell is another promising technology in automobiles in future replacing IC engines. After researching on many possible fuels and membranes, hydrogen seems to be the best fuel for fuel cell. However, carrying hydrogen on vehicle is difficult and dangerous. Hence, production of hydrogen from water by electrolysis on the running vehicle is tried but has certain limitations like the time and energy required for electrolysis process to produce the desired amount of hydrogen for fuel cell. Fuel cells can also be used with natural gas or other fuels by external or internal reforming which normally run on hydrogen [16]. Fuel cells are still in the R&D stage [20]. The benefits of fuel cells are: higher efficiency (up to 60% electric), negligible pollution, fuel cells are very quiet [16, 17, 18, 19]. The major problem of fuel cells is its shorter lifetime of the membrane and its high cost [16, 19].

HEV and FEV, Solar cars, etc. are other good solutions as alternate sources of energy and at the same time reduction in emissions. However, these technologies are also in their early stage and commercial acceptance of these might take couple of decades. Some of the constraints are high cost to power ratio, maximum speed, etc.

1.4 Stationary diesel engines

Stationary engines are often used where there is no access to the grid to supply electric power or as emergency generators when there is a shortage of continuous supply of the main source of power from grid. However, in certain cases, it is also cheaper to generate power through a diesel generator set than to buy electric power from the supply of grid.

CHAPTER 2

LITERATURE REVIEW

As seen in the previous chapter, lots of focus and purpose is there on reduction of usage of fossil fuels and replacement of the same with alternate energy sources. These alternate energy sources are (i) alternate fuels viz., bio-diesels, alcohols, LPG, CNG, bio-gas, hydrogen, acetylene, etc., (ii) renewable energy sources viz., solar energy, hydel energy, wind energy, tidal energy, etc., (iii) nuclear power, (iv) fuel cells, etc. As far as IC engines are concerned, the alternatives available (for the purpose of reduction of fossil fuels' usage as well as emission reduction) are (i) alternate fuels as mentioned above, (ii) HEV and FEVs, (iii) fuel cells, etc. Lots of research has been done in the above areas and a gist of the same is presented in this chapter.

2.1 Alternate fuels for IC engines

The principal oxygenate fuels such as vegetable oils,methanol and ethanol, and methyl and ethyl esters produced from vegetable oils are under active investigation as alternate fuels [21].

2.1.1 Biodiesel

In an agrarian nation like India the utilization of vegetable oil would be economically viable due to its reduced dependence on import of oil based commodities and large productivity. Vegetable oils appear to be a precursor as they are sustainable and are effectively accessible [22]. Due to the poor atomization and high viscosity of SVO causes improper mixing and combustion. Moreover, usage of plant oils raise technical, economic and environmental issues [23].

Oner et al. reported reduction of 15%, 38.5%, 56.8%and 72.7% for that CO, NO_x, smoke and SO_2 respectively while using animal tallow methyl ester in diesel engine (B100) compared to diesel [24].

Pradhan et al. carried out experimental study using preheated Jatropha oil (PJO) in diesel engine. The results showed increment in BSFC and EGT while reduction in BTE with PJO as compared to high speed diesel (HSD) for all engine loads. CO_2, HC and NO_x were reduced while CO increased for PJO as compared to those of HSD [25].

Alcohol can be utilized as alternate fuel for CI Engines. Different studies have been conducted using methanol and ethanol, using various techniques with different alcohol-diesel blends in dual fuel mode.

2.1.2 Ethanol

Ethanol is also known as ethyl alcohol. It is a colorless liquid with a characteristic, acceptable odor. Ethanol (CH_3CH_2OH) molecule contains a hydroxyl group. Ethanol obtained from cellulosic biomass materials is called bioethanol[26].

Alcohols appear to be the most attractive alternative fuel from the perspective of its availability, storage and handling. Though complete replacement of diesel with alcohol is not easy, still several investigations have been done using alcohols with different techniques and different quantities of alcohols in dual fuel mode [27]. Wang et al. reported increase in HC, CO, NO_x and NO_2while adding ethanol with diesel [28]. Padala et al. investigated the effect of ethanol utilization in diesel engine and found that, a 10% efficiency gain was achieved with 60% ethanol energy fraction and on increasing ethanol energy fraction, increase in HC, CO and NO_x emissions was observed [29]. The performance of CI engine improved and the exhaust emissions were fairly reduced on using BE20 (80% biodiesel and 20% ethanol) in diesel engine [30]. The use of ethanol–diesel blends with a CLZ, a novel emulsifier improved engine performance, reduced smoke and NO_x emissions, while the total hydrocarbon (THC) emission increased [31]. Advantages of the ethanol-diesel dual fuel operation were energy security, sustainability of the renewable fuel with reduced CO_2 and smoke[32].

2.1.3 Methanol

Methanol (CH_3OH)is oxygenated fuel having high latent heat of vaporization. It has high burning speed. The particulate and NO_x emissions can be reduced by using it in diesel engines [33].Wei et al. studied the effect of methanol to diesel ratio, R_{MD} and diesel injection timing (DIT) in methanol port premixed diesel engine and found that BTE remained stable at low R_{MD}, but showed a slight decrease at high R_{MD}. NO_x and soot emissions decreased while HC and CO emissions increased as R_{MD} increased. On retarding DIT, HC emission initially increased and then decreased, while CO emission always increased [34]. Wang et al. carried out experimental investigation in methanol fumigated diesel engine. The experimental results showed that the viable diesel-methanol dual fuel (DMDF) operating range in terms of load and methanol substitution percent (MSP) was achieved over a load range from 6% to 100%.

[35]. Wei et al. studied the effects of pilot injection of diesel-methanol dual fuel engine. They found that pilot injection strategy could reduce most of gaseous emissions in comparison to single injection. Increasing pilot quantity could reduce HC, CO and most of unregulated emissions of DMDF engine. Advancing pilot injection timing caused an increase in some unregulated emissions on M50 mode[36].

Methanol can be used in diesel engines in the fumigation mode with diesel fuel injected directly into the engine cylinder and with methanol injected into the air intake. Fumigation methanol influences engine combustion and particulate emissions. It reduces diesel fuel consumed and increases heat released in premixed mode. Peak cylinder pressure is increased at high engine load but reduced at low engine load. It increases ignition delay and peak heat release rate but not combustion duration. [37].

Unlike ethanol-gasoline blend, ethanol-diesel blend has some concerns regarding lubricity, reduced flash point and startability problems.

The high production cost and performance losses of liquid fuels encourage the use of gaseous fuels as better alternative fuels for IC engines. Fuels like CNG, LPG and hydrogen are prominent gaseous fuels.

2.1.4 Hydrogen

Hydrogen is the most abundant element in the universe. Hydrogen gas (H_2) is being explored to use in IC engines and fuel cell electric vehicles. On burning, it creates only water vapor as a by-product. It also produces small amounts of NO_x, UHC and CO because of engine lubricants still the exhaust is free from CO_2. Being a gas at NTP, it faces problems like transportation and storage [38].

The addition of hydrogen as a combustion enhancer can be used to counteract the increase in THC emissions seen with the butanol fuel blends and can further reduce CO and PM emissions [39]. Yadav et al. conducted experimental study using hydrogen in dual fuel mode with diesel. The results showed lower exhaust emissions and improved performance. At 70% load, the BTE was increased by 10.71% with the supply of 120 g/h of hydrogen in comparison to neat diesel due to better combustion characteristics of hydrogen [40]. Yadav et al. conducted experiments with hydrogen in DF mode, with varying injection timings (18.5 to 27.5° CA) and flow rates of hydrogen (80, 120 and 150 g/hr). Maximum BTE and minimum

BSEC were obtained at 120 g/h flow rate and 20º IT [41]. Santoso introduced hydrogen to the intake manifold using a mixer before entering the combustion chamber. At low load, hydrogen enrichment reduced cylinder peak pressure and efficiency. The combustion rate of reaction was slower as per the CFD calculations [42].

2.1.5 Liquefied Petroleum Gas (LPG)

LPG is a by-product of natural gas processing. It is a product that comes from crude oil refining. It is composed primarily of propane and butane. Although small amounts of propylene and butylene is also present in it. The characteristics of propane are considered closely to those of LPG because LPG's mostly part is propane,

LPG dual fuel engines are modified diesel engines. LPG is used as primary fuel and diesel as secondary fuel in DF engines. LPG DF engines have a good thermal efficiency at high loads but less during part load [43]. LPG can be used in diesel engines with significant reductions in nitrous oxides and smoke emissions [44]. As per the experimental results of Tira et al.,up to 60% of liquid fuel was replaced by LPG. Engine combustion variability was kept within the acceptable range. Clear benefits in the soot-NO_x trade-off were obtained [45]. LPG_4 (25% Propane) is showing the best performance among the other fuel types with the highest level of efficiency with small noise. Compression ratio of 20 seems to be the best among other tested [46]. Exhaust emissions and fuel conversion efficiency of DF engine were affected using different LPG composition. 30% butane with 70% propane was found to be the best LPG composition at peak loads in the DF operation [47].

2.1.6 Biogas

The biogas can reduce the diesel fuel consumption significantly in dual fuel mode. BTE of CI engine run in dual fuel mode is strongly affected by biogas flow rate and methane concentration [48]. Biogas when used in stationary engines, resulted in significant reduction in HC and CO emission. It offers reliable idling, easy starting & stumble free acceleration. Storage is the biggest challenge for the use of biogas. It was experimentally observed that methane enriched biogas exhibits performance similar to that of CNG. Hence, methane enriched biogas is equally good as natural gas [49].Bora et al. used biogas in dual fuel engine at various CRs (18, 17.5, 17 and 16) under varying loading conditions at IT of 23º bTDC. The highest BTE in DF mode was found at CR 18 as against that at CR 17.5 in neat diesel mode. CO and HC emissions got reduced but NO_x and CO_2 emissions increased in dual fuel

mode [50]. Barik et al. found that the ignition delay in DF mode was longer than diesel for all loads. About 11 bar higher peak pressure was found in DF mode as compared to diesel mode. Nitrogen oxide and smoke were reported to be lower in DF operation compared to that of diesel mode [51]. Yilmaz experimentally investigated the effect of biogas on the thermal barrier coated (TBC) dual-fuel engine using biogas (60% methane) as main fuel where smoke emissions got reduced substantially [52].

2.1.7 Compressed Natural Gas (CNG)

Among all alternative fuels, CNG has been considered as one the best solutions for fossil fuel substitution because of its availability throughout the world, inherent clean burning, economical as a fuel and its adaptability to the gasoline and diesel engines. CNG is meeting the maximum needs of countries worldwide to switch over to alternate fuels.

Liu et al. conducted experiment on CNG-diesel DF engine. They reported that NO_x emission of DF mode was reduced by average 30% compared to diesel mode. With increase ofrpm, NO_x emission reduced due to reduced residence time in high temperature [53]. High thermal efficiency and clean combustion of diesel-natural gas DF engines at light loads can be achieved with two-stage auto-ignition mode, which can be obtained by optimizing pilot diesel injection timing [54].

2.2 Acetylene gas as fuel for I.C. engines

Among the new alternative fuels, acetylene gas has also been suggested as a possible alternative to petroleum-based fossil fuels since it can be produced from non-petroleum resources (coal, limestone and water) [55].

Wide flammability range of acetylene,and requires minimum ignition energy. since engine can run in lean mode with a higher specific heat ratio leading toincrease in thermal efficiency. Having high flame speed and hence has faster energy release. Larger compression ratios are allowed than diesel engines because of high self-ignition temperature of acetylene. The physical and combustion properties of the fuels used for this investigation (diesel and acetylene) and their comparison with hydrogen are given in Table 2.1.

Table 2.1 Physical and combustion properties of acetylene & other fuels [56].

Properties	**Acetylene**	**Diesel**	**Hydrogen**
Formula	C_2H_2	$C_8 – C_{20}$	H_2
Density kg/m^3 (At 20 ^{o}C & 1 atm)	1.092	840	0.08
Auto ignition temperature (^{o}C)	305	257	572
Stoichiometric air fuel ratio (kg/kg)	13.2	14.5	34.3
Flammability Limits (Vol %)	2.5 – 81	0.6 – 5.5	4 – 74.5
Flammability Limits(Equivalent ratio)	0.3 – 9.6	-	0.1 – 6.9
LCV (kJ/kg)	48,225	42,500	1,20,000
LCV (kJ/m^3)	50,636	-	9600

2.2.1 Production of acetylene

Conventional method of acetylene production is by reacting calcium carbide with water that produces acetylene and lime as given in equation 2.2. This reaction is spontaneous. Lime is separated as a co-product in the reactor.Acetylene is then dried, purified and compressed into cylinders. Acetylene is produced in acetylene gas generators as given by the following reactions [57].

$$CaCO_3 + C \text{ (graphite)} \longrightarrow CaC_2 \quad (2.1)$$

$$CaC_2 + H_2O \longrightarrow Ca(OH)_2 + C_2H_2 \quad (2.2)$$

The second method consists of thermal cracking of hydrocarbons or partial combustion of methane with oxygen.

2.2.2 Application of acetylene gas in I.C. engines

Lakshmanan et al. aspirated acetylene gas at 3 lpm in the inlet manifold, and used diesel as an ignition source. In dual fuel mode operated at full load, the BTE was found lower than diesel. It was suggested that using techniques like TPI, TMI, etc., BTE can be improved along with reduction in NO_x emissions [58]. Lakshmanan et al. used TMI to investigate the performance of acetylene in dual fuel mode. The BTE in case of DF mode was lower at part load and more

at higher loads than neat diesel. HC, CO, NO_x, and CO_2 emissions were reduced in DF operation than diesel while smoke level went higher in dual fuel mode [59]. Lakshamanan et al. conducted experiments using acetylene in dual fuel mode. Results obtained were lower thermal efficiency with reduced CO, HC & smoke emissions when compared to baseline diesel, while NO_x emission increased with acetylene introduction, due to the high combustion rates. Maximum rate of pressure rise and peak pressure were higher in the dual fuel mode of operation [56]. Lakshmanan et al. used EGR with acetylene-diesel dual fuel mode and used TMI for inducting acetylene in inlet manifold. NO_x emissions were found to be low in comparison to diesel operation and slight increase in smoke was observed. The BTE in case of dual fuel was higher using TMI than diesel operation. With EGR, HC, CO, CO_2 emissions were more [60]. Lakshmanan et al.conducted an experiment where acetylene was used as a secondary fuel with diesel. Reduction in NO_x, HC and CO with increased smoke level was observed as compared to diesel operation. BTE was closer to that in diesel operation [61].

Nathan et al. conducted used acetylene in homogenous charge compression ignition (HCCI) mode. The thermal efficiencies were comparable to diesel mode and with optimized EGR operation, slight increase in BTE was observed. Smoke and NO_x were reduced by HCCI mode. HC emissions were more than diesel mode [62]. Another researcher Wulff et al. used mixture of alcohol and acetylene in SI engine and CI engine in dual fuel mode. Higher efficiency than conventional engine was observed, with cleaner burning as compare to diesel.[63].Wulff et al. observed reduction in NO_x, HC and CO emissions while using acetylene in dual fuel mode[64].Reversing the cooling water direction in acetylene operated CI engine in HCCI mode resulted in 5-10% improvement in BTE with higher NO_x and CO emissions [65]. Sharma et al. used acetylene gas with alcohol in SI engine. The results came with lower CO_2, NO_x, SO_x [66]. Mahla et al. inducted acetylene and diethyl ether (DEE) with diesel in DF mode with different blend ratios. An increment in BP and BTE was observed for all loads with 20% DEE 20% addition [67].

Srivastava et al. used acetylene in DF mode in CI engine. BTE in case of dual fuel mode followed the same trend as of diesel during low load conditions. The BSEC increased with the induction of acetylene. The EGT, CO, CO_2 and HC emissions in case of dual fuel mode was higher as compared to that for neat diesel [68]. Brusca et al. carried out theoretical and experimental analysis of an IC engine running on acetylene and alcohol using two standard commercial injectors for acetylene and alcohol. An optimization technique based on genetic

algorithms and neural networks to optimize the engine performance was used. A reduction in CO, HC and NO_x emissions was observed while using acetylene alcohol combination compared to the baseline gasoline case [69]. Acetylene when used in DF mode with diesel and Used Transformer Oil (UTO) gave lower Exhaust gas temperature (EGT) and smoke emission while NO_x level was higher compared to neat diesel or neat UTO operation [70]. Sudheesh et al. carried out experimental analysis using acetylene in HCCI mode and DEE. BTE was comparable to that of diesel operation. High CO, HC and lower NO, smoke emissions were observed in case of acetylene-DEE mode [71].

Dual-fuel operation can be one of the prominent methods for conserving fossil fuels like diesel and petrol [72]. In DF engine the gaseous fuel is mixed homogeneously with air in cylinder, while diesel is used as a pilot fuel for ignition of the charge. DF engines can be modified to operate on natural gas. Diesel can be used as pilot fuel, or it can be operated on 100% diesel fuel [73]. NO_x and soot emissions are controlled by the help of dual fuel concept. In gas diesel operations, HC, CO and BSFC were higher at part load condition in CI Engine, but with the help of increasing in engine speed and amount of pilot fuel and advancement in IT, the thermal efficiency could be improved in dual fuel engine [74]. Longer ignition delays and short combustion durations were characterized for DF operations. NO_x emission for DF operation was found to be lower than diesel case. Lower PM emission but increased UHC emissions were measured for biogas–diesel DF operations [75].

2.4 Effect of operation parameters

It has been observed that operation parameters like compression ratio, injection pressure, injection timing, etc. have considerable effects on the performance and emissions of diesel engines.

2.4.1 Effect of Compression Ratio (CR)

Muralidharan et al. conducted experiments using methyl esters of waste cooking oil with diesel on VCR engine varying CR from 18 to 22, and found maximum BTE at CR 21 [76]. Sivaramakrishnan conducted experiment using 20%, 25% and 30% of Karanja oil blended with diesel in a multi-fuel VCR engine at CRs of 15 to 18. The best results were obtained with 25% biodiesel–diesel blend with CR 18 [77]. Hariram et al. observed reduction in BTE and increase in EGT when CR was reduced from 18 to 16 [78]. Nagaraja et al. used pre heated palm oil and their blends with diesel on CI Engine at different CR. Experiments were

conducted at CR 16 to 20. EGT was low for all the blends compared to diesel. CO and HC reduced with an increase in blending ratio and CR at maximum load. The engine performance was found to be optimum when using O20 blend at CR 20 at full load condition [79]. De et al. evaluated the effects of Jatropha oil combustion on performance and emissions in VCR diesel engine at three CRs of 16, 17 and 18 and different Jatropha oil blending rates (10%, 30%, 50%, 80% and 100%). They concluded that the thermal efficiency, EGT and emission such as NO_X and CO at CR of 18 for up to 30% Jatropha oil blend was close to that of diesel. [80]. Senthil et al. studied the effects of CR and IT on the performance with Annona methyl ester (A20). It was found that CR 19.5 and IT 30º bTDC, A20 gave better performance and lower emission which was very close to diesel and also concluded that the improvement in BTE and SFC was observed, when CR and IT increased [81]. Lal et al. studied the performance and emission using downdraft gasifier with DI VCR diesel engine. It was observed that increasing the CR from 12 to 18 maximum diesel saving attained was 8.7% to 64.3% respectively along with reduction of 63.62% in HC emission was achieved [82]. Selim investigated the effect of CRs using HCNG. Highest brake torque, lowest BSFC was observed at high CR 12.5 for all blends[83]. Hirkude et al. concluded that higher CR improves the engine efficiency and also results in reduced CO and PM but with an increase in NO_x emission [84]. EL_Kassaby et al. observed the outcome of blending ratio and compression ratio on a CI Engine varying the CR from 14 to 16 to 18. On increasing the CR from 14 to 18, engine torque increased and BSFC decreased. CO_2 emission was increased by 14.28%. HC and CO emission were reduced by 52%, 37.5% respectively [85].

2.4.2 Effect of Injection Pressure (IP)

Fuel injection pressure affects the performance and emissions in diesel engine and is one of the most important operating parameters [86]. Higher fuel injection pressure improves the performance and reduces emissions [87]. Aalam et al. used mahua methyl ester blend at varying injection pressure from 22 MPa to 88 MPa where higher BTE and better combustion characteristics were observed at highest injection pressure of 88 Mpa compared to other injection pressures. There was a gradual fall in HC, CO and smoke emissions with increase in injection pressure. It was due to better mixture formation because of the well-atomized spray at higher injection pressure [88]. Quadri et al. conducted experiment using hydrogen in dual fuel mode with diesel on three different injection operating pressures (IOP) i.e. 200, 220 and 240 bar at full load condition. It was observed that on using 20% hydrogen with diesel,

highest BTE and NO_x emission along with lowest unburnt hydrocarbon (UHC) and CO emissions were obtained at 220 bar [89]. Liu et al. observed the result of IP on the performance and emissions characteristics with common-rail fuel system in diesel-methanol dual fuel (DMDF) combustion mode. With the increase of IP, BSFC, CO, HC and smoke emissions decreased while NO_x emission, maximum cylinder pressure and HRR increased in DMDF mode [90]. Gumus et al. studied the effects of IP using biodiesel–diesel blends at IPs of 18, 20, 22 and 24 MPa. Increase in IP resulted in reduction in BSFC at different biodiesel diesel blends (Blend of 20%, 50% and 100%).There was decrease in CO, smoke opacity, and UHC and increased the value of NO_x, CO_2, and O_2emissions with increase in IP [91]. Ryu et al. studied effects of pilot IP using biodiesel–CNG dual fuel combustion (DFC) system. There was increase in combustion stability of DFC mode with increase of IP. Smoke decreased and NO_x emissions increased as the pilot IP increased in biodiesel–CNG DFC system [92]. Nathagopal et al. studied the effect of IP using calophylluminophyllum biodiesel in DI diesel engine fuelled with 100% biodiesel. Tests were conducted at different IPs of 200, 220 and 240 bar. The experimental results revealed that at higher IP there was a reduction in BSEC of calophylluminophyllum methyl ester. There was significant reduction in emissions of UHC, CO and smoke at 220 bar IP of biodiesel compared to other IPs. However, NO_x increased with increase in IP of calophylluminophyllum methyl ester and was always higher than that of neat diesel [93]. Shehata et al. conducted test on DI diesel engine at different IPs of 180, 190 and 200 bar. Increased IP gave better performance in comparison to the original IP for all tested fuels, and hence, it was concluded that the best results were obtained at high injection pressure of 200 bar [94]. Sayin et al. studied the effect of IP with methanol blended diesel fuel. Different IPs of 180, 200 and 220 bar were used. The best results in terms of BSFC were obtained at 200 bar IP for all engine loads. BSFC, NO_x and CO_2 increased while smoke, CO and UHC decreased on increasing methanol % in fuel. It was thus suggested to use high IP for decreasing smoke, CO and UHC emissions and low IP for decreasing NO_x and CO_2 emissions [95]. The effect of injection pressure on DI diesel engine using orange skin powder diesel solution (OSPDS) at different IPs of 215, 235 and 255 bar was studied. It was found that at 235 bar the combustion, performance and emission characteristics of OSPDS were better than those at other injection pressures [96]. Behera et al. carried experimental investigation using UTO at different injection pressures (200, 210, 220, 230, 240 and 250bar). Better performance with less emissions were observed at 230 bar injection pressure as compared to 200 bar [97].Channapattana et al. investigated the effect of Honne biodiesel and diesel blends at different IPs (180, 210 and 240 bar). At 240 bar higher BTE

and lower BSFC were obtained compared to that at other IP for all blends. CO, HC and smoke emissions at 240 bar were lower compared to those at other IPs while NO_x emission increased with increase in IP [98]. Sastry et al. used isobutanol and ethanol as additives to the diesel-biodiesel blends at different IPs of 200, 225, 250 and 275 bar. It was found that on increasing nozzle opening IP up to 250 bar, the BTE and fuel economy of the engine were improved and CO and smoke emissions were reduced significantly. However, NO_x emission decreased marginally in some blends [87]. Syed et al. studied the influence of IOP for 20% blend (B20) of mahua oil methyl ester (MOME) and 22.5 liters per minute of hydrogen in dual fuel mode at four different IOPs of 200, 225, 250 and 275 bar. At IOP of 250 bar maximum BTE, minimum BSFC, and lowest HC, CO and smoke emissions with increased concentration of NO_x were obtained for B20-hydrogen dual fuel mode [99]. Anbarasu et al. investigated the effect of IP on canola biodiesel emulsion at 200, 220 and 240 bar. Results showed an improvement in BTE of 28.8% at 240 bar accompanied by the drastic reduction in NO_x at 200 bar using emulsified fuel [100]. Balusamy et al. observed the result of IT and IP on CI engine using thevetia peruviana seed oil methyl ester. Increasing the injector opening pressure and advancing the IT from the base diesel value increased BTE while CO, HC and smoke emissions reduced significantly [101]. Belaguret al. conducted experiment to study the effect of honne oil-diesel blend (H50) at different IP (200, 220, 240 and 260 bar). It was observed that with H50, increasing the IP increased the BTE. CO, HC and smoke emissions got reduced while NOx increased. Optimum IP was observed at 240 bar for H50 based on BTE and emissions [102]. Sayin et al. conducted experiment using canola oil methyl esters (COME) blends with diesel fuel at different IPs (18, 20, 22 and 24 MPa). The results showed that the increased IP gave better results for BSFC, BSEC and BTE compared to the original and decreased IP. Increased IP boosted maximum cylinder gas pressure due to increase in premixed combustible mixture [103].

2.4.3 Effect of Injection Timing (IT)

Injection timing is an important parameter that affects the performance, emission and combustion characteristics of diesel engine. Advanced IT seems to be a good choice for improving performance and combustion of dual-fuel engine at low loads in terms of cost and benefit [104]. Mani et al. performed tests at four ITs (23^o, 20^o, 17^o and 14^o bTDC) and found that NO_x, CO and UHC emissions decreased while BTE, CO_2 and smoke emissions increased at retarded IT of 14^0bTDC [105]. Kannan et al. performed experiment using waste cooking

oil at different IP and IT and found that BTE, cylinder gas pressure and HRR improved while there was reduction in NO_x and smoke emissions for advanced IT of 25.5° bTDC at 280 bar IP [106]. Liu et al. conducted experiment on diesel engine using diesel-methanol compound combustion (DMCC) mode and found that PCP, maximum HRR and NO_x increased while BSEC, EGT and smoke decreased for DMCC with advanced IT [107]. Suresh et al. varied IT from 19° to 27° bTDC and IP from 210 to 240 bar and concluded that increased BTE and reduced HC, CO and smoke emissions were obtained for retarded injection timing of 19° bTDC and increased IOP of 230 bar [108]. Saravanan studied the effect of EGR at advanced ITin diesel engine. Long delay period, high peak pressure, high maximum HRR were observed at advanced IT when compared to those at standard IT. Using EGR at advanced IT delay period, peak pressure, MHRR and combustion duration were higher than those without EGR [109]. Aljamali et al. investigated the effect of various ITs of (EOI 120, EOI 180, EOI 300, EOI 360) bTDC on the performance and emissions of stratified combustion CNGDI engine. High power, torque, brake mean effective pressure (BMEP) and CO_2were observed at 120 bTDC (at high engine speed) while BSFC, NO, HC and CO emissions were found to be reduced [110]. Ayetor et al. experimented the effect of IP and ITin diesel engine fuelled with biodiesel. It was found that IT had profound effect on BSEC and engine emissions. Low HC and CO while high NO_x emission was obtained at advanced IT [111]. Bora et al. reported improved efficiency and reduction in emissions at 29° bTDC IT on using biogas DF engine at different ITs of 23°,26°, 29° and 32° bTDC [112].Sayin et al. conducted tests for different ITs (21°, 24°, 27°, 30° and 33° CA bTDC) with ethanol in DF diesel engine. CO and UHC decreased while NO_x and CO_2 increased with advanced IT [113, 114]. Sayin et al. observed the effect of IT in CI engine using diesel–methanol blends for different ITs (15°, 20° and 25° CA bTDC) and found that smoke, HC and CO decreased while CO_2 and NO_x increased with advanced IT (25° CA bTDC) [115]. Datta et al. numerically founded the outcome of IT on diesel engine fuelled with diesel and methyl soyate. Simulations were carried out for three different ITs of 17°, 20° and 23° bTDC. Decrease in BTE and an increase in BSFC were predicted with the advancement in IT for both the fuels. EGT, NO_x and CO_2 increased while particulate matter and smoke emission decreased with advanced IT. NO_x and CO_2 emissions and EGT were more, while PM and smoke emissions were less for methyl soyate compared to those in diesel [116]. Barik et al. investigated the effect of IT in biodiesel dual fuel mode (BDFM) at give different ITs from 21.5° CA bTDC to 27.5° CA bTDC. Biodiesel dual fuel mode at 24.5° CA (BDFM24.5) gave better performance, combustion and emissions than

those at other ITs [117]. Balusamy et al. studied the effect of IT and IP in CI engine fuelled with methyl ester of thevetiaperuviana seed oil. On advancing the IT from 23º to 27º bTDC and increasing IP from 210 bar to 225 bar, BTE increased and CO, HC and smoke emissions reduced significantly. The optimum IT and IP were found to be 27º bTDC and 225 bar respectively [118]. Sakthivel studied the consequence of IT in DI CI engine fuelled with ethyl ester of fish oil (EEFO) at different ITs (21º, 24º and 27º bTDC). Retarding the IT increased BTE and decreased NO_x, HC and CO emissions [119]. Ryu investigated the effect of IT in CI engine using biodiesel and CNG DF mode and found that at low loads, BSEC of DF mode improved with advanced IT while at high loads, BSEC improved with delayed IT. Smoke emission decreased while NO_x increased with advanced IT while CO emission decreased with delayed IT for biodiesel–CNG DFC [120]. Yadav et al. used TWTO (trans-esterified waste transformer oil) as a fuel in CI engine. Experiments were conducted at four ITs (23º, 22º, 21º and 20º bTDC). NO_x, CO and UHC decreased with retarded IT of 20º bTDC while BTE and smoke increased under all the load conditions when compared to that of standard IT [121]. Ganapathy et al. studied the influence of Jatropha biodiesel blend in CI engine at different ITs. On advancing the IT, BSFC, CO, HC and smoke reduced. BTE, P_{max} (maximum cylinder pressure), HRR_{max} and NO increased on advancing the IT [122]. Hwang et al. conducted experiment at different IPs and ITs using waste cooking oil biodiesel and found that PCP, HRR and NO_x emission increased with advanced IT.CO emissions decreased with higher IP and retarded IT. Smoke emission decreased with advanced IT [123]. Park et al. used ethanol blends for different loads and ITs in four cylinder diesel engine and reported that advanced IT caused active combustion process. NO_x emissions increased while CO and HC decreased with increase in load and advanced IT [124].

2.5 Research gaps

A remarkable development has taken place in the field of alternate fuels in IC engines all over the world, especially during the last 2 decades. However, following research gaps were observed from the detailed literature review:

- Acetylene gas has not been explored much as an alternative fuel in IC engines. Thus exhaustive study is required to study it as a suitable alternate fuel for IC engines.
- Not much research has been carried out using acetylene in multi cylinder engines.
- No research work has been found using acetylene in medium and large capacity engines.

- Performance variation using acetylene with change of compression ratio has not been reported.
- Majority of research has been done using acetylene stored at high pressure in cylinders. Very little study has been done using onboard generation of acetylene.
- No study has been found on constant delivery onboard acetylene generator.
- Modeling and simulation work has not been carried out using acetylene as a fuel.

2.6 Objectives

After going through the observed research gaps, the present work proposed to use acetylene gas as an alternative fuel for a CI engine and to test its feasibility with the following objectives:

- To develop a fuelling system for stationary CI engine operated on Acetylene and Diesel in dual fuel mode.
- To optimize the engine operating parameters and study the performance parameters, combustion characteristics and exhaust emissions using acetylene as alternate fuel.
- Modeling and simulation of the performance of stationary CI engine operated on Acetylene and Diesel in dual fuel mode.

2.7 Research methodology

The following methodology / research plan was proposed to carry out the current research:

1. Detailed literature review regarding the use of alternate fuels in CI engine, including acetylene gas around the world in the past few years.
2. Selection of appropriate stationary CI engine for testing of acetylene in dual fuel mode.
3. Selection of optimum acetylene generator and other components for CI engine.
4. Procurement of the selected acetylene gas generator and other components.
5. Verification of the optimum operating conditions of the selected engine.
6. Development of experimental set up for evaluation of engine performance parameters, exhaust emissions and combustion characteristics.
7. Development of the acetylene fuelled CI engine operated end-utility system.
8. Calibration of 5 gas analyser, smoke meter, dynamometer, etc.

9. Engine test runs to be carried out with the developed / modified system for its accuracy, reliability, and durability. Further improvement/modification to be carried out if required in the developed system.
10. Development / calibration of engine instrumentation for acetylene gas fuelling, and long-term operation over a wide range of operating parameters such as load, injection pressure, injection timing and compression ratios, etc., if required.
11. Experimental evaluation of engine performance, emissions and combustion characteristics with Acetylene-Diesel (dual fuel mode) fuelling, including determination and comparison of various parameters.
12. Determination of optimum compression ratio for neat diesel operation.
13. Determination of optimum injection pressure for neat diesel operation.
14. Determination of optimum injection timing for neat diesel operation.
15. Determination of optimum flow rate of acetylene for dual fuel mode.
16. Determination of optimum compression ratio for dual fuel mode.
17. Determination of optimum injection pressure for dual fuel mode.
18. Determination of optimum injection timing for dual fuel mode.
19. Calculation and comparison of performance parameters (BTE, BSEC and EGT) of acetylene-diesel operated (dual fuel mode) engine with that of neat diesel operation at varying (i) loads, (ii) compression ratios, (iii) injection pressures and (iv) injection timings.
20. Study the combustion phenomenon using p-θ plots obtained from the system.
21. Comparison of engine exhaust emissions (CO, HC, smoke and NO_x) of acetylene-diesel operated (dual fuel mode) engine with that of neat diesel operation at varying (i) loads, (ii) compression ratios, (iii) injection pressures and (iv) injection timings.
22. Selection of software application for modelling and simulation.
23. Building of a model for the acetylene-diesel fuelled VCR engine.
24. Simulation of the model and its validation from experimental results obtained.
25. Documentation of the research work and final report writing.

CHAPTER 3

EXPERIMENTAL SETUP, PLAN AND PROCEDURE

3.1 Experimental set-up

The purpose of the current research was to test the feasibility of acetylene as a fuel in a stationary, single cylinder CI engine in dual fuel mode along with diesel. Hence, in the present research work, the experimental investigation of the performance, emission and combustion characteristics for a diesel-acetylene fuelled, stationary, water-cooled, constant speed, single cylinder, 4-stroke, compression ignition engine was carried out at varying (i) flow rates of acetylene, (ii) compression ratio (CR), (iii) injection pressure (IP) and (iv) injection timing (IT). Load was determined with the help of an eddy current dynamometer coupled with the engine. For this research, acetylene gas was required to be supplied at constant pressure and constant flow for accurate estimation of the mass of acetylene consumed in each set. For the same, an acetylene generator was used, specifications of which are mentioned later in this section. For safety, flame traps and non-return valves were used.

The performance parameters viz., brake thermal efficiency, brake specific energy consumption and exhaust gas temperature were determined whereas exhaust emission parameters like NO_x, HC, CO and smoke opacity were recorded. The various indicators of combustion behavior of diesel-acetylene fuelled CI engine included in-cylinder pressure histories, heat release rate and rate of pressure rise.

Flow meter was used for the measurement of flow rate of acetylene. Air box arrangement was used to determine the air flow rate. Fuel supply system consisted of a burette method to measure the volumetric fuel consumption. AVL Ditest-444 5-gas analyzer was used to measure CO, CO_2, HC, NO_x and O_2 in exhaust gas. Smoke percentage in the exhaust gas was measured using AVL 480 BT smoke meter.

The detailed description of the instruments used is discussed in this section.

3.2 Diesel engine and dynamometer

The study was carried-out on a computerised experimental engine test rig, comprising of a single cylinder, water-cooled, four-stroke, stationary, constant speed, variable compression ratio (VCR) diesel engine coupled to an eddy current dynamometer. The photograph of the engine along with the dynamometer is shown in Fig. 3.1. The detailed technical specifications of the engine are shown in Table 3.1. The data acquisition device of the VCR engine consisted of an interface unit and suitable analogue-digital-converter, which were connected to the computer. The interface-unit gets the pressure signals from the output of charge amplifier which after getting processed were stored in the internal memory and are digitally displayed on computer, after completion of 10 combustion cycles.

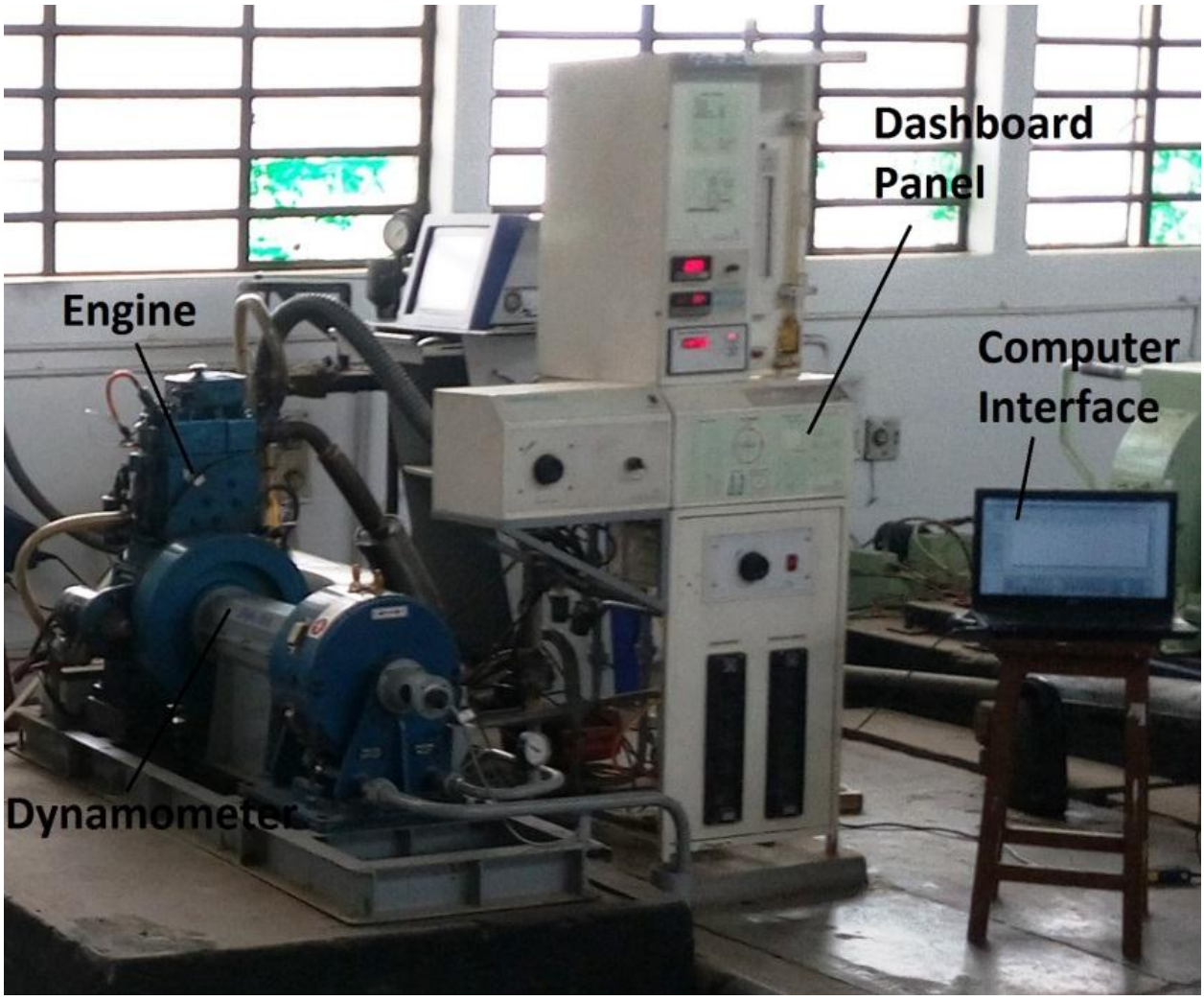

Fig. 3.1 Pictorial view of engine coupled with eddy current dynamometer and computer interface

Table 3.1 Specifications of the diesel engine [125]

Particular	**Description**
Type of engine	Research engine test setup - single cylinder, 4 stroke, multi-fuel, VCR, computerized
Make and model	Apex Innovation 240PE (with modified Kirloskar TV1 engine)
Bore	87.5 mm
Stroke	110 mm
Cubic capacity	661 cc
Connecting rod length	234 mm
Engine speed	1500 rpm (constant speed)
Maximum power	3.5 kW @ 1500 rpm
Type of cooling	Water cooled
Compression ratio	18:1 to 22:1
Injection variation	0 – 25° bTDC
Combustion chamber	Hemispherical bowl in piston type
Rotameters	Engine cooling 40-400 LPH; Calorimeter 25-250 LPH
Fuel tank	15 litres, dual compartment, glass fuel metering pipe
Air box	MS fabricated with orifice meter and manometer (water filled)
Orifice diameter	0.020 m (20 mm)
Engine performance analysis software	'Enginesoft' supplied by Apex Innovation, India

SAJ make eddy current dynamometer was used to measure brake power. The dynamometer was bidirectional. The shaft mounted finger type rotor ran in a dry gap. A closed circuit type cooling system permitted for a sump. Dynamometer load measurement was obtained from a strain gauge load cell and speed measurement was done from a shaft mounted 360 PPR (pulses per revolution) rotary encoder.Specifications of the dynamometer are given in Table 3.2.

Table 3.2 Specifications of dynamometer [125]

Particular	**Description**
Manufacturer	Saj Test Plant Pvt. Ltd
Model	AG10
Type	Eddy current
Cooling	Water cooled
End flanges both side	Cardan shaft model 1260 type A
Water inlet pressure	1.6 bar
Maximum Torque	50 Nm
Continuous current	5.0 amps
Cold resistance	9.8 ohms
Maximum speed	10000 rpm
Weight	130 kg
Load cell	Apex AX-155, constant speed, 230V AC
Dynamometer arm length	0.185 m

3.3 Air flow measurement

Flow of air to the engine was measured with the help of an Air box. As the air flow is pulsating, for measurement of air consumption, an air box of suitable volume was fitted with orifice of diameter 20 mm having C_d = 0.6. The air box was used for damping out the pulsations. The differential pressure across the orifice was measured by manometer. The outlet was connected to the air filter mounted on the engine. The amount of air inducted was obtained with the help of the following relation:

$$\text{Air Flow (kg / hr)} = C_d \times \frac{\pi}{4} \times D^2 \times \sqrt{2g \times h_w \times \frac{\rho_w}{\rho_a}} \times \rho_a \times 3600 \qquad (3.1)$$

Where,

C_d = Coefficient of discharge of orifice = 0.6

D = Orifice diameter in m = 0.02 m (= 20 mm)

g = Acceleration due to gravity (m/s^2) = 9.81 m/s^2

h = Differential head across orifice (m of water)

ρ_w = Water density (kg/m^3) = 1000 kg/m^3

ρ_a = Air density (kg/m^3) = 1.15 kg/m^3

3.4 Fuel flow measurement

3.4.1 Diesel flow measurement

Flow rate of diesel was measured on volumetric basis, using 100 ml glass burette and a stop-watch. The glass burette mounted on the dashboard panel of the engine had graduated scale for measurement of diesel flow rate as shown in Fig. 3.2 (a). Time elapsed for a fixed quantity of fuel (20 ml) before feeding to engine was measured by a stop watch to calculate the volumetric flow rate of fuel. The mass flow rate of diesel was calculated using fuel density and volumetric flow rate. Speed governor adjusted the quantity of diesel injected to keep the engine speed almost constant at different load conditions.

(a) **(b)**

Fig. 3.2(a) Glass burette for measuring diesel flow rate **(b)** Calibrated gas flow meter

3.4.2 Acetylene gas flow rate

The flow rate of acetylene gas was measured with the help of calibrated gas flow meter as shown in Fig. 3.2 (b). The outlet of constant pressure acetylene gas generator was connected to the gas flow meter and the quantity of the gas was regulated with the help of the valve attached to the outlet of generator.

3.5 Water flow measurement

Globe valves were used to control the flow of cooling water to the engine and calorimeter. Two rotameters were provided for cooling water and calorimeter water flow measurement. Rotameters used in the experiment shown in Fig. 3.3. Technical specifications of rotameters are given in Table 3.3.

Fig. 3.3 Rotameters for water flow measurement in engine and calorimeter

Table 3.3 Specifications of Rotameter [125]

Particular	**Description**
Make	Eureka
Model	PG-5 and PG-6
Flow rate	25-250 LPH and 40-400 LPH
Packing/Gaskets	Neoprene
Measuring tube	Borosilicate glass
Float	316SS
Cover	Glass
Accuracy	+/- 2% full flow
Range ability	10:1
Scale length	175-200 mm
Max. Temp.	2000^0C
Connection	Flanged and threaded, vertical

3.6 Temperature measurement

RTD 100 type temperature sensor with output 4-20mA, supply 24VDC and range: 0-100^0 C and thermocouples (type K), output 4-20 mA, supply 24 VDC, range: 0-1200^0 C were used to measure the temperature of water and exhaust gas in the experimental setup.

3.7 In cylinder pressure measurement

In-cylinder pressure is one of the important quantity recorded, the analysis of which and the derived parameters, thereof, furnished information about the complex process of combustion. Piezo-electric pressure transducers are most commonly used form of pressure transducers for the purpose of acquiring in-cylinder pressure histories. For combustion pressure and fuel line pressure measurement, two piezo-type sensors were mounted on the cylinder head and fuel injector respectively. Pressure pick-up assembly consisting of piezoelectric transducer was mounted to the cylinder head and crank angle encoder, which was connected to NI USB-6210, 16 bit, 250 kS/s card, with digital input. Specifications of pressure sensors are given in Table 3.4. The measured cylinder pressure was displayed on the computer by data acquisition

system. The shaft encoder was used for delivering signals for TDC and crank angle with a precision of 1 crank angle degree.

Table 3.4 Specifications of pressure sensors [125]

Particular	**Description**
Sensor name	Dynamic pressure transducer with built in amplifier
Make	PCB Piezotronics, Inc.
Model	M111A22
Range, FS (5V output)	5000 psi
Useful range (10V output)	10000 psi
Maximum pressure	15000 psi
Resolution	0.1 psi
Sensitivity	1 mV/psi
Resonant frequency	400 kHz
Rise time	2 µs
Discharge time constant	500 s
Low frequency response (-5%)	0.001 Hz
Linearity (Best straight line)	2 %
Acceleration sensitivity	0.002 psi/g
Temperature coefficient	0.03 % / ºF
Temperature range	-100 to +275 ºF
Flash temperature	3000 ºF
Vibration / Shock	2000 / 20000 g peak
Ground isolation	No (2)
Excitation (Constant current)	2 to 20 mA
Voltage to current regulator	+18 to 28 VDC
Sensing geometry	Compression
Sensing element	Quartz
Housing material	17-4 SS
Diaphragm	Invar
Sealing	Welded hermetically

3.8 Crank angle measurement

A rotary encoder is fitted on the engine shaft for crank angle signal detecting each degree (1^0) rotation of the crank for each cycle. Hence, for a particular cycle, a total of 720 data for both cylinder pressure and volume are recorded at each load. Signals are scanned by an engine indicator (electronic unit) and communicated to computer. The software in the computer draws pressure crank-angle and pressure volume plots. Specifications of crank angle sensor are given in Table 3.5.

Table 3.5 Specifications of crank angle sensor [125]

Particular	**Description**
Make	Kubler, Germany
Model	8.3700.1321.0360
Resolution	1°
Supply voltage	5-30 V DC
Output	Push Pull (AA, BB, OO)
PPR	360
Speed	5500 rpm with TDC pulse
Diameter	37 mm
Shaft size	Dia. 6 mm × length 12 mm
Weight	120 gm

3.9 Acetylene generator

An acetylene generator is a device which delivers and keeps up a regular supply of acetylene gas, which can be utilized in welding, repair, construction. Installation, use, and maintenance of an acetylene generator are liable to strict safety measures since acetylene is extremely hazardous gas which can easily explode at a wide range of gas to air concentrations.

Acetylene generators are of two types. In the first type calcium carbide is fed in granular or powdered form into the tank containing water while in the second type, water is fed over calcium carbide. Both the types of generators work on the principle of reaction of calcium carbide with water which produces acetylene gas. Both types of generators ought to be outfitted with pressure safety valves to safeguard against spikes in the internal pressure of the

gas generated and the generator should be sealed well. In the current research water on carbide type generator was used.

A constant pressure acetylene gas generator was used for production of acetylene gas as shown in Fig. 3.4. It consisted of a carbide chamber where calcium carbide was fed and a tank where water was filled. The reaction of calcium carbide and water produced acetylene gas which was collected in the floating drum type arrangement. The specifications of the acetylene gas generator are given in Table 3.6.

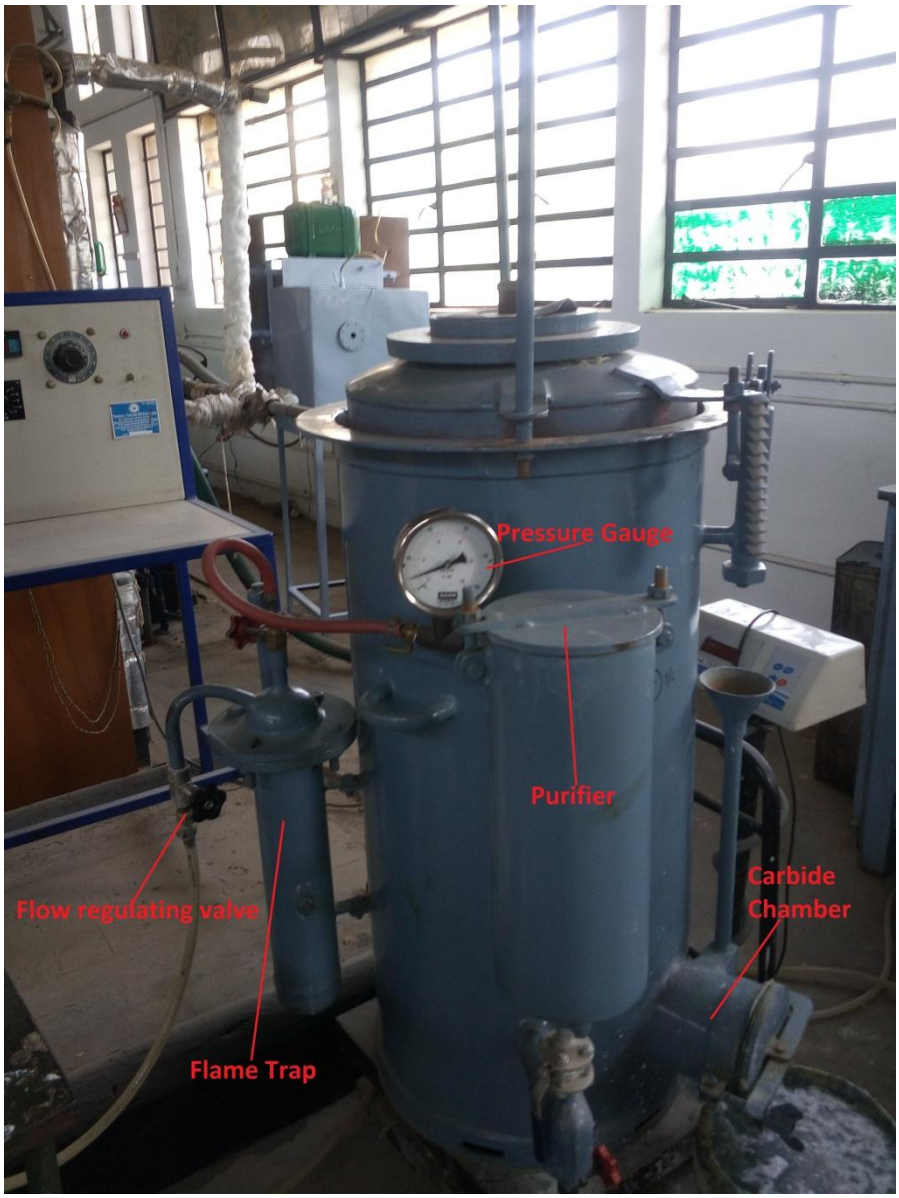

Fig. 3.4 Acetylene gas generator

Table 3.6 Specifications of acetylene gas generator [126]

Particular	**Description**
Make	International Industrial Gases Limited, India
Model	B-0
Carbide charge in each chamber	3.2 kg
Maximum output per hour	608 litres
Total output per hour	851 litres
Number of carbide chambers	1
Gas holding capacity	71 litres
Gas output Line	15 mm
Weight (empty)	90 kg
Tank dimensions	Diameter: 432 mm, height: 940 mm
Overall assembled height	1600 mm

3.10 Development of acetylene fueling system

Acetylene is highly explosive gas. It can form a flammable mixture with air over a wide range of concentrations (2.5% to 81%), the widest among commonly used gas, and very low energy is required to ignite acetylene-air mixtures. The minimum ignition energy of acetylene is 0.017 mJ. This means that acetylene can ignite easily and form a flammable mixture with oxygen or air. Therefore acetylene must be stored and handled with great care. The experimental area was well ventilated for this purpose. Two flame traps were provided: one attached to the gas generator and the other before the engine so as to prevent flash black. Non return valves were also used for safety purpose. Acetylene gas is reactive in nature with copper alloys and therefore the materials other than copper alloys were used in experimental set up.

Acetylene was first passed through a flame trap coupled with the acetylene gas generator to prevent explosions inside the acetylene-containing system, followed by a flow control valve to adjust the flow rate. Then acetylene was then passed through a non-return valve (NRV) preventing reverse flow of acetylene into the system. Then it was passed through another

flame trap connected before the engine. 2 NRVs were attached to the flame trap and one on the intake manifold as shown in Fig. 3.5 (a) and (b) respectively. The flame trap was made of cast iron (5 mm thick sheet) that contained a sleeve to suppress the flame and water to put off the flame. There were two pipe lines, one (inlet) was dipped in the water just above the bottom of the trap and the second (outlet) was above the water level in the trap. One pressure gauge was also mounted on the trap to measure the pressure level.

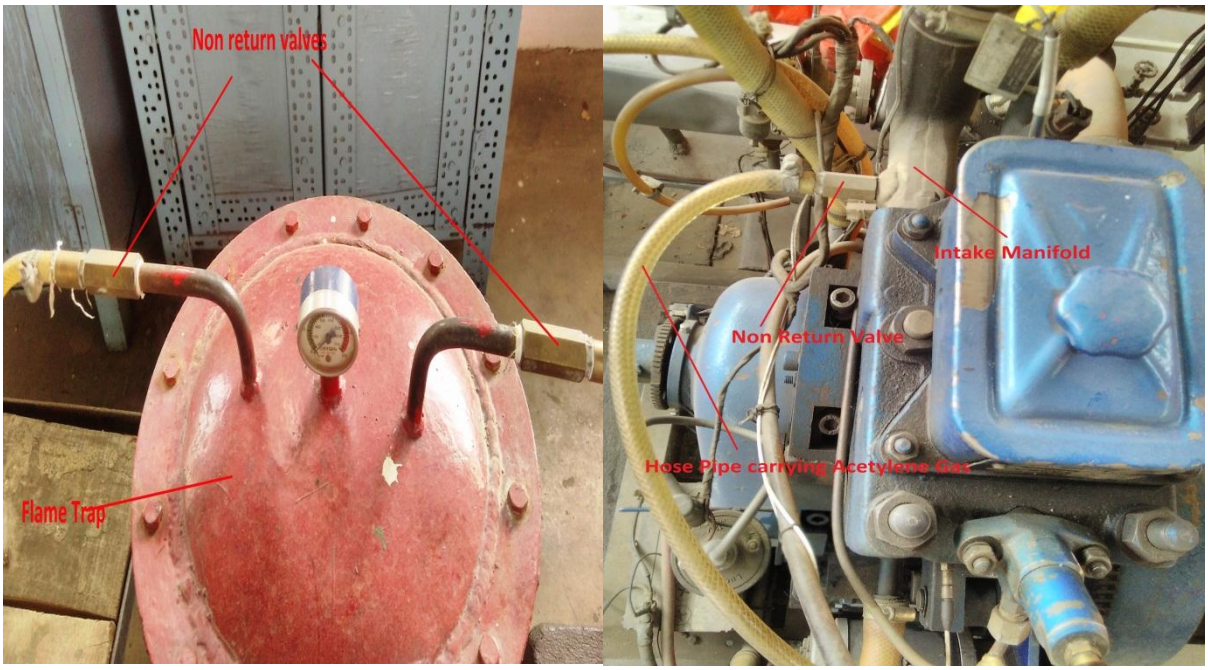

(a) **(b)**

Fig. 3.5 Non return valves attached to (a) flame trap (b) intake manifold

3.10.1 Flame trap

A flame trap is a safety feature which prevents fire from reaching a fuel supply line as shown in Fig 3.6. Flame Trap reduces the risk of explosion or fire, making the system safer to operate. The flame trap extinguishes the fire, ensuring that it does not comes into contact with the fuel supply. Flame traps are widely used in internal combustion engines, fuel gas lines and other types of equipment which rely on combustion for heat or energy.

Over time, a flame trap can become blocked with particulates and other material. By products of combustion can build up inside the trap, slowly blocking it. The flame trap may still be able to extinguish flame, but the flow through the system will be obstructed. It can create a fire hazard, if it is clogged enough, as the particulates may catch fire. Therefore, regular

maintenance of flame traps is required so as to ensure people that they are in good working condition.

Fig. 3.6 Flame trap

3.11 Engine optimization for alternate fuel used

The optimum combination of compression ratio (CR), injection pressure (IP) and injection timing (IT) was desired while working with acetylene as an alternate fuel in diesel engine, so as to obtain maximum BTE and minimum BSEC.

3.11.1 Compression ratio adjustment

Compression ratio (CR) was varied without stopping the engine and without altering the combustion chamber geometry by specially designed tilting cylinder block arrangement provided on the engine. CR was adjusted by loosening the 6 Allen bolts provided on the cylinder block. Then the lock nut provided on the adjuster was loosened. The adjuster was rotated as desired to set the given CR based on the markings on the CR indicator. Adjuster was locked by tightening the lock nut. Finally the 6 Allen bolts were tightened. The compression ratio adjustment mechanism is shown in Fig. 3.7.

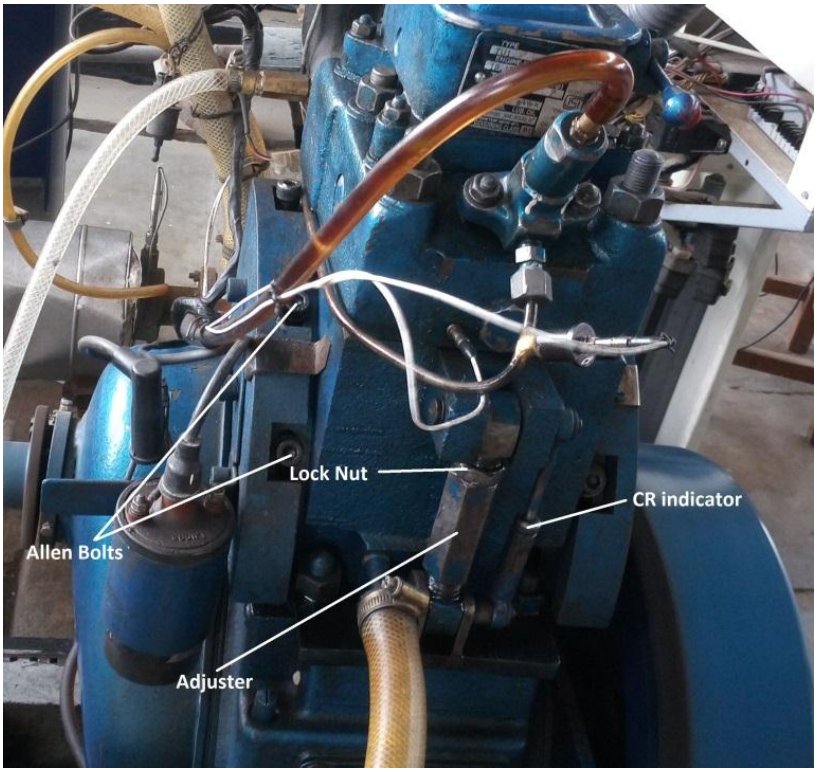

Fig. 3.7 CR adjustment mechanism

3.11.2 Injection pressure adjustment

The injection pressure (IP) is the opening pressure of fuel nozzle. Optimum IP is that value in which maximum BTE and minimum BSEC is obtained. IP was changed by testing the injector

assembly in a nozzle tester, as shown in Fig. 3.8. To obtain the different fuel injection pressure values, spring tension of the injector needle with setting screw was varied. In order to identify the trend, one lower and one higher injection pressure was selected.

Fig. 3.8 Fuel injection pressure tester

3.11.3 Injection timing adjustment

Injection timing was varied with the help of injection point nut provided on the engine. The injection point nut was turned in one direction @ ¼ turn. The readings were then observed on the monitor. Injection point adjustment nut was gradually turned and its effect on diesel injection plot was noted. The diesel injection plot shifted horizontally to retard / advance the injection point, depending upon the direction of rotation. The nut was adjusted till the desired injection point was obtained. The injection timing adjustment mechanism is shown in Fig. 3.9.

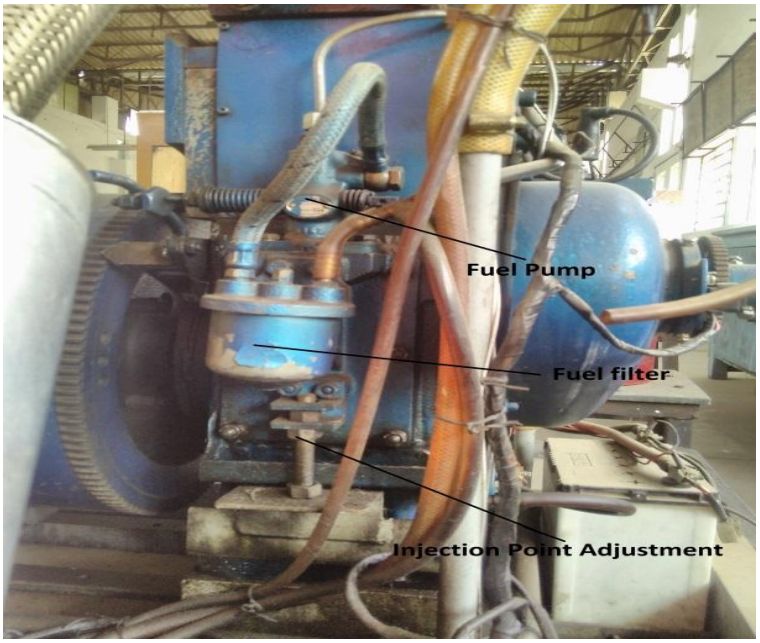

Fig. 3.9 Injection timing (IT) adjustment mechanism

3.12 Exhaust emissions' measurement

The major pollutants in the diesel engine exhaust are smoke and oxides of nitrogen. The exhaust gases were sampled from the exhaust line using the probe of the gas analyzer, and the gas-composition was digitally displayed on its screen. Prior calibrated five gas analyzer (AVL DIGAS 444) was used to measure CO, HC and NO_x in the exhaust gas.

In this gas analyzer, measurement of CO_2, CO, and HC emissions was based on the principle of non-diffractive infrared radiation (NDIR) and that of O_2 and NO_x on electrochemical method. CO, CO_2 and O_2 are measured in percentage by volume, while NO_x and HC are

measured as n-hexane equivalent ppm. The five gas analyzer is shown in Fig. 3.10 while its specifications are given in Table 3.7.

Fig. 3.10 AVL DIGAS 444 5 Gas Analyser

Table 3.7 Specifications AVL DIGAS 444 5 Gas Analyser [127]

Measured quality	**Measuring range**	**Resolution**	**Accuracy**
CO	0... 10 % vol	0.01 % vol	< 0.6 % vol: ± 0.03 % vol ≥ 0.6 % vol: ± 5 % of ind. val.
CO_2	0... 20 % vol	0.1 % vol	< 10 % vol: ± 0.5 % vol ≥ 10 % vol: ± 5 % v. M.
HC	0... 20000 ppm vol	≤ 2000: 1 ppm vol, > 2000: 10 ppm vol	< 200 ppm vol: ± 10 ppm vol ≥ 200 ppm vol: ± 5 % of ind. val.
O_2	0... 22 % vol	0.01 % vol	< 2 % vol: ± 0.1 % vol ≥ 2 % vol: ± 5 % v. M.
NO	0... 5000 ppm vol	1 ppm vol	< 500 ppm vol: ± 50 ppm vol ≥ 500 ppm vol: ± 10 % of ind. val.
Engine speed	400... 6000 min^{-1}	1 min^{-1}	± 1 % of ind. val.
Oil temperature	- 30... 125 °C	1 °C	± 4 °C
Lambda	0... 9.999	0.001	Calculation of CO, CO_2, HC, O_2

Prior calibrated smoke meter (AVL DISMOKE 480 BT), as shown in Fig. 3.11 was used tomeasure the smoke level of the exhaust gas as percent opacity. It is a filter-type smoke meterfor measuring the soot content in the exhaust of diesel engines. This smoke meter is basedon light extinction principle. Light is passed in a standard tube containing the sample fromthe engine exhaust. Then, intensity of transmitted light is measured by a photovoltaic deviceat the other end. Specifications of smoke meter are given in Table 3.8.

Fig. 3.11 AVL DISMOKE 480 BT Smoke meter

Table 3.8 Specifications of AVL DISMOKE 480 BT smoke meter [128]

Measuring principle	Extinction measurement	
Operating temperature	+5 … +45°C : Adhering to measurement accuracy +1 … +50°C : Ready for measurement	
Air humidity	Max. 90%, non-condensing	
Measurement chamber heating	100 °C	
Effective length	0.215 m ± 0.002 m	
Maximum exhaust temperature	200 °C	
	Measuring range	Resolution
Turbidity	0–100%	0.1%
Absorption (k value)	0–99.99 1/m	0.01 1/m

3.13 The complete experimental set-up

After integration and adjustment of all the equipments as explained above in this chapter, the experimental set-up was ready for start of experimentation. The pictorial view of the complete experimental set-up is shown in Fig. 3.12 and schematic layout of the same is shown in Fig. 3.13.

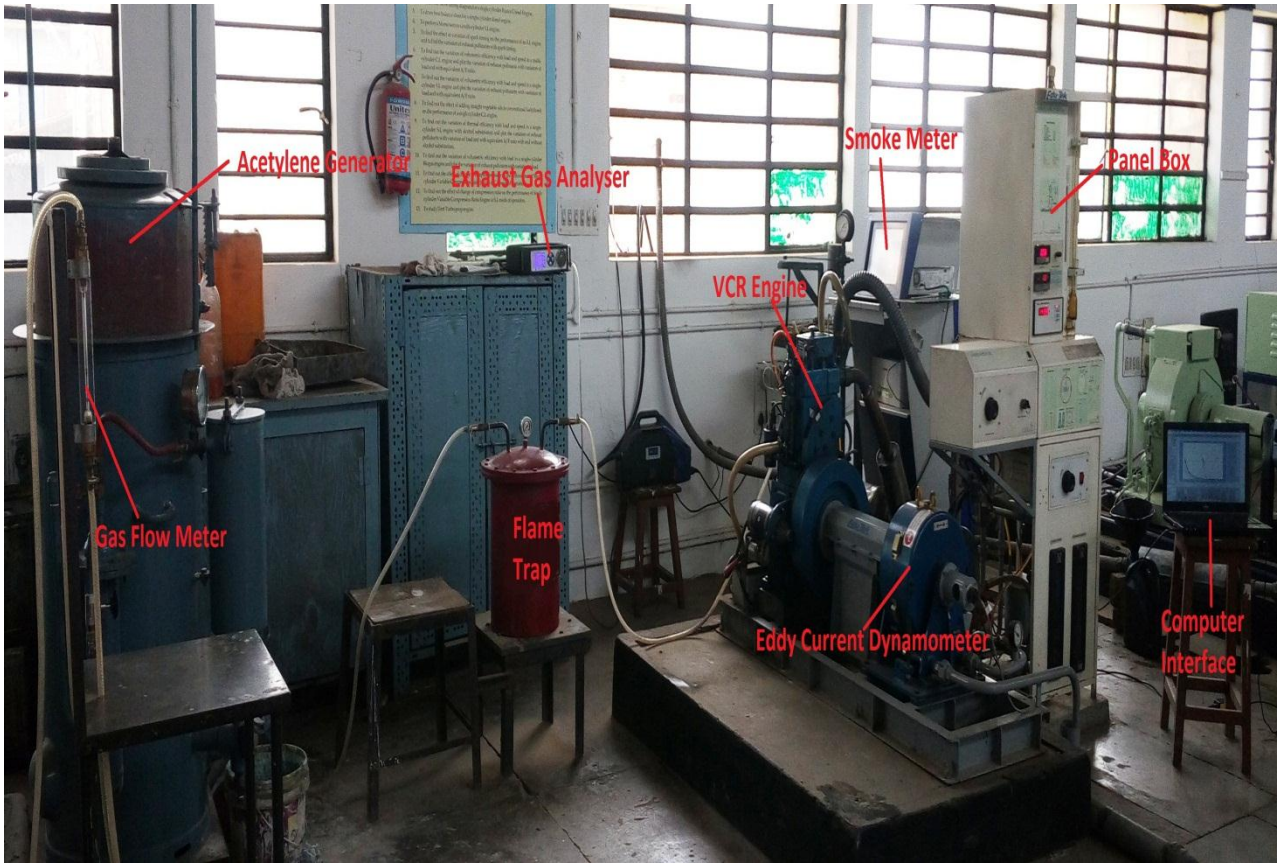

Fig. 3.12 Pictorial view of experimental setup

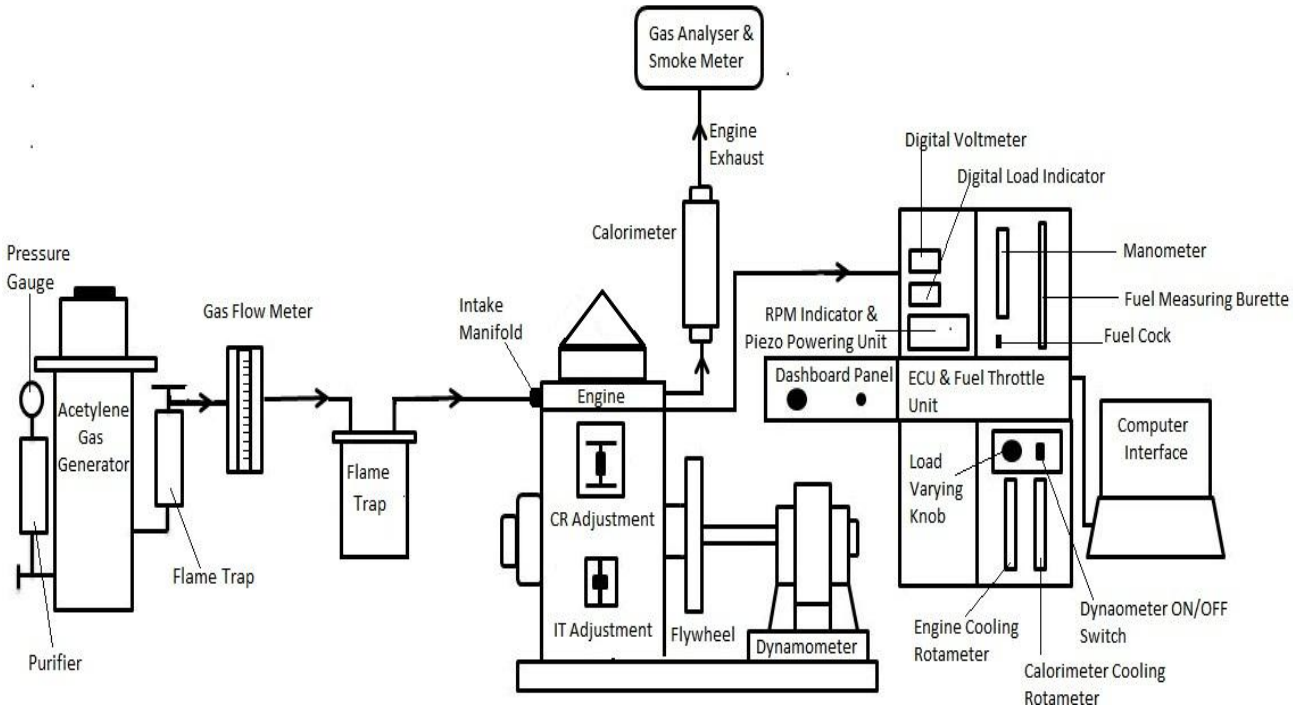

Fig 3.13 Schematic diagram of experimental setup

3.14 Experimental plan and procedure for engine performance, emission analysis

The engine load was changed by varying the current to the eddy current dynamometer and hence, the load of the dynamometer. At each load, after the engine reached the stabilized condition, the performance and emission parameters were recorded. Different physical quantities viz., temperature at various points of the test rig (viz. inlet and outlet of the cooling water, exhaust gas and intake air), consumption rates of diesel, pressure head at manometer, flow rate of cooling water and engine speed were recorded to calculate various performance indicators.

Experiments were carried out at five compression ratios (18, 19, 20, 21 and 22), different injection pressures (180 to 220 bar at the intervals of 10 bar), at four injection timings (18º, 20º, 23º and 25º CA bTDC). For each step of observations for engine performance, exhaust emissions and combustion characteristics readings were taken at 0%, 20%, 40%, 60%, 80% and 100% (3.5 kW) load with the rated engine speed of 1500 rpm for each load.

Phase I

- In the first step, tests were carried out for each set of load as mentioned above for diesel at different compression ratios (18, 19, 20, 21 and 22) at fixed injection

pressure of 210 bar and injection timing of 23° bTDC CA and optimum CR (corresponding to maximum BTE) was found.

- In the second step, tests were carried out at different injection pressures (190, 200, 210 and 220 bar) keeping the compression ratio (optimum CR as found in the previous step) constant and injection timing (23° bTDC) constant so as to find out the optimum injection pressure at these conditions.

- In the third step, tests were carried out at different injection timings (18°, 20°, 23° and 25° bTDC) keeping the compression ratio (optimum CR as found in the 1st step) constant and injection pressure (optimum IP as found in the 2nd step) constant so as to find out the optimum injection timing.

In this way optimum compression ratio, optimum injection pressure and optimum injection timing was obtained for neat diesel which was taken as baseline.

Phase II

- After obtaining the baseline conditions, engine was tested for dual fuel mode (i.e. diesel + acetylene). To find the optimum flow rate of acetylene, acetylene gas was injected at different flow rates (60, 120, 180 and 240 LPH) at optimized conditions of baseline diesel (as obtained at the end of Phase I) and thus, optimum flow rate of acetylene was obtained.

- Then, similar steps as mentioned for the diesel case in Phase I above were followed at different compression ratios (18, 19, 20, 21 and 22), injection pressures (180, 190, 200 and 210 bar) and injection timings (18°, 20°, 23° and 25° bTDC) to find out the optimum compression ratio, optimum injection pressure and optimum injection timing for dual fuel mode at the optimum flow rate of acetylene.

After all the readings were taken, different graphs were plotted under various conditions for performance, emissions and combustion characteristics for neat diesel mode and dual fuel mode. Readings of dual fuel mode were then compared with those of baseline. Then the results were analyzed and conclusions were drawn.

3.15 Calculation of performance parameters

3.15.1 Brake power

Brake power (BP) is given by:

$$BP = (2\times \pi \times N \times W \times R) / (60 \times 1000) \quad (3.2)$$

Where, N is engine speed in rpm, W is load in N and R is dynamometer arm length in m.

3.15.2 Brake Thermal Efficiency

Brake Thermal efficiency (BTE) (η^{th}) is defined as the ratio of useful power (i.e., brake power) to the chemical energy input in the form of fuel(s). BTE is expressed by the following equation:

For diesel mode,

$$BTE = BP \times 3600 \times 100 / (m_d \times CV_d) \quad (3.3)$$

Where, BP is brake power in kW, m_d is mass flow rate of diesel in kg/h, CV_d is calorific value of diesel in kJ/kg.

For dual fuel mode,

$$BTE = BP \times 3600 \times 100 / (m_d \times CV_d + m_a \times CV_a) \quad (3.4)$$

Where, BP is brake power in kW, m_d and m_a are mass flow rates of diesel and acetylene respectively in kg/h, CV_d and CV_a are calorific value of diesel and acetylene respectively in kJ/kg.

3.15.3 Brake Specific Energy Consumption (BSEC)

BSEC, for diesel mode, is given by:

$$BSEC = m_d \times CV_d / BP \quad (3.5)$$

BSEC, for dual fuel mode, is given by:

$$BSEC = (m_d \times CV_d + mf_a \times CV_a) / BP \quad (3.6)$$

3.15.4 Temperature measurement

RTD 100 type temperature sensor with output 4-20mA, supply 24VDC and range: 0-100° C and thermocouples (type K), output 4-20 mA, supply 24 VDC, range: 0-1200° C were used to measure the temperature of water and exhaust gas in the experimental setup.

3.15.5 Calculation of Net Heat Release rate (NHRR)

The calculation of net heat release rate for both diesel and dual fuel run engines needs the instantaneous P–V data recorded during experiments. The crank angle encoder connected to the engine shaft detects each degree (1°) rotation of the crank for each cycle. Hence, for a particular cycle, a total of 720 data for both cylinder pressure and volume was recorded at each load. Each heat release calculation at a particular load was made by considering 10 cycles. The equation used for the net heat release rate (NHRR) is obtained from the first law analysis [129, 130] by implementing the rate of pressure rise and rate of volume change, which is given by:

$$\frac{dQ_n}{d\theta} = \left(\gamma \times P \times \frac{dV}{d\theta}\right) / (\gamma - 1) + \left(V \times \frac{dP}{d\theta}\right) / (\gamma - 1) \quad (3.7)$$

Where, $\frac{dQ_n}{d\theta}$, γ , P and V are net heat release rate (J/°CA), ratio of specific heats, instantaneous cylinder pressure (N/m^2) and cylinder volume (m^3) respectively. The value of γ is considered as 1.35 as taken by some researchers [129, 130] in their respective works.

3.15.6 Calculation of rate of pressure rise (RPR)

The data acquisition device (DAD) can record cylinder pressure variation with each degree of crank angle change. The values of change of pressure per unit change of crank angle $\frac{dP}{d\theta}$ were evaluated by using the first order finite differential equation with fourth order accuracy [131] as given by:

$$\frac{dP}{d\theta} = \{(P_{n-2}) - 8(P_{n-1}) + 8(P_{n+1}) - (P_{n+2})\}/\{12(\Delta\theta)\} \quad (3.8)$$

3.16 Assumptions and limitations

In the current research, the following assumptions were made / limitations handled / challenges encountered:

(a) Steady-state conditions are assumed for all observations.

(b) Heat transfers and pressure drops in pipings are ignored.
(c) Ideal gas principles have been applied to air and exhaust gas treatment.
(d) Lower heating value (LHV) of the fuel is used for calculations.
(e) Emission reduction techniques like EGR were kept out of scope of this research.
(f) Due to set-up limitations, actual in-cylinder temperatures could not be verified against those obtained from simulations.

3.17 Challenges faced during research work

(a) Due to excessive vibrations, Allen bolts (used for change of CR by tilting the cylinder block) of VCR engine sheared thrice. Whenever this happened, the entire engine was to be dismantled and repaired as the broken bold used to get stuck in the groove of the tilting mechanism. Also, many readings had to be taken again whenever this happened.
(b) Oil started coming out from the cylinder block due to damaged gasket. Cylinder block was opened, gasket was replaced and hence, the problem got fixed.
(c) When the flow rate of acetylene was increased beyond 240 LPH, the rpm of the constant speed engine rated at 1500 rpm started rising and went upto around 1600 rpm and engine stopped suddenly. Due to this it was decided not to go beyond the flow rate of 240 LPH of acetylene.
(d) The fuel pump broke down once while changing the injection timing and the same was fixed.
(e) Procurement of acetylene generator took more than a year due to quite strict regulations for manufacturing / production of acetylene generators in India. Further, since the identified manufacturer did not usually make the desired type of acetylene generator (small capacity, constant pressure, constant flow type), it was needed to have extended sittings with the supplier to design the desired generator. Also, before selling the generator, the supplier was required to get certain inspections done by Government of India officials (Factory Inspector, Fire and Safety officials, Explosives Controller, etc.). Hence, procurement of acetylene generator was quite a challenge.
(f) The electronic system of the 5 gas analyzer went bad mid-way the experimentation and the same needed to be repaired. Due to this, many sets of experimental readings with doubt were repeated.

CHAPTER 4

RESULTS AND DISCUSSIONS

4.1 Introduction

Before carrying out detailed experimentation on acetylene, verification of engine parameters was done for neat diesel operation to find optimum compression ratio, injection pressure and injection timing for proper comparison as explained in Chapter 3. Acetylene flow rate was optimized for the best performance of the engine at the optimized CR, IP and IT for neat diesel. It was found that acetylene substitution at 120 LPH was optimum because at lower than 120 LPH flow rate of acetylene substitution was not giving significant improvement in performance and above 120 LPH flow rate, engine started knocking and it was difficult to run the engine at higher loads with acetylene above 120 LPH flow rate. Once it was decided that 120 LPH is the optimum flow rate of acetylene, optimum CR, IP and IT were determined for dual fuel mode using the procedure mentioned in Chapter 3. It was found that the optimized flow rate of acetylene, compression ratio, injection pressure and injection timing of the acetylene operated (dual fuel mode) CI engine were 120 LPH, 21, 200 bar and 23^{o} bTDC respectively.

4.2 Optimization of engine parameters for neat diesel

The performance parameters were taken for different compression ratios, injection pressures and injection timings. Experimental data show that the modified Kirloskar TV1 VCR engine, which was used for this research, had 20:1, 210 bar and 23^{o} bTDC as optimum CR, optimum IP and optimum IT respectively for neat diesel. At these conditions, engine had maximum brake thermal efficiency and lowest brake specific energy consumption.

4.2.1 Effect of compression ratio on engine performance for neat diesel

4.2.1.1 Brake Thermal Efficiency (BTE)

Fig. 4.1 shows the variation of brake thermal efficiency with load at different compression ratios for neat diesel. As the CR was increased, the BTE improved till a certain CR (20) and beyond that it decreased.

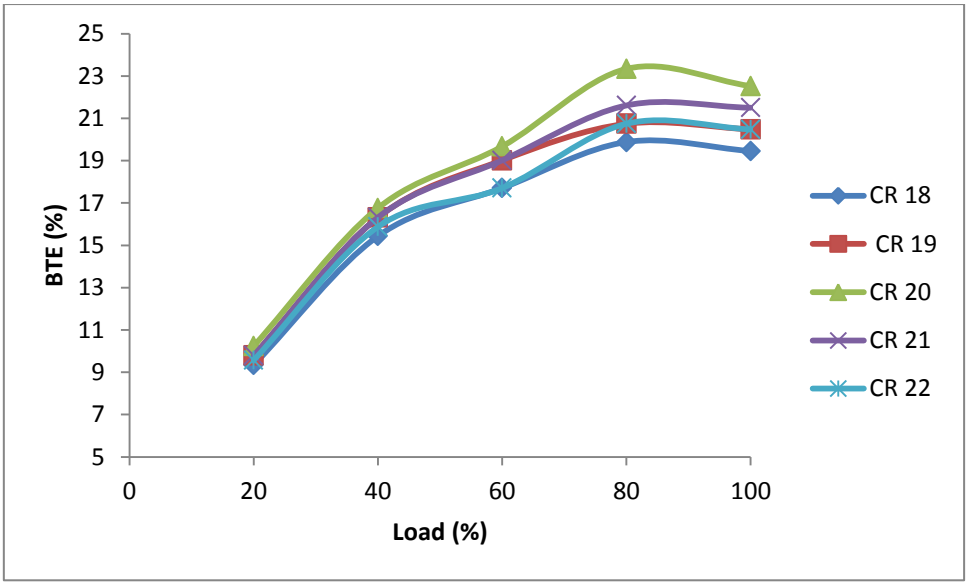

Fig. 4.1 Variation of BTE with load at different compression ratios for neat diesel

Hence, the highest brake thermal efficiency was obtained at CR of 20 in diesel mode. The in-cylinder pressure and temperature increased with increase in CR, and resulted in increase in the burning rate and thus, thermal efficiency. While on further increasing CR, thermal efficiency decreased due to increase in surface to volume ratio of the combustion chamber at TDC which increased the heat transfer rate and heat loss. At 80% load (where the BTE was highest for all CRs), the BTE in diesel mode was found to be 19.88%, 20.74%, 23.34%, 21.61% and 20.74% for CR 18, 19, 20, 21 and 22 respectively.

4.2.1.2 Brake Specific Energy Consumption (BSEC)

BSFC cannot be considered a reliable parameter if the calorific value and densities of various test fuels vary considerably. Hence, brake specific energy consumption proves to be a more reliable assessment method in the case of dual fuel mode. Brake specific energy consumption is the product of BSFC and calorific value of the fuel. It means how efficiently energy is obtained from the given fuel. BSEC decreases with the increase in brake power. This trend was maintained at all compression ratios for neat diesel operation. The BSECs obtained at 80% load were 17965.68, 17217.11, 15304.1, 16528.43 and 17217.11kJ/kWh for CR 18, 19, 20, 21 and 22 respectively. As seen from Fig. 4.2 BSEC decreased with increase in CR up to 20, beyond which it increased with increase in CR. The lowest BSEC was obtained at CR 20 in case of neat diesel operation.

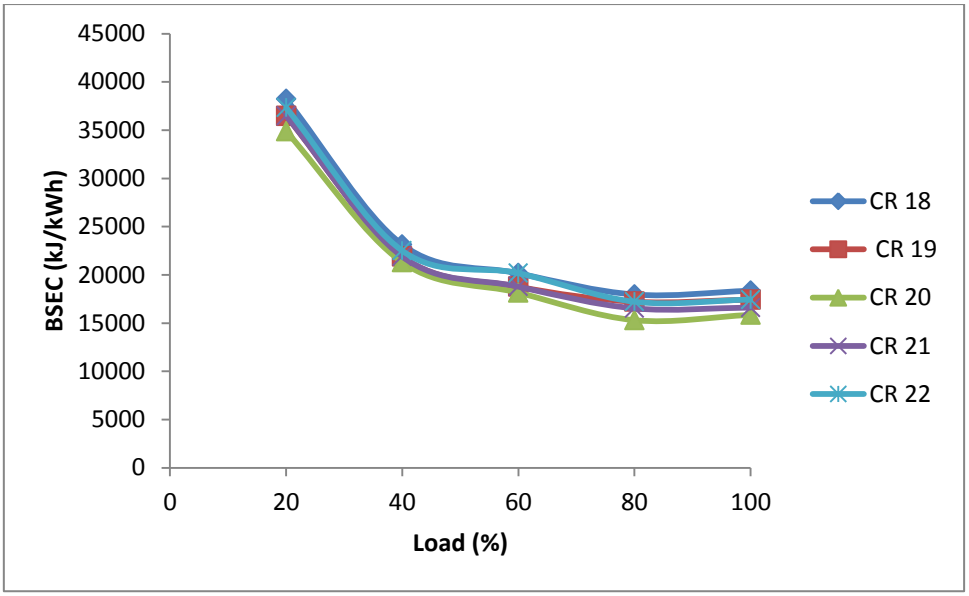

Fig. 4.2 Variation of BSEC with load at different compression ratios for neat diesel

4.2.1.3 Exhaust Gas Temperature (EGT)

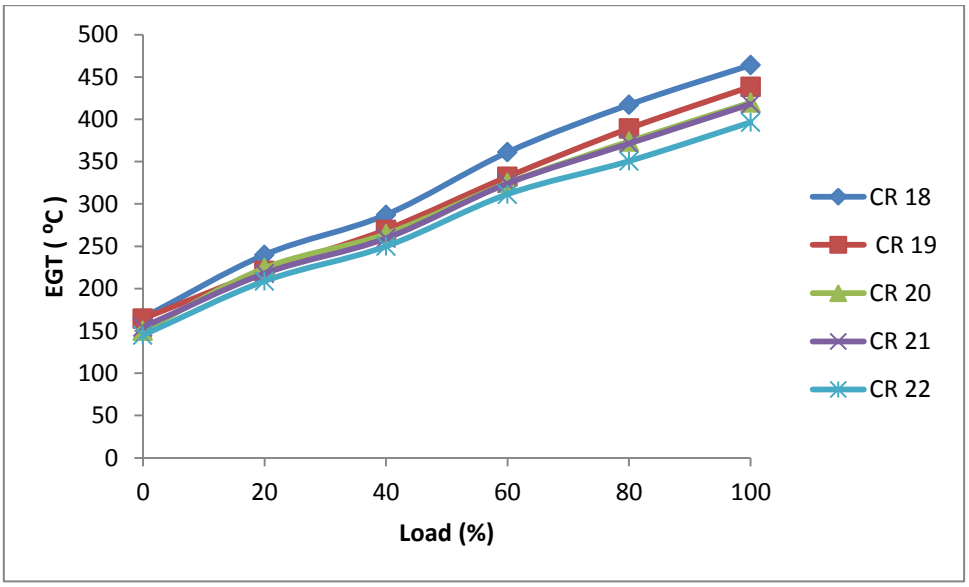

Fig. 4.3 Variation of EGT with load at different compression ratios for neat diesel

As can be seen in Fig. 4.3, EGT increased with increase in load for all compression ratios. EGT decreased on increasing CR from 18 to 22. Decrease in EGT on increasing CR could be due to increase in increased flame propagation speed and also because of the fact that the time interval for complete combustion got reduced, at increased CR, which reduced EGT.

4.2.2 Effect of injection pressure on engine performance for neat diesel

4.2.2.1 Brake Thermal Efficiency (BTE)

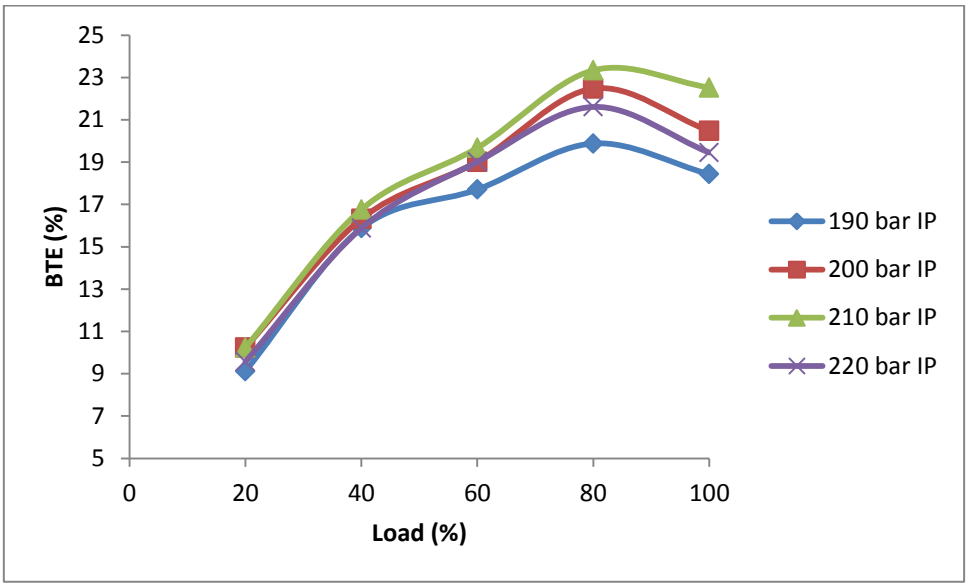

Fig. 4.4 Variation of BTE with load at different injection pressures for neat diesel

Fig. 4.4 shows the variation of BTE with load at different injection pressures for neat diesel. BTE increased with increase in injection pressure from 190 to 210 bar beyond which it decreased. The increase in BTE might be due to fine spray, better atomization of diesel and better combustion at higher IP [33]. The highest BTE of 23.34% was obtained at IP of 210 bar in comparison to 19.88%, 22.47% and 21.61% at 190, 200 and 220 bar respectively. When the IP was too high (220 bar), ignition delay period became shorter which might have resulted in decrease in homogeneous mixing of air and fuel and hence, combustion efficiency decreased. Also, when the IP was too high, the fuel droplets became extremely fine which reduced the depth of penetration of fuel particles. This resulted in poor combustion leading to lesser BTE.

4.2.2.2 Brake Specific Energy Consumption (BSEC)

Fig. 4.5 shows the variation of BSEC with load at different injection pressures for neat diesel. BSEC decreased with increase in injection pressure from 190 to 210 bar beyond which it increased. The lowest BSEC of 15304.1 kJ/kWh was obtained at IP of 210 bar in comparison to 17965.68, 15892.72 and 16528.43 kJ/kWh at 190, 200 and 220 bar respectively. Increase in BSEC at 220 bar was due to poor combustion as when the IP was too high (220 bar), ignition delay period became shorter which resulted in decrease in homogeneous mixing of

air and fuel and hence, combustion efficiency decreased. Also, when the IP was too high, the fuel droplets became extremely fine which reduced the depth of penetration of fuel particles leading to incomplete combustion.

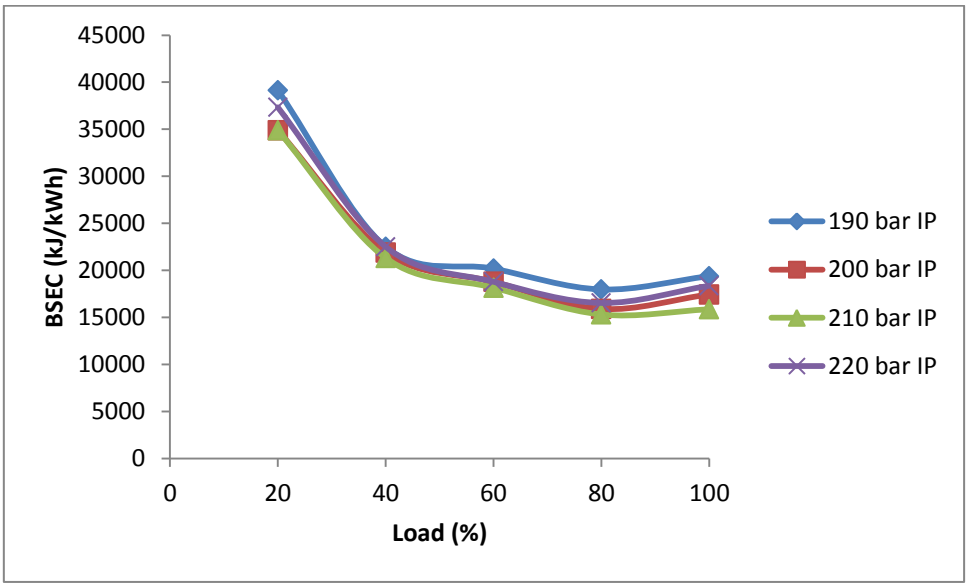

Fig. 4.5 Variation of BSEC with load at different injection pressures for neat diesel

4.2.2.3 Exhaust Gas Temperature (EGT)

The EGT increased with increase in load for all IPs as shown in Fig. 4.6.EGT decreased with increase in injection pressure from 190 to 210 bar. As the IP increased the droplet size became finer resulting in better fuel air mixing and smooth and faster combustion resulting in lower EGT. The lowest EGT was obtained at 210 bar in comparison to other injection pressures.

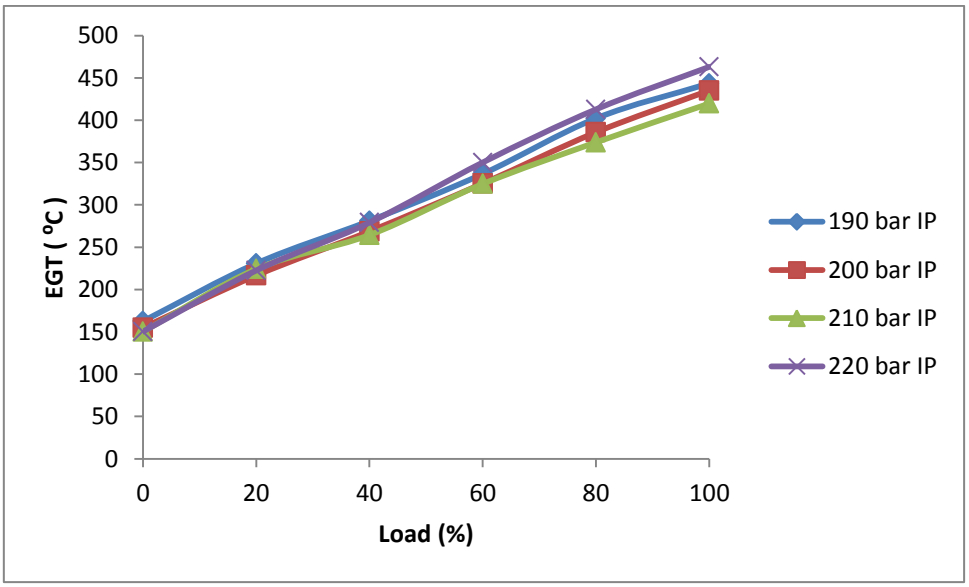

Fig. 4.6 Variation of EGT with load at different injection pressures for neat diesel

4.2.3 Effect of injection timing on engine performance for neat diesel

4.2.3.1 Brake Thermal Efficiency (BTE)

Fig. 4.7 shows the variation of BTE with load at different ITs for neat diesel. BTE increased when the IT was advanced from 18^0 to 23^0 bTDC. The highest BTE of 23.34% was obtained at IT of 23° bTDC in comparison to 19.94%, 21.6% and 21.98% at IT of 18°, 20° and 25° bTDC respectively. The advancement of IT from 18° to 23° bTDC resulted in injection of diesel earlier into the combustion chamber, therefore giving sufficient time for the diesel to form a homogeneous mixture with air resulting in proper combustion and higher BTE. Hence, it was found that IT of 23° bTDC was the optimum giving maximum BTE.

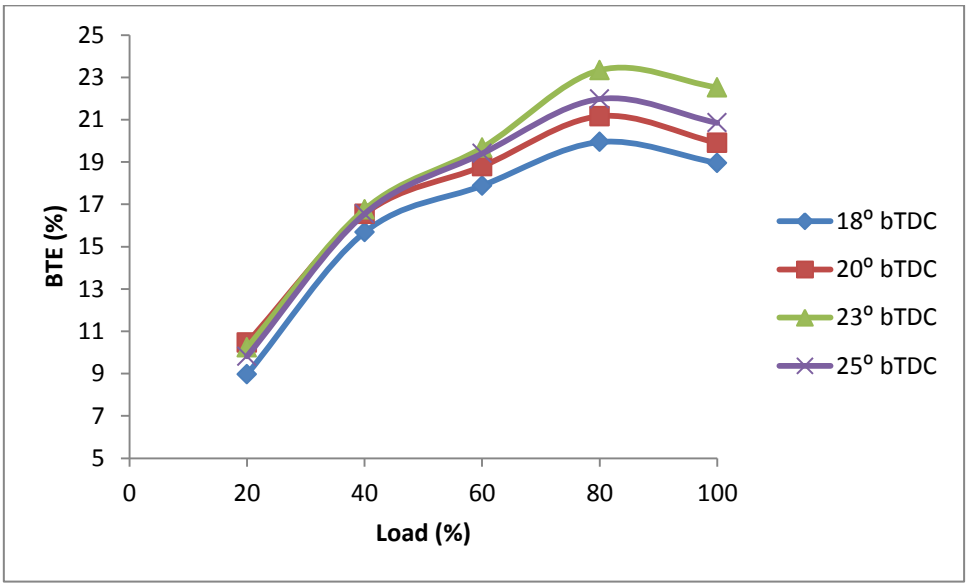

Fig. 4.7 Variation of BTE with load at different injection timings for neat diesel

4.2.3.2 Brake Specific Energy Consumption (BSEC)

Fig. 4.8 shows the variation of BSEC with load at different injection timings for neat diesel. The lowest BSEC of 15304.1 kJ/kWh was obtained at IT of 23° bTDC in comparison to BSEC of 17910.09, 16876.82 and 16251.75 kJ/kWh at IT of 18°, 20° and 25° bTDC. BSEC decreased with advancing IT from 18° to 23° bTDC because it resulted in injection of diesel earlier into the combustion chamber, therefore giving sufficient time for the diesel to form a homogeneous mixture with air resulting in proper combustion and higher BTE. Hence, it was found that 23° bTDC was the optimum IT giving minimum BSEC. Further advancing of IT laid down to reduction in BTE, probably due to achieving of peak pressure before the piston reaches the TDC.

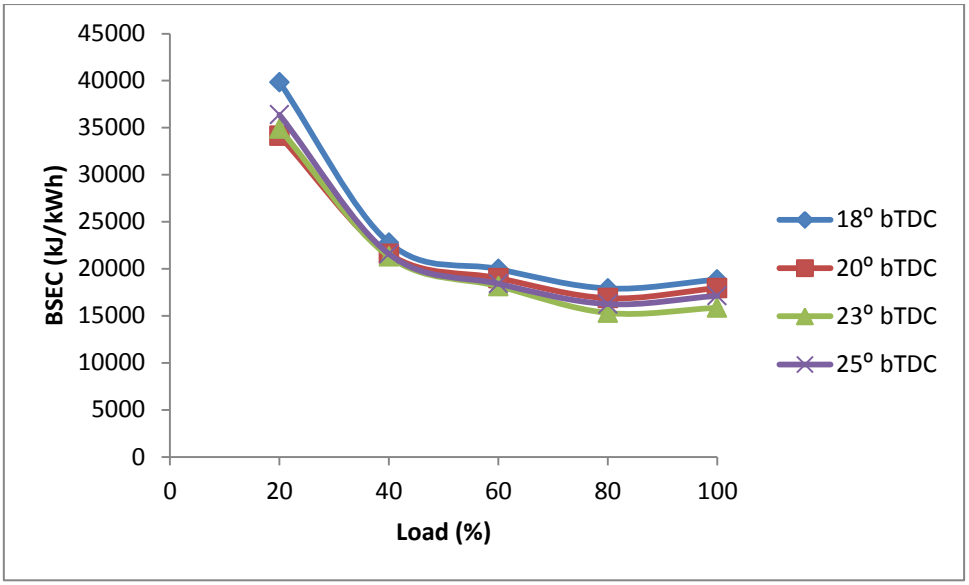

Fig. 4.8 Variation of BSEC with load at different injection timings for neat diesel

4.2.3.3 Exhaust Gas Temperature (EGT)

Variation of EGT with load at different IT is depicted in Fig. 4.9. EGT increased with increase in load at all ITs. It was found that the variation in EGT was not significant with change in the injection timing at low load conditions while at higher load the lowest EGT was obtained at 23° bTDC IT as compared to those at IT of 18°, 20° and 25° bTDC though the difference was found to be negligible.

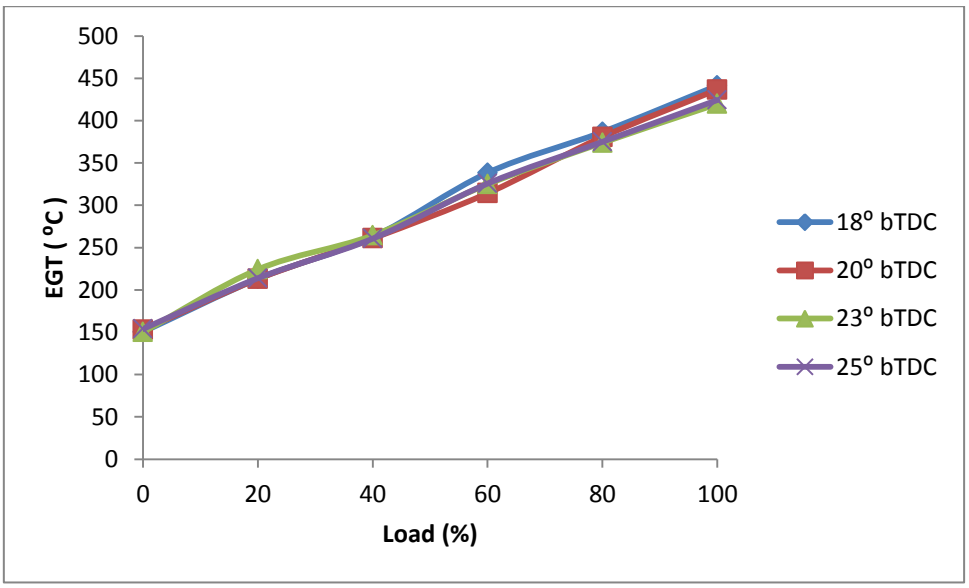

Fig. 4.9 Variation of EGT with load at different injection timings for neat diesel

4.3 Optimization of flow rate of acetylene

The optimized compression ratio (CR), injection pressure (IP) and injection timing (IT) for neat diesel was found to be 20, 210 bar and 23° bTDC respectively. After the optimization of compression ratio, injection pressure and injection timing for neat diesel, the flow rate of acetylene (in dual fuel mode) was optimized at the above conditions (as baseline) and the following results were obtained.

4.3.1 Effect of flow rate of acetylene on engine performance

4.3.1.1 Brake Thermal Efficiency (BTE)

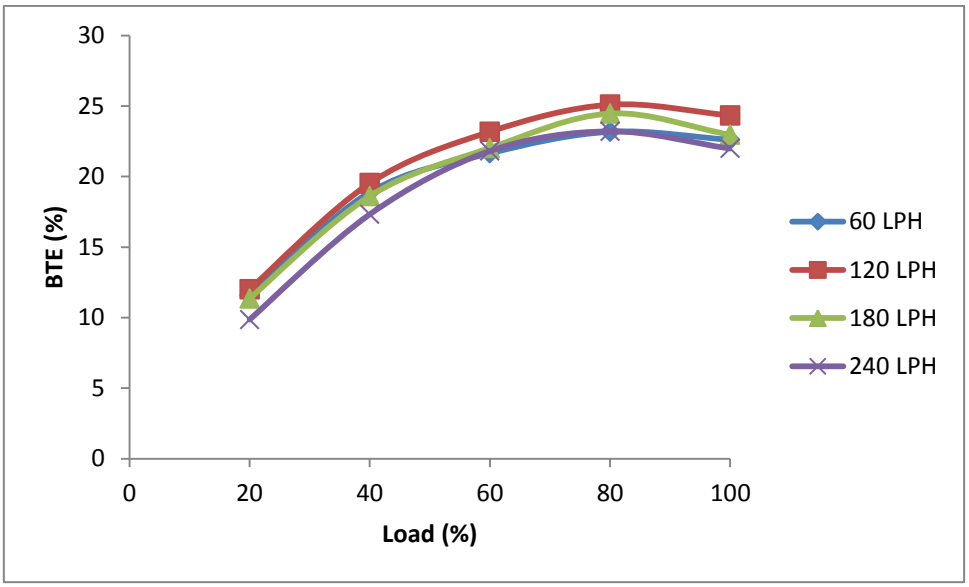

Fig. 4.10 Variation of BTE with load in dual fuel mode at different flow rates of acetylene

The variation of brake thermal efficiency against load for diesel-acetylene dual fuel mode with different flow rates is shown in Fig. 4.10. It was observed that as flow rate of acetylene increased from 60 LPH to 120 LPH, there was an increase in BTE at all loads. However, on further increase in flow rate of acetylene to 180 and 240 LPH, BTE decreased due to reduced availability of oxygen, However at 240 LPH flow rate of acetylene, the rpm of engine suddenly increased due to excessive amount of acetylene the governor could not control the speed by decreasing the quantity of diesel hence the engine had to be shut down. Hence, highest BTE was achieved at 120 LPH flow rate of acetylene which was therefore considered as the optimum flow rate of acetylene.

It was observed that 120 LPH flow rate of acetylene gave maximum thermal efficiency at around 80% load. The highest BTE of 25.09% was obtained at the flow rate of 120 LPH at

80% load compared to those of 23.17%, 24.46% and 23.20% at the flow rates of 60, 180 and 240 LPH respectively at 80% load.

4.3.1.2 Brake Specific Energy Consumption (BSEC)

Variation of BSEC with load in dual fuel mode at different flow rates of acetylene is shown in Fig. 4.11. While using acetylene at different flow rates of 60, 120, 180 and 240 LPH, BSEC was found to be 15412.70, 14233.99, 14599.18 and 14756.62 kJ/kWh respectively at 80% load in each case. The lowest BSEC was obtained at the flow rate of 120 LPH in comparison to those at other flow rates.

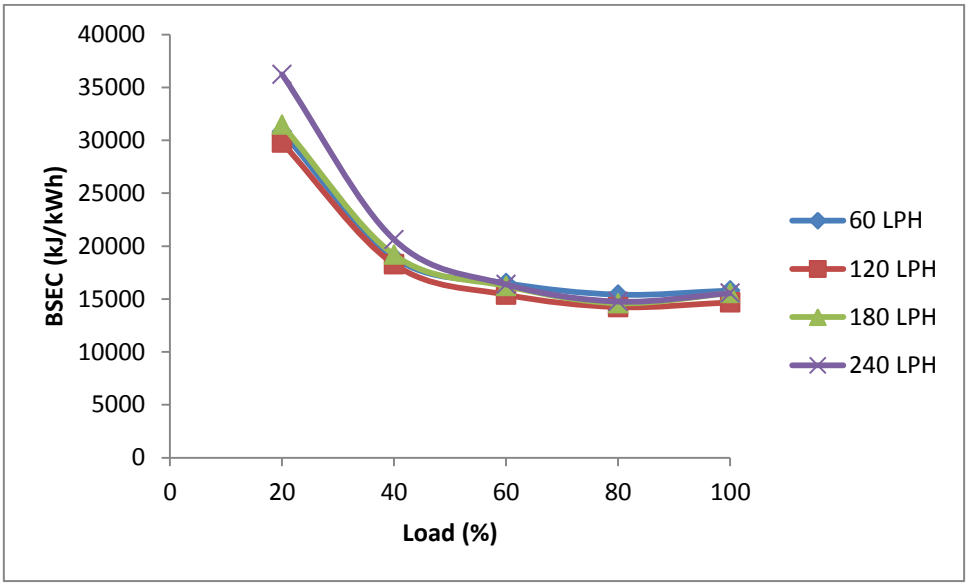

Fig. 4.11 Variation of BSEC with load in dual fuel mode at different flow rates of acetylene.

4.3.1.3 Exhaust Gas Temperature (EGT)

EGT increased with increase in load in all cases as shown in Fig. 4.12. EGT reduced when the flow rate of acetylene was increased from 60 LPH to 120 LPH beyond which EGT increased as the flow rate was increased. The highest EGT was found at the flow rate of 60 LPH followed by 180 LPH while the lowest EGT was obtained at 120 LPH as depicted in Fig. 4.23. However, the difference in EGT was considered insignificant as the variation was less 20 ºC in most cases.

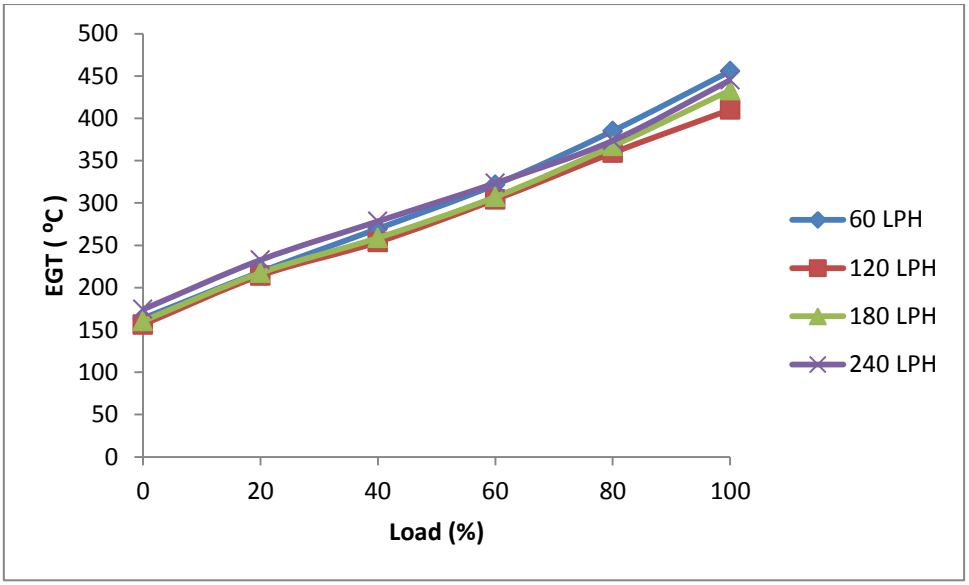

Fig. 4.12 Variation of EGT with load in dual fuel mode at different flow rates of acetylene

4.3.2 Effect of flow rate of acetylene on exhaust emissions

4.3.2.1 Carbon monoxide (CO)

As can be seen in Fig. 4.13, lowest CO emission at 80% load and full load was obtained at the acetylene flow rate of 120 LPH in comparison to other flow rates. Since, the engines are usually run at 80% load most of the times, 120 LPH was considered to be the best flow rate of acetylene from CO emission point of view also.

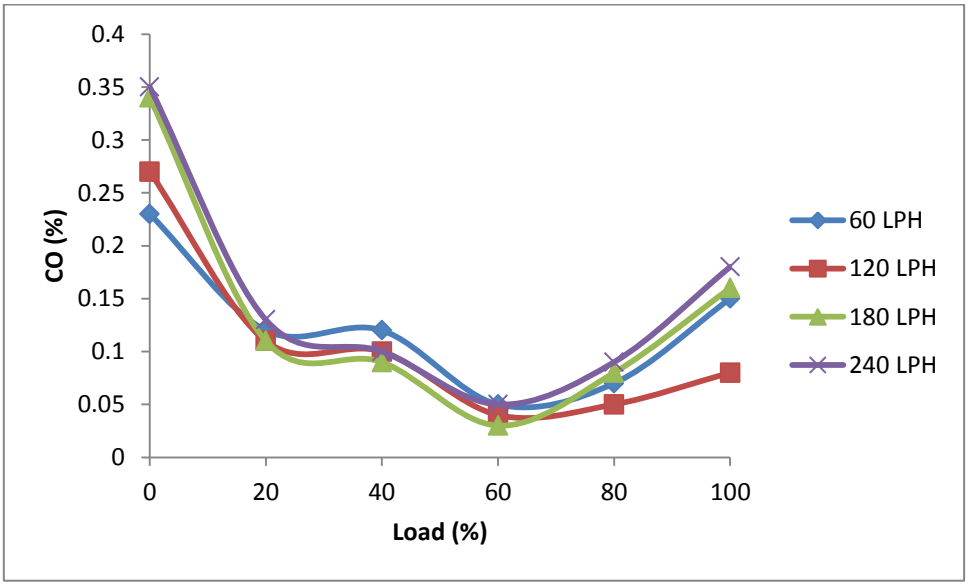

Fig. 4.13 Variation of CO with load in dual fuel mode at different flow rates of acetylene

4.3.2.2 Hydrocarbon (HC)

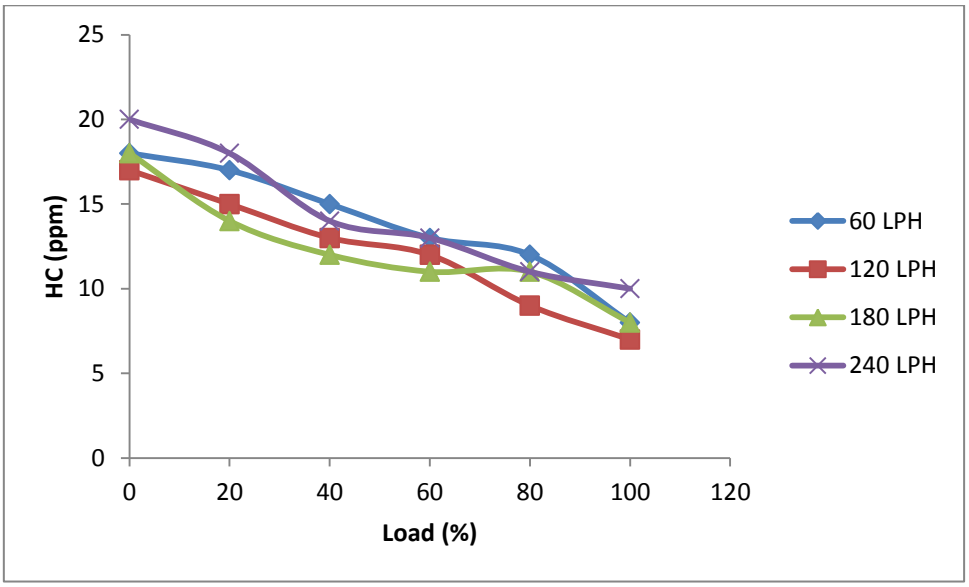

Fig. 4.14 Variation of HC with load in dual fuel mode at different flow rates of acetylene

From Fig. 4.14, it is seen that HC emission was unpredictable with change in flow rate of acetylene. However, HC emission reduced with increase in load for all cases.

4.3.2.3 Oxides of Nitrogen (NO_x)

From Fig. 4.15, it is evident that NO_x emission increased with increase in flow rate of acetylene. Maximum NO_x emission was observed at 40% load for all flow rates of acetylene. The increase in NO_x emission with increase in flow rate of acetylene was might be due to the fact that, with increase in acetylene flow rate, the amount of fuel (diesel + acetylene) in the cylinder increased substantially resulting in release of much higher amount of heat and thus, increasing in-cylinder temperature substantially, which is the main cause of NO_x formation.

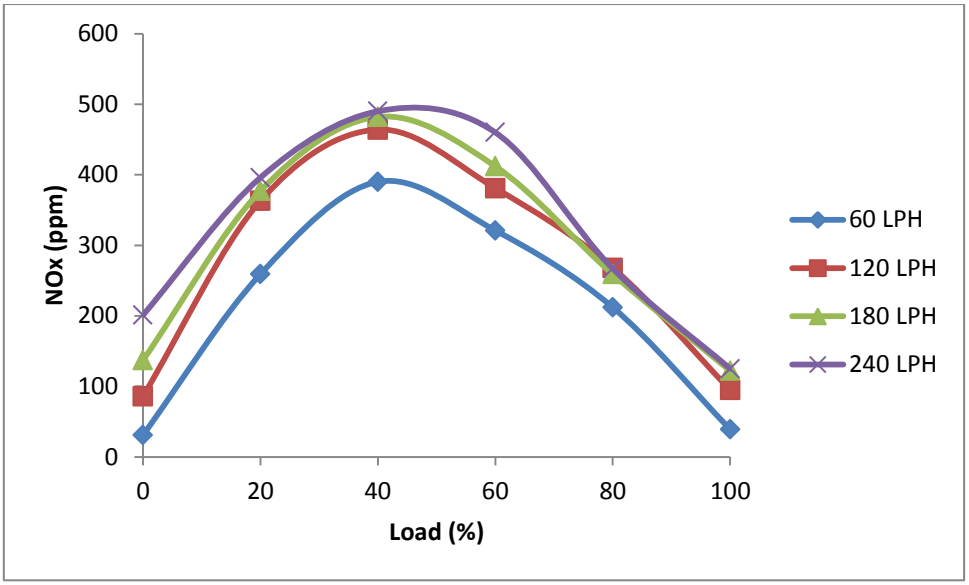

Fig. 4.15 Variation of NO_x with load in dual fuel mode at different flow rates of acetylene

4.3.2.4 Smoke

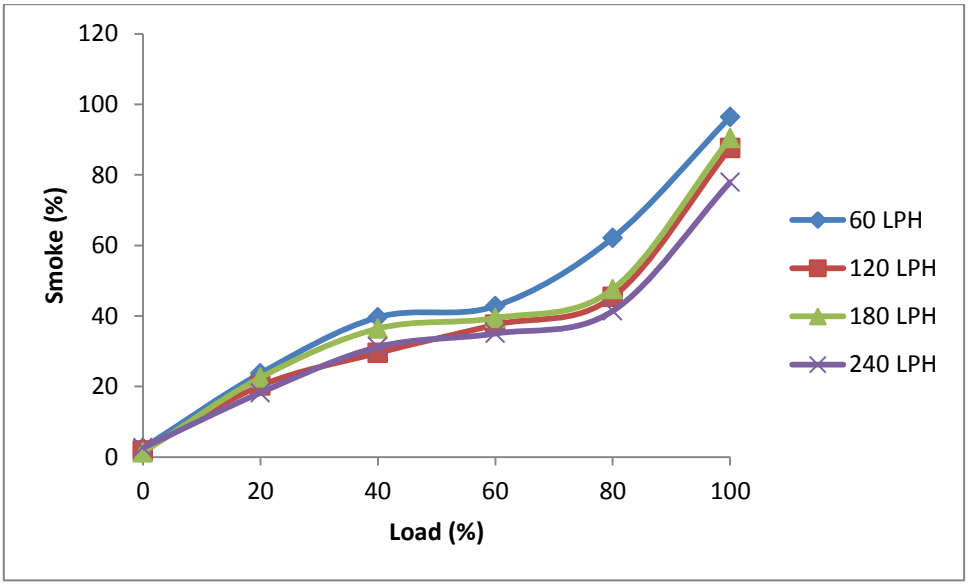

Fig. 4.16 Variation of smoke density (opacity) with load in dual fuel mode at different flow rates of acetylene.

Smoke formation is much higher for diesel fuel burning as compared to acetylene burning since it contains much lesser carbon. The inducted acetylene forms a homogeneous mixture that burns more rapidly and the overall mixture contains less carbon from which smoke can be formed. Hence, as the flow rate of acetylene was increased, the smoke density percentage got reduced as shown in Fig. 4.16. Smoke density increased with increase of load for all cases

since with increased load, more diesel was burnt while flow rate of acetylene was kept constant.

Based on the engine performance with different flow rates of acetylene, it was observed that 120 LPH was the optimum flow rate of acetylene in dual fuel mode.

4.4 Optimization of engine performance parameters for diesel-acetylene dual fuel mode and their comparison with neat diesel (baseline)

4.4.1 Effect of compression ratio on engine performance for dual fuel mode

4.4.1.1 Brake Thermal Efficiency (BTE)

Variation of BTE in the dual mode at different compression ratios is shown in Fig. 4.17. The BTE at 80% load was 21.8%, 22.53%, 25.09%, 25.72% and 24.46% for CRs of 18, 19, 20, 21 and 22 respectively. Hence, the highest BTE of 25.72% was obtained in dual fuel mode at CR of 21 which was 10.2% higher than the BTE of baseline diesel. The BTE of the engine run on dual fuel mode was more than diesel mode because of the high flame speed of acetylene leading to higher combustion rate. As the CR is increased, the BTE improves and further it tends to decrease.

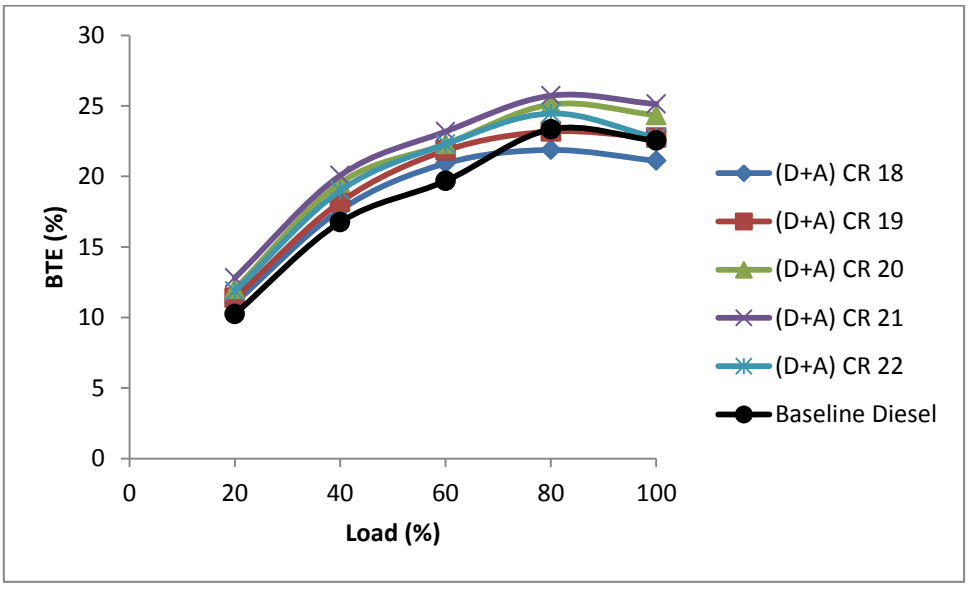

Fig. 4.17 Variation of BTE with load in dual fuel mode at different compression ratios

4.4.1.2 Brake Specific Energy Consumption (BSEC)

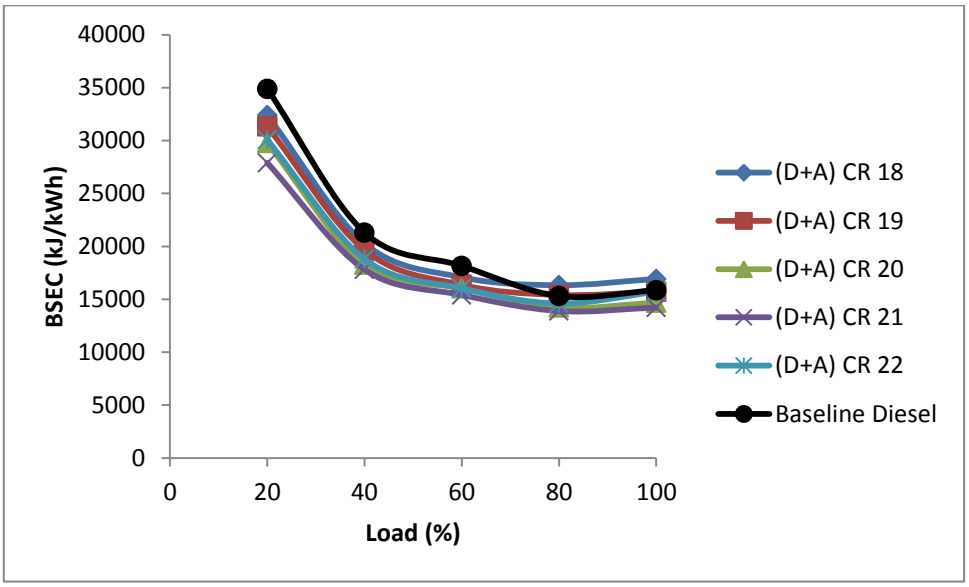

Fig. 4.18 Variation of BSEC with load in dual fuel mode at different compression ratios

Fig. 4.18 shows the variation of BSEC with load for different compression ratios. BSEC at 80% load in dual fuel mode was 16329.38, 15410.12, 14233.99, 13886.76 and 14602.27 kJ/kWh for CR 18, 19, 20, 21 and 22 respectively. Lowest BSEC was obtained at CR 21 in dual fuel mode. BSEC in case of baseline diesel was 15304.09 kJ/kWh which was 9.3% higher than BSEC in dual fuel mode at CR of 21. BSEC in case of dual fuel mode was lower than that in diesel mode due to higher conversion of acetylene gas into work.

4.4.1.3 Exhaust Gas Temperature (EGT)

As seen from Fig. 4.19, EGT increased with increase in load. Maximum EGT in dual fuel mode was 433.3° C, 424.3° C, 410.2° C, 402.6° C and 382.5° C at CRs of 18, 19, 20, 21 and 22 respectively while in case of baseline diesel it was 419.7. EGT decreased on increasing CR in dual fuel mode since the burning velocity increased on increasing CR and the duration for combustion got reduced which resulted in reduced EGT. The EGT in case of dual fuel mode was lower than diesel mode because of the higher flame speed of acetylene and advancement in the heat release rate in case of dual fuel mode. Reduction in EGT in dual fuel mode could also be due to higher thermal conductivity of gases due to which heat loss from the gas to the wall increased, leading to higher losses and lower EGT [132].

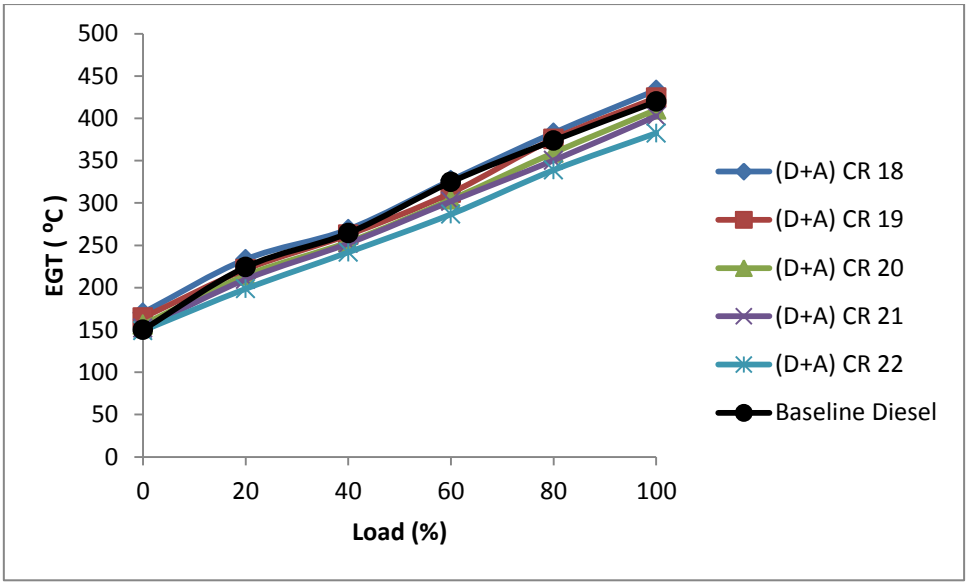

Fig. 4.19 Variation of EGT with load in dual fuel mode at different compression ratios

4.4.2 Effect of compression ratio on exhaust emission for dual fuel mode

4.4.2.1 Carbon monoxide (CO)

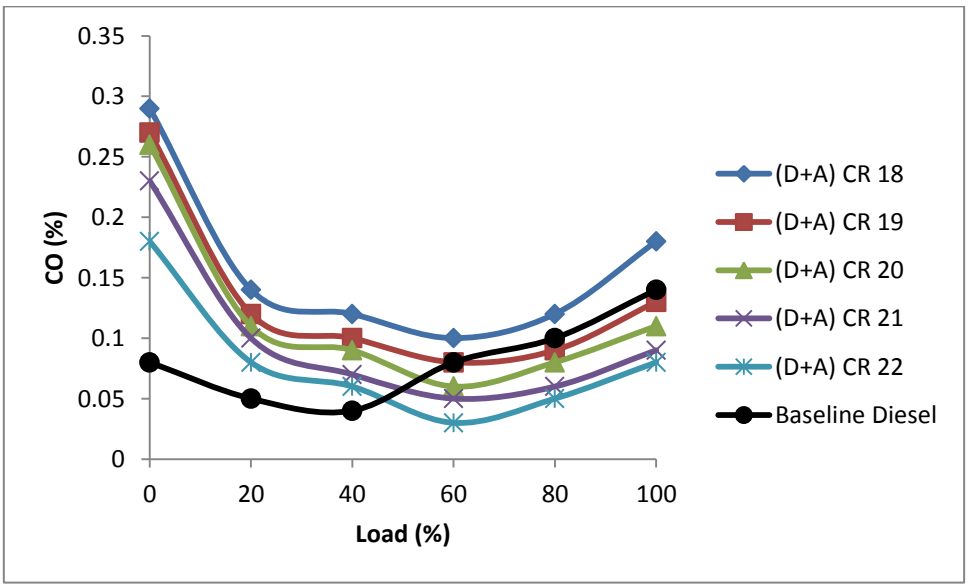

Fig. 4.20 Variation of CO with load in dual fuel mode at different compression ratios

Variation of CO emission in dual fuel mode at different CRs is shown in Fig. 4.20. CO emission decreased with increase in CR in case of dual fuel mode due to better combustion and higher temperature at higher CR. CO emission above 60% load was lower at CR 20, 21 and 22 in case of dual fuel mode as compared to the baseline diesel mode. At higher loads due to high temperature and pressure complete burning of fuel took place which led to lower CO emission in comparison to emission at low loads in dual fuel mode. CO emission in dual

fuel mode at full load for CR 18 was 28.5% higher than baseline diesel while for CR 19, 20, 21 and 22 it was 7.1%, 21.4%, 35.7% and 42.8% lower than baseline diesel respectively.

4.4.2.2 Hydrocarbon (HC)

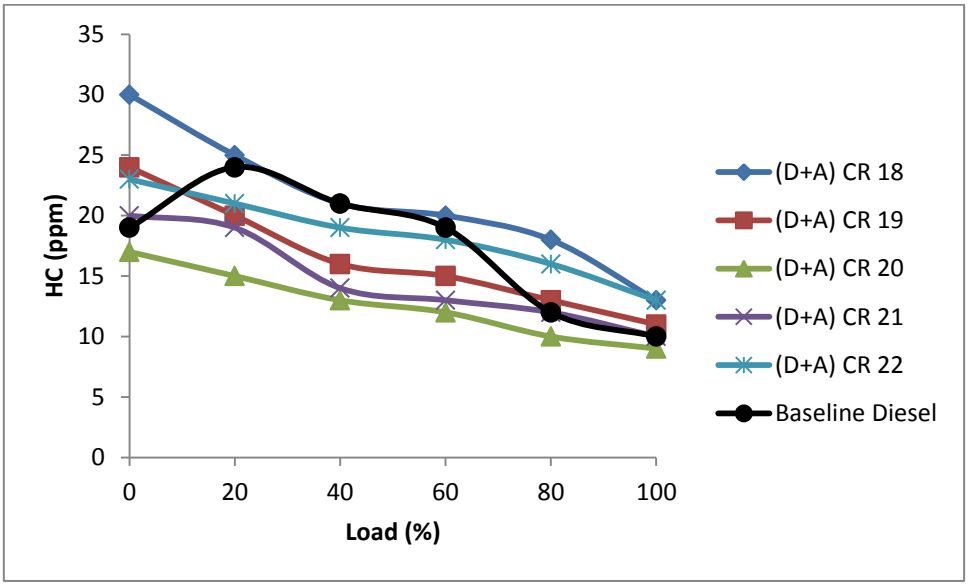

Fig. 4.21 Variation of HC with load in dual fuel mode at different compression ratios

Variation of HC emission in dual fuel mode at different CR is shown in Fig. 4.21. In case of dual fuel mode, HC emission decreased with load at all CRs. HC decreased with increase in CR up to CR 20 after which it increased as the CR increased. The minimum HC emission in case of dual fuel mode was obtained at CR 20 which was 10.5%, 37.5%, 38.1%, 31.6%, 16.7% and 10% lower than baseline diesel for 0%, 20%, 40%, 60%, 80% and 100% load respectively. This was due to the complete combustion in case of dual fuel mode due to wide ignition limit, higher flame velocity of acetylene and higher energy content which resulted in lower HC emission.

4.4.2.3 Oxides of Nitrogen (NO_x)

Fig. 4.22 shows the variation of NO_x emission with load at different CRs for dual fuel mode. NO_x emission increased with increase in CR in dual fuel mode due to high in-cylinder temperature at higher CR which increased NO_x emission. NO_x emission was higher in dual fuel mode compared to diesel mode may be because in dual fuel mode the combustion chamber temperature was higher than diesel due to higher calorific value of acetylene gas compared to that of diesel. Also, induction of acetylene facilitated quicker formation of more homogeneous air-fuel mixture in cylinder, resulting in complete combustion, thus raising in-

cylinder temperature, which is the main cause of NO_x formation. Maximum NO_x was obtained at 40% load in dual fuel mode while in case of diesel mode maximum NO_x was obtained at 20% load. The NO_x emission in case of baseline diesel was lower compared to the dual fuel mode for all CRs. NO_x emission at full load in case of dual fuel mode was 60, 75, 95, 131 and 250 ppm which was much higher than that of 46 ppm in baseline diesel.

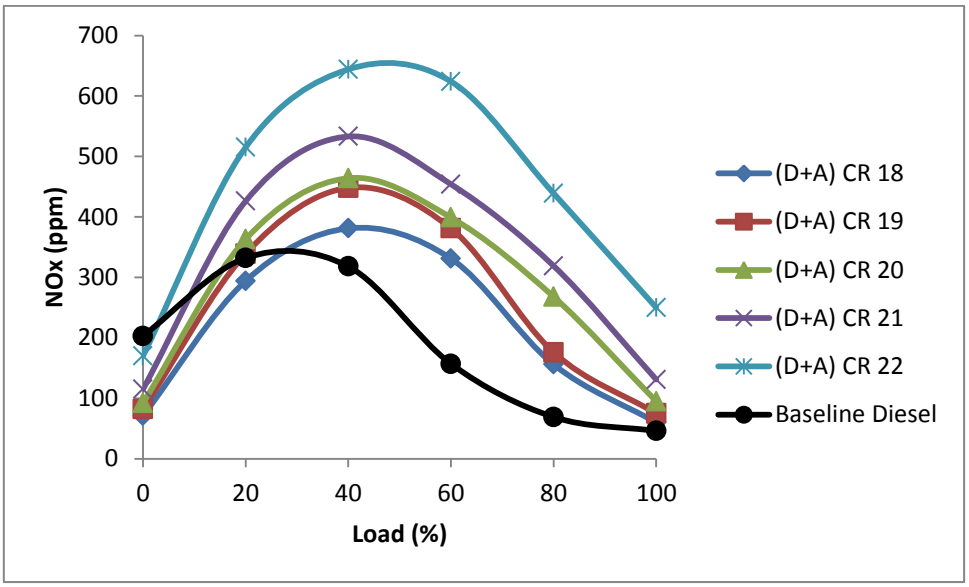

Fig. 4.22 Variation of NO_x with load in dual fuel mode at different compression ratios

4.4.2.4 Smoke

Fig. 4.23 shows the variation of smoke density with load at different CRs for dual fuel mode. Smoke density in dual fuel mode was lower as compared to the diesel mode. The addition of acetylene lessened the amount of injected fuel (diesel) and brought down the smoke level. Also the inducted acetylene formed a homogeneous mixture that burnt rapidly resulting in less carbon from which smoke could be formed. Smoke density decreased with increase in CR. The maximum temperature during combustion increased as CR increased resulting in complete combustion and this in turn decreased smoke density. Maximum smoke density at full load was 0.8%, 3%, 9.1%, 11.4% and 26.5% lower than baseline diesel for CRs of 18, 19, 20, 21 and 22 respectively.

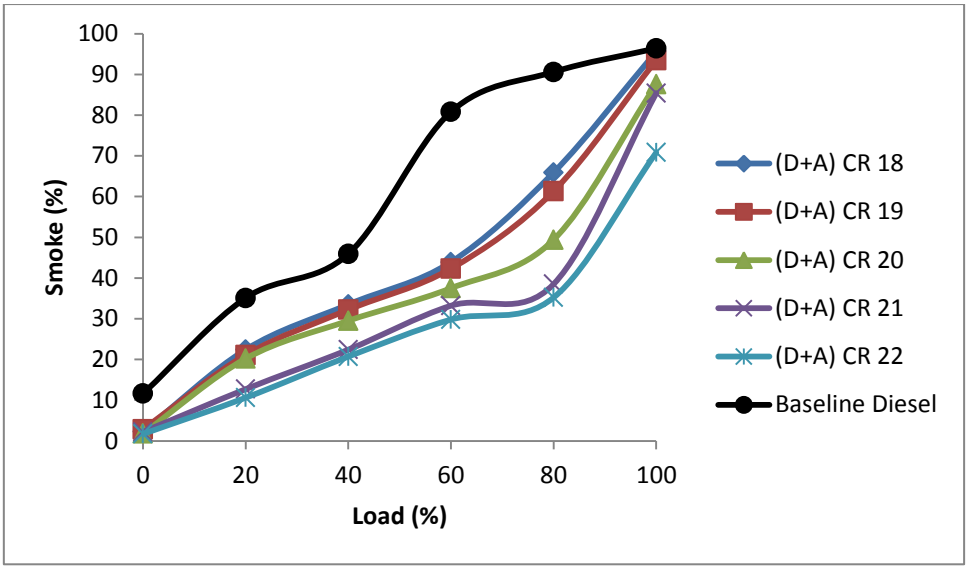

Fig. 4.23 Variation of Smoke density (opacity) with load in dual fuel mode at different compression ratios

4.4.3 Effect of compression ratio on combustion characteristics for dual fuel mode

4.4.3.1 Pressure-Crank Angle

Fig. 4.24 shows the variation of cylinder pressure with crank angle at full load for different CRs in dual fuel mode. The maximum cylinder pressure in case of dual fuel operation was 68.74, 73.16, 74.03, 81.41 and 91.53 bar for CRs of 18, 19, 20, 21 and 22 respectively at full load. Cylinder pressure increased with increase in CR in dual fuel mode. The maximum cylinder pressure in case of baseline diesel was 71.88 bar.

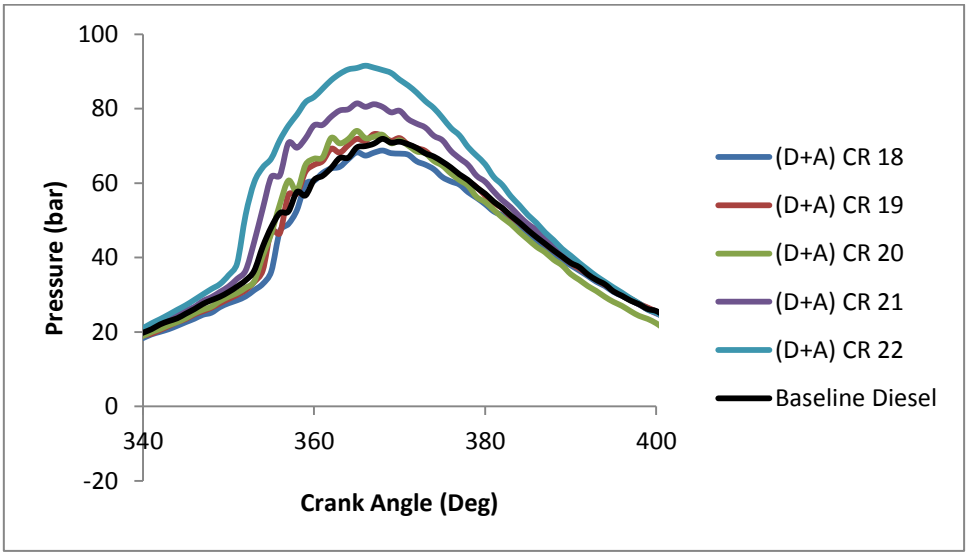

Fig. 4.24 Variation of cylinder pressure (p) with respect to crank angle (Θ) at full load in dual fuel mode at different compression ratios

4.4.3.2 Net Heat Release Rate (NHRR)

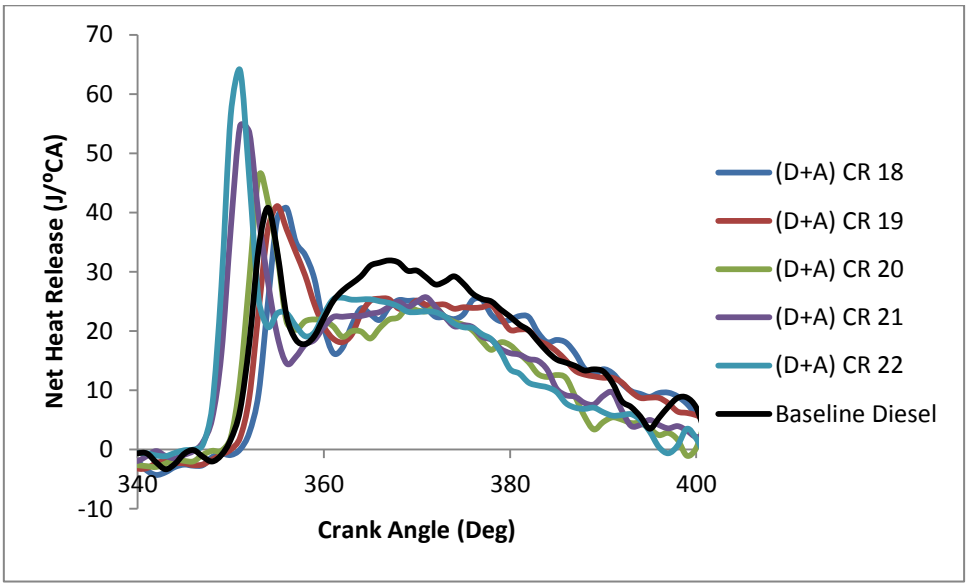

Fig. 4.25 Variation of net heat release rate with respect to crank angle at full load in dual fuel mode at different compression ratios

Fig. 4.25 shows the variation of net heat release rate (NHRR) with respect to crank angle at full load in dual fuel mode at different CRs. NHRR increased with increase in CR due to increase in cylinder pressure and combustion temperature. In case of dual fuel mode the maximum HRR was 40.76 J/° CA, 41.09 J/° CA, 46.053 J/° CA, 54.57 J/° CA and 64.01 J/° CA at CR 18, CR 19, CR 20, CR 21 and CR 22 respectively. The NHRR in case of baseline diesel was 40.81 J/° CA. The NHRR in case of dual fuel mode was higher compared to that in diesel mode because of higher energy density of acetylene diesel air mixture.

4.4.3.3 Rate of Pressure Rise (RPR)

Fig. 4.26 shows the variation of rate of pressure rise (RPR) with respect to crank angle at full load in dual fuel mode at different CRs. The maximum RPR obtained in dual fuel mode was 5.42, 5.51, 6.62, 7.30 and 8.51 bar/°CA for CR 18, 19, 20, 21 and 22 respectively. RPR increased with increase in CR in dual fuel mode. The maximum RPR in case of baseline diesel was 4.92 bar/°CA which was lower than those in dual fuel mode at different CRs. As CR was increased complete combustion took place which caused an increase in the rate of pressure rise.

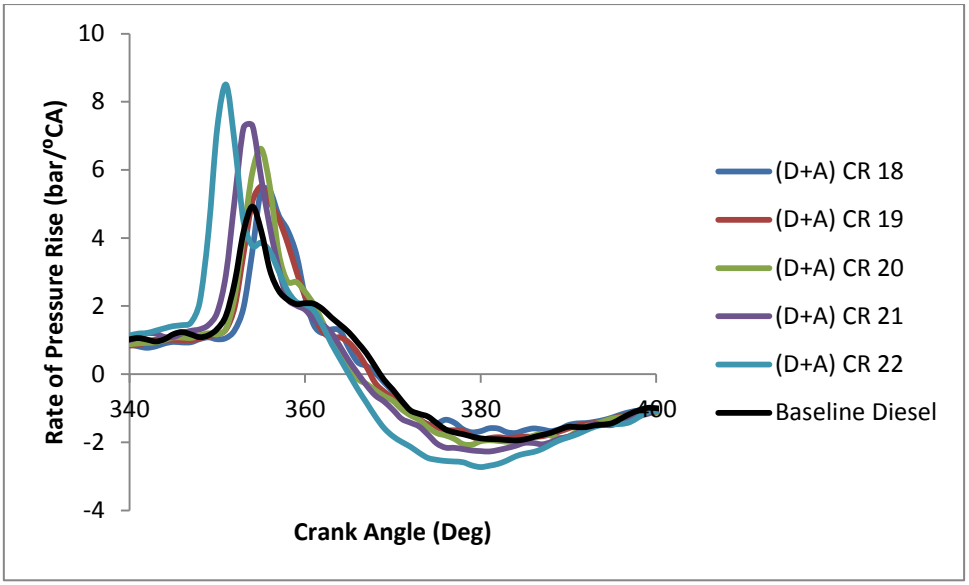

Fig. 4.26 Variation of rate of pressure rise with respect to crank angle at full load in dual fuel mode at different compression ratios

Though best emission results were obtained at CR of 22 in dual fuel mode, however, since CR of 21 gave best BTE and BSEC results, CR of 21 was considered as optimum CR for dual fuel mode.

4.4.4 Effect of injection pressure on engine performance for dual fuel mode

After the optimization of compression ratio (CR) in dual fuel mode on the basis of performance, emission and combustion characteristics, the effect of injection pressure (IP) on performance, emission and combustion characteristics in dual fuel mode was studied by varying injection pressure from 180 to 210 bar at the interval of 10 bar. The readings were taken at optimum flow rate of 120 LPH, compression ratio 21 and standard injection timing of 23° bTDC for different loads in dual fuel mode and the results were compared with baseline diesel (CR 20, IP 210 bar and IT 23° bTDC).

4.4.4.1 Brake Thermal Efficiency (BTE)

Fig. 4.27 shows the variation of BTE with load at different injection pressures in dual fuel mode. The brake thermal efficiency increased with increase in load for all the cases. The BTE in case of dual fuel operation was higher than that with baseline diesel because of wide flammability limits, minimum ignition energy and higher flame velocity of acetylene gas. BTE increased with increase in IP up to 200 bar and then it decreased with increase in IP.

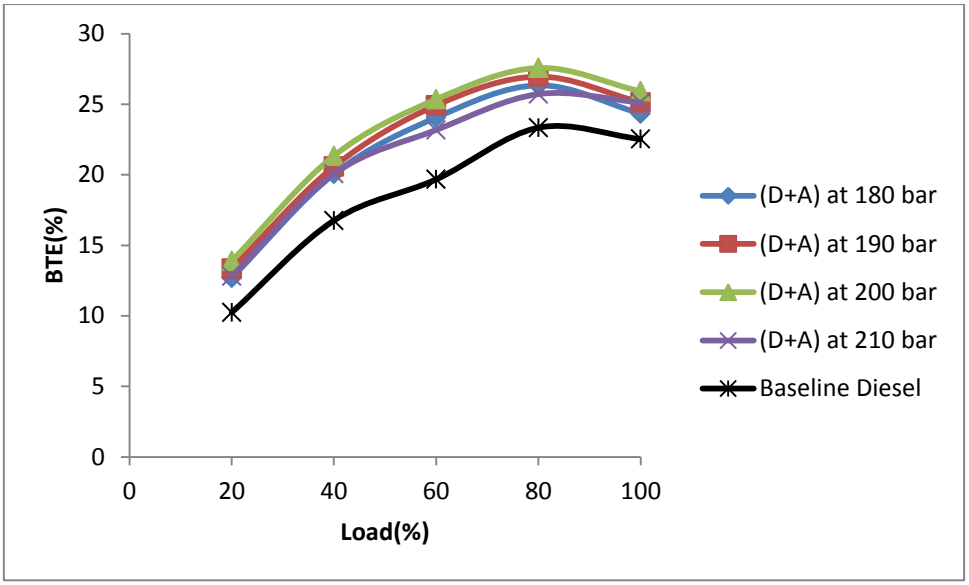

Fig. 4.27 Variation of BTE with load in dual fuel mode at different injection pressures

The increase in BTE might be due to fine spray, better atomization of diesel and better combustion at higher IP. While on further increasing IP, BTE reduced which might be due to reduction in the size of fuel droplets that had lesser momentum which affected the fuel distribution (penetration) in the air leading to incomplete combustion [99]. At 80% load, highest BTE of 26.34%, 26.96%, 27.57% and 25.72% was obtained at 180, 190, 200 and 210 bar respectively in dual fuel mode as compared to the BTE of 23.34% for baseline diesel. BTE in dual fuel mode was 12.9%, 15.5%, 18.1% and 10.2% higher than baseline diesel for 180, 190, 200 and 210 bar IP respectively. Thus, the highest BTE was obtained at 200 bar in case of dual fuel mode.

4.4.4.2 Brake Specific Energy Consumption (BSEC)

Fig. 4.28 shows the variation of brake specific energy consumption (BSEC) with load in dual fuel mode at different injection pressures. BSEC in case of dual fuel mode was 13558.8, 13248.6, 12954.7 and 13886.8 kJ/kWh at 180, 190, 200 and 210 bar respectively. BSEC in dual fuel mode was 11.4%, 13.4%, 15.4% and 9.3% lower than baseline diesel. BSEC in dual fuel mode decreased with increase in IP up to 200 bar may be because of better atomization, vaporization of the fuel and improved air-fuel mixing that led to better combustion. BSEC increased on further increasing IP up to 210 bar due to poor combustion as explained above. The highest BSEC of 15304.1 kJ/kWh was found in the case of baseline diesel.

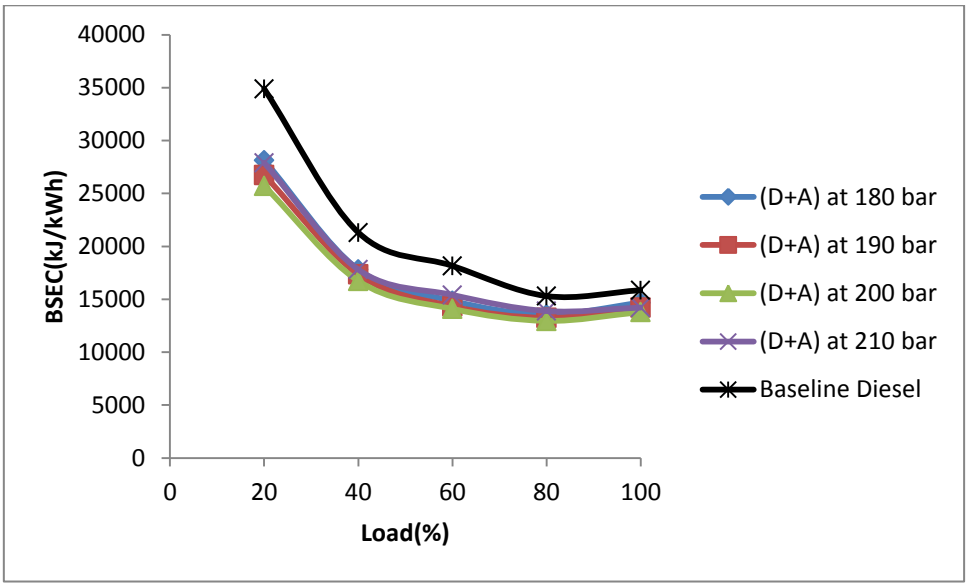

Fig. 4.28 Variation of BSEC with load in dual fuel mode at different injection pressures

4.4.4.3 Exhaust Gas Temperature (EGT)

Fig. 4.29 shows the variation of EGT with load at different injection pressures for dual fuel mode. EGT increased with increase in load. Maximum EGT in dual fuel mode was 423.9° C, 411.4° C, 391.1° C and 402.6° C at 180, 190, 200 and 210 bar respectively at full load while in case of baseline diesel it was 419.7° C. The EGT in case of baseline diesel was higher compared to that in dual fuel mode at all IPs. The EGT in case of dual fuel mode was lower than diesel mode because of the higher flame speed of acetylene and advancement in the heat release rate in case of dual fuel mode. In dual fuel mode the EGT decreased with increase in IP upto 200 bar, which could be due to the sluggish combustion leading to higher EGT at lower IP [102].

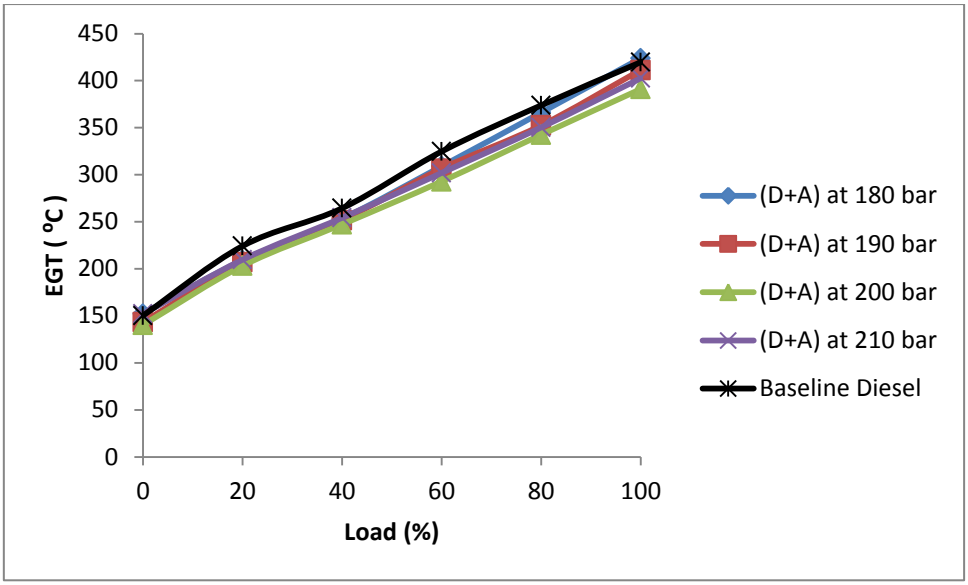

Fig. 4.29 Variation of EGT with load in dual fuel mode at different injection pressures

4.4.5 Effect of injection pressure on exhaust emission for dual fuel mode

4.4.5.1 Carbon monoxide (CO)

Fig. 4.30 depicts the variation of CO emission with load at different IPs. At full load CO emission was 14.3%, 28.6%, 42.9% and 35.7% lower than baseline diesel at 180, 190, 200 and 210 bar respectively in dual fuel mode. The CO emission decreased with increase in IP up to 200 bar. Increasing the injection pressure caused better fuel air mixing leading to complete combustion and reduced CO emission. At 210 bar the formation of CO increased, this might be due to lack of mixing of fuel and air and insufficient time for combustion [89].

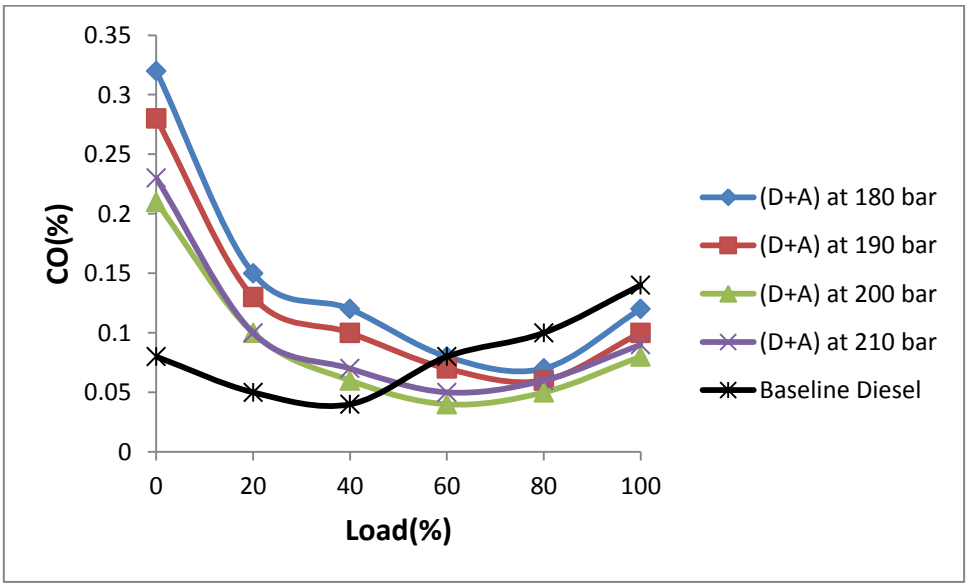

Fig. 4.30 Variation of CO with load in dual fuel mode at different injection pressure.

4.4.5.2 Hydrocarbon (HC)

Fig. 4.31 shows the variation of HC emission with load for different IPs. HC emission in dual fuel mode decreased with increase in IP up to 200 bar. The fuel air mixing was more proper on increasing the injection pressure which caused low HC emissions at high injection pressure than that at low injection pressures. HC emission increased with further rise in injection pressure (210 bar). HC emission in case of dual fuel mode at 200 IP, full load was 10% lower than that for baseline diesel.

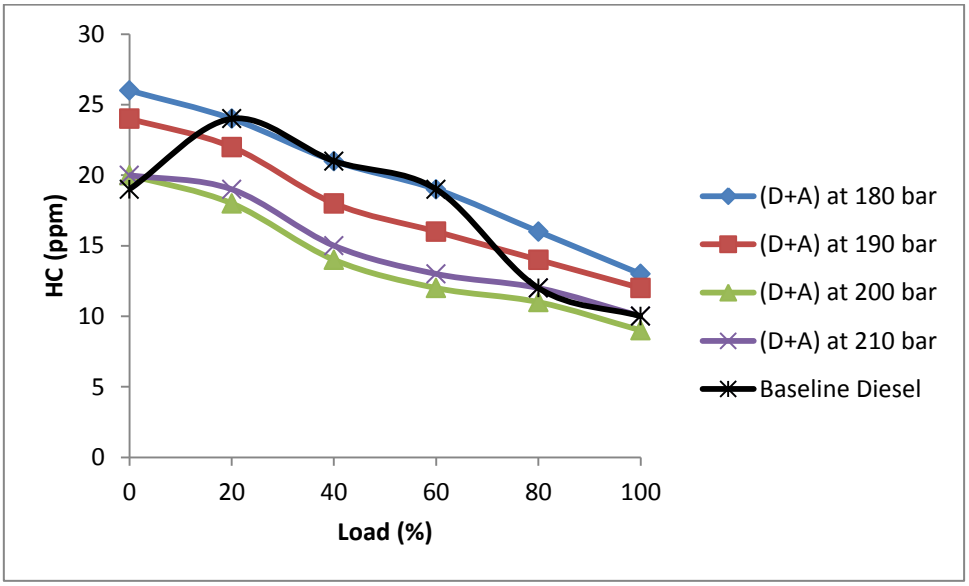

Fig. 4.31 Variation of HC with load in dual fuel mode at different injection pressures

4.4.5.3 Oxides of Nitrogen (NO_x)

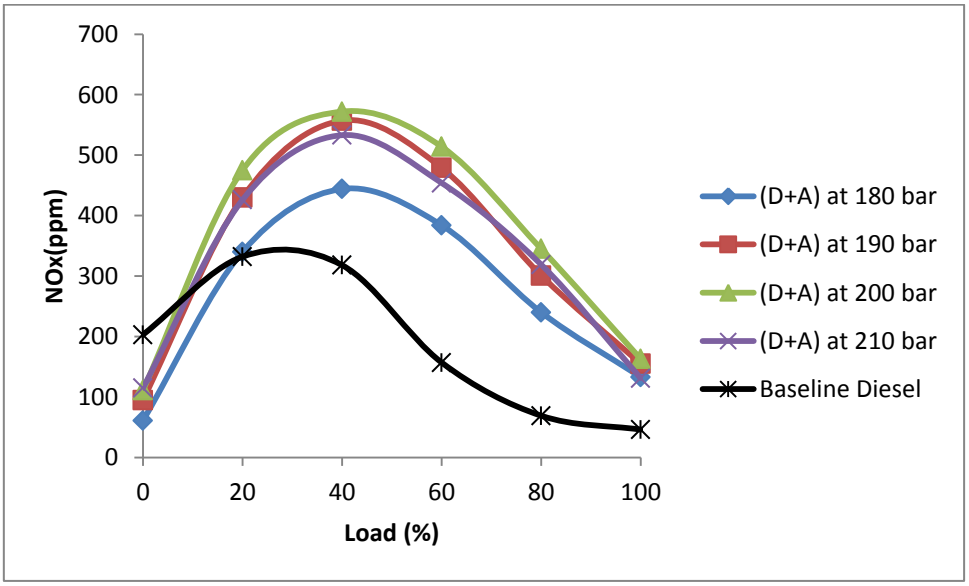

Fig. 4.32 Variation of NO_x with load in dual fuel mode at different injection pressures

Fig. 4.32 shows the variation of NO_x emission with load at different IPs in dual fuel mode. NO_x emission was higher in dual-fuel mode compared to that in diesel mode because in dual-fuel mode the combustion chamber temperature was higher than diesel due to higher calorific value of acetylene gas compared to that of diesel. Maximum NO_x was obtained at 40% load in dual fuel mode while in case of diesel mode maximum NO_x was obtained at 20% load. NO_x emission increased with increase in injection pressure up to 200 bar. Increase in NO_x emission was due to rapid combustion, high in-cylinder temperature and high peak pressure attained with higher injection pressure. Further increase of IP to 210 bar lowered the NO_x emissions, which was due to improper combustion resulting in lower in-cylinder temperatures when compared to IP of 200 bar. NO_x emission in case of dual fuel mode at full load and 200 bar IP was 163 ppm which was much higher than 46 ppm in case of baseline diesel.

4.4.5.4 Smoke

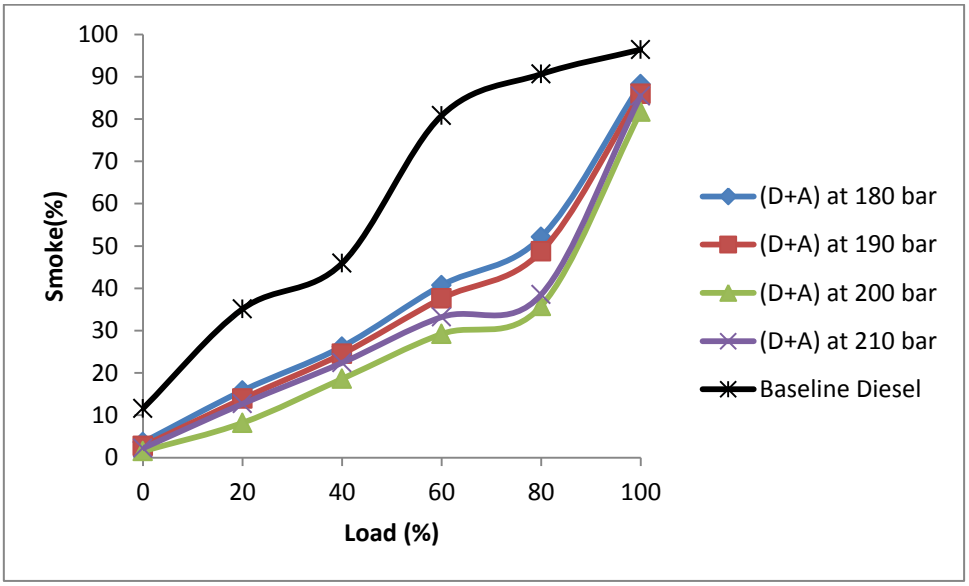

Fig. 4.33 Variation of smoke density (opacity) with load in dual fuel mode at different injection pressures

Fig. 4.33 shows the variation of smoke density with load at different injection pressures. Smoke density (in opacity %) in dual fuel mode at full load was 8.5%, 10.9%, 15.2% and 11.4% lower than baseline diesel. Smoke density in dual fuel mode was found decreasing with increase in injection pressure upto 200 bar. The higher smoke density at lower injection pressure was due to the large droplet size leading to poor atomization, while at higher injection pressure, droplet size reduced resulting in better fuel-air mixing and complete combustion which led to lower smoke emission. On increasing injection pressure above 200

bar, smoke density increased, which was due to the fact that too high an injection pressure led to formation of extremely fine droplets of fuel which lacked depth of penetration resulting in incomplete combustion.

4.4.6 Effect of injection pressure on combustion characteristics for dual fuel mode

4.4.6.1 Pressure-Crank Angle

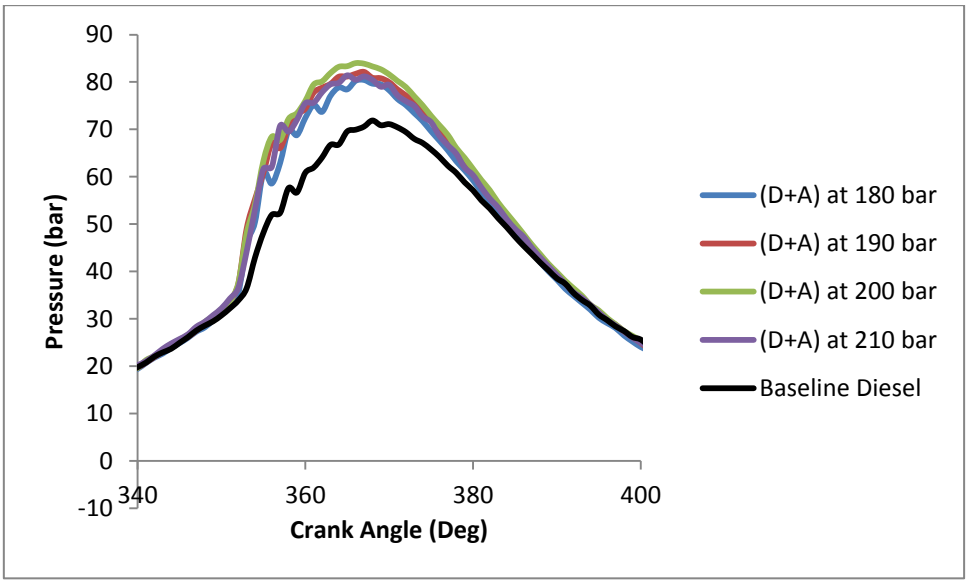

Fig. 4.34 Variation of cylinder pressure (p) with crank angle (Θ) at full load in dual fuel mode at different injection pressures

Fig. 4.34 shows the variation of cylinder pressure with crank angle at full load for different injection pressures. The maximum cylinder pressure at 100% load in case of dual-fuel operation was found to be 80.44, 82.15, 83.99 and 81.41 bar for IP 180, 190, 200 and 210 bar respectively as compared to the maximum cylinder pressure of 71.88 bar for baseline diesel. The maximum cylinder pressure in dual fuel mode increased with increase in IP upto 200 bar. The highest maximum cylinder pressure of 83.99 bar was obtained at IP 200 bar in case of dual-fuel mode beyond which it decreased. The increase in maximum cylinder pressure from 180 to 200 bar injection pressure might be due to better atomization, air-fuel mixing and enhanced combustion. Further increase in injection pressure to 210 bar lowered maximum cylinder pressure, which could be due to improper mixing of fuel leading to improper combustion.

4.4.6.2 Net Heat Release Rate (NHRR)

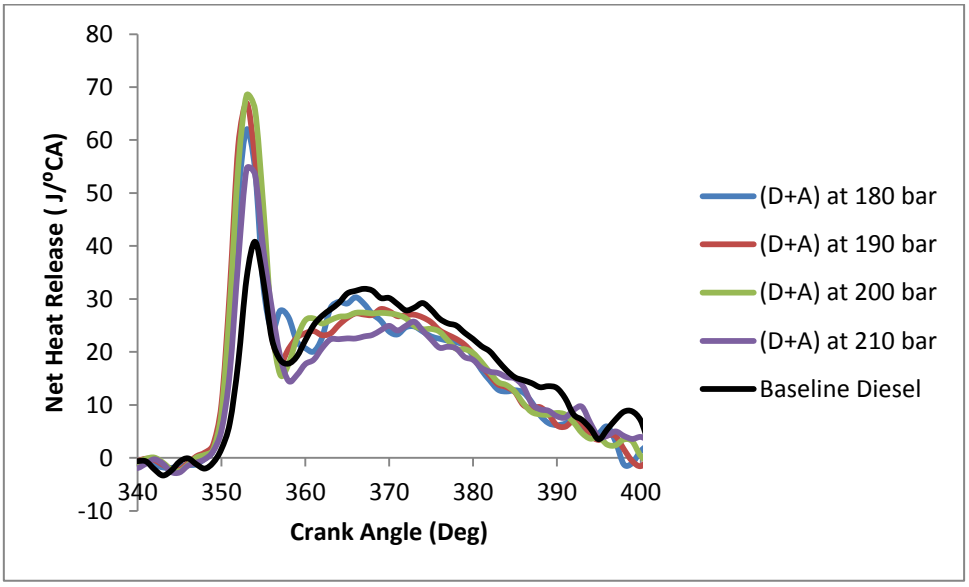

Fig. 4.35 Variation of net heat release rate with crank angle at full load in dual fuel mode at different injection pressures

Fig. 4.35 shows the variation of net heat release rate (NHRR) with crank angle at full load in dual fuel mode at different injection pressures. The NHRR increased with increase in IP due to increase in cylinder pressure and combustion temperature. In case of dual-fuel mode at full load, the maximum NHRR was 62.01, 67.01, 68.45 and 54.57 J/° CA at 180, 190, 200 and 210 bar respectively. NHRR for baseline diesel was 40.81 J/° CA. The NHRR in case of dual-fuel mode was higher compared to that in diesel mode. Higher energy density of acetylene diesel air mixture resulted in higher NHRR when compared to baseline diesel operation. NHRR increased from 180 to 200 bar injection pressure because with the increase in injection pressure heat release rate increased due to improved premixed combustion phase which was due to better atomization and improved air fuel mixing. On further increasing IP to 210 bar, NHRR decreased.

4.4.6.3 Rate of Pressure Rise (RPR)

Fig. 4.36 illustrates the trends for the rate of pressure-rise (RPR) with the crank angle for dual fuel mode at different IP and also for baseline diesel. At full load, the maximum rate of pressure rise (bar/° CA) for dual fuel mode was found to be 7.05, 7.60, 7.71 and 7.30 for IPs of 180, 190, 200 and 210 bar respectively while for baseline diesel the maximum rate of pressure rise was 4.92 bar/° CA. The maximum rate of pressure rise in case of dual fuel mode

increased consistently with increase in injection pressure up to 200 bar beyond which it decreased.

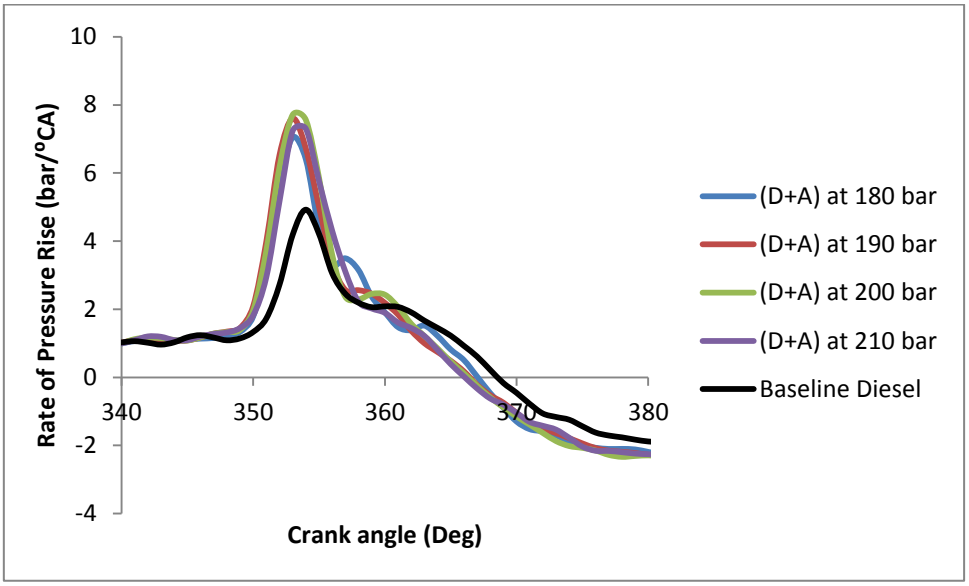

Fig. 4.36 Variation of rate of pressure rise with crank angle at full load in dual fuel mode at different injection pressures

Based on the engine performance at different injection pressures, it was found that IP of 200 bar was optimum for dual fuel mode.

4.4.7 Effect of injection timing on engine performance for dual fuel mode

After the optimization of injection pressure (IP) in dual fuel mode on the basis of performance, emission and combustion characteristics, the effect of injection timing (IT) on performance, emission and combustion characteristics in dual fuel mode was studied at different injection timings of 18º, 20º, 23º and 25º bTDC. The readings were taken at optimum flow rate of 120 LPH, CR 21 and IP of 200 bar for different loads in dual fuel mode and the results were compared with baseline diesel (CR 20, IP 210 bar and IT 23° bTDC).

4.4.7.1 Brake Thermal Efficiency (BTE)

Fig. 4.37 shows variation of brake thermal efficiency (BTE) with different injection timings (ITs) of 18º, 20º, 23º and 25º bTDC for dual fuel mode. BTE increased with increase in load upto 80% for all ITs in dual fuel mode. BTE in dual fuel mode increased with advancing IT from 18º to 23º after which it decreased. The highest BTE of 27.57% was obtained at 23º bTDC in comparison to 24.46%, 26.34% and 25.72% at 18º, 20º and 25º bTDC respectively.

BTE in dual fuel mode was 4.8%, 12.9%, 18.1% and 10.2% higher than baseline diesel for 18°, 20°, 23° and 25° bTDC ITs respectively. The advancement of IT from 18° to 23° bTDC resulted in injection of diesel earlier into the combustion chamber, therefore giving sufficient time for the diesel to form a homogeneous mixture with air and acetylene. This resulted in more efficient burning of acetylene air diesel mixture. When the IT was further advanced to 25° bTDC, the delay period increased which resulted in lower peak pressure and hence BTE reduced.

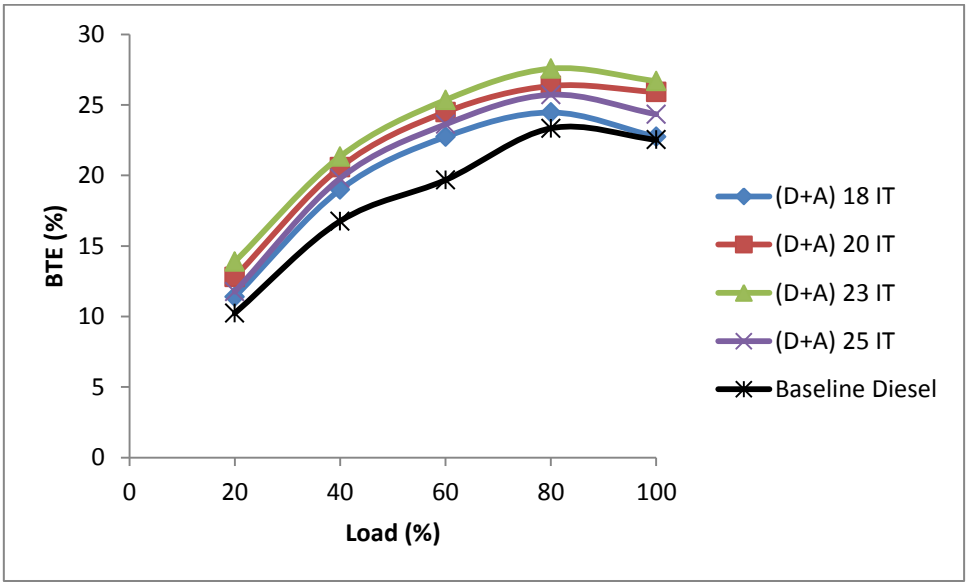

Fig. 4.37 Variation of BTE with load in dual fuel mode at different injection timings

4.4.7.2 Brake Specific Energy Consumption (BSEC)

Fig. 4.38 shows the variation of BSEC with load for all ITs. BSEC in case of dual-fuel mode was lower than that in diesel mode due to higher conversion of acetylene into work. The lowest BSEC obtained in dual fuel mode at 80% load was 14602.3, 13558.8, 12954.7 and 13886.8 kJ/kWh for 18°, 20°, 23° and 25° bTDC respectively in comparison to 15304.1 kJ/kWh for baseline diesel. BSEC decreased with advancement of IT from 18° to 23° bTDC beyond which it increased. Thus, the lowest BSEC was obtained at standard IT of 23° bTDC. The highest BSEC was found in the case of baseline diesel.

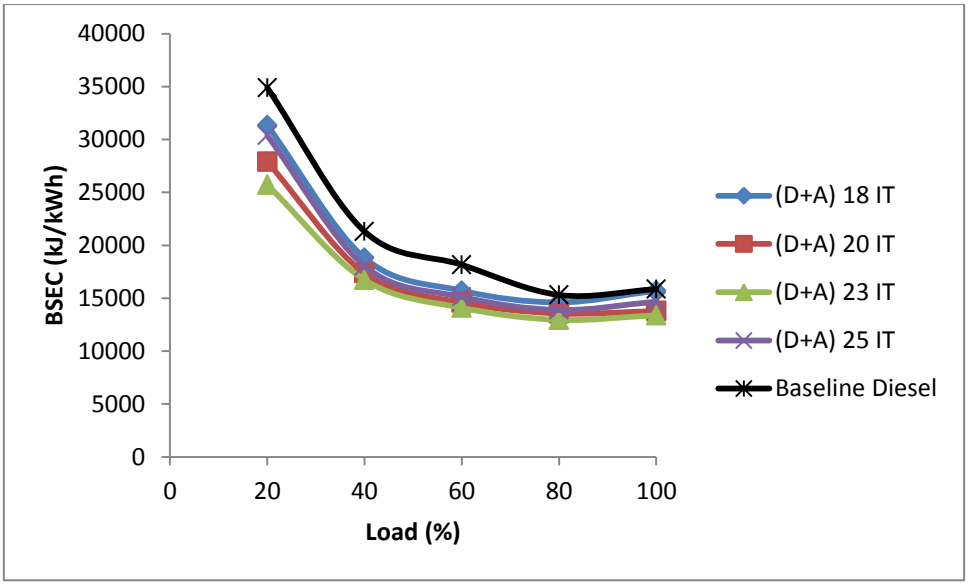

Fig. 4.38 Variation of BSEC with load in dual fuel mode at different injection timings

4.4.7.3 Exhaust Gas Temperature (EGT)

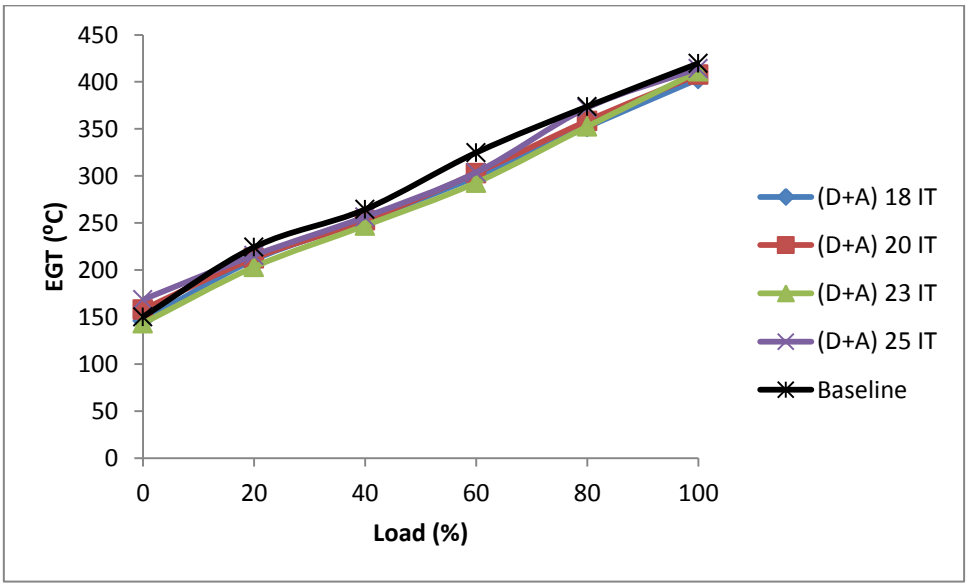

Fig. 4.39 Variation of EGT with load in dual fuel mode at different injection timings

Fig. 4.39 shows variation of EGT with load for different ITs. The EGT increased with increase in load for all the cases. Maximum EGT in dual fuel mode was 403°C, 407.7°C, 411.1°C and 414.4°C at 18°, 20°, 23° and 25° bTDC respectively at full load while in case of baseline diesel it was 419.7°C. The EGT is found to decrease as the IT was advanced from 18° to 23° bTDC, beyond which EGT increased. Although no significant effect on EGT was observed with change in IT.

4.4.8 Effect of injection timing on emission characteristics for dual fuel mode

4.4.8.1 Carbon monoxide (CO)

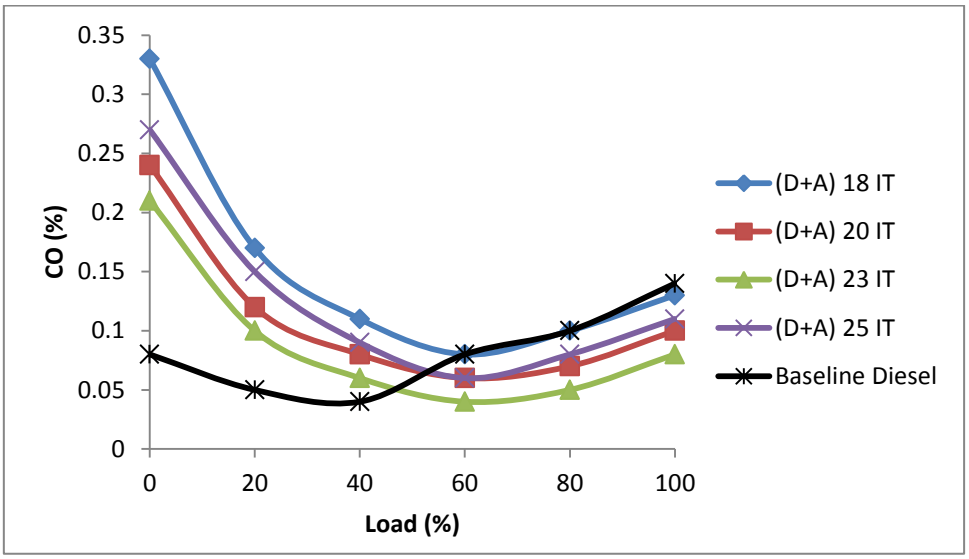

Fig. 4.40 Variation of CO with load in dual fuel mode at different injection timings

Fig. 4.40 depicts the variation of CO emission with load at different ITs. CO emissions at full load in dual fuel mode was 7.1%, 28.6%, 42.9% and 21.4% lower than baseline diesel for 18°, 20°, 23° and 25° bTDC IT respectively. As the IT was advanced from 18° to 23° bTDC CO emissions reduced due to complete combustion as a result of proper mixing of air-fuel mixture because of availability of more time for mixing process. On further advancing IT to 25° bTDC, CO emissions increased which might be due to improper combustion.

4.4.8.2 Hydrocarbon (HC)

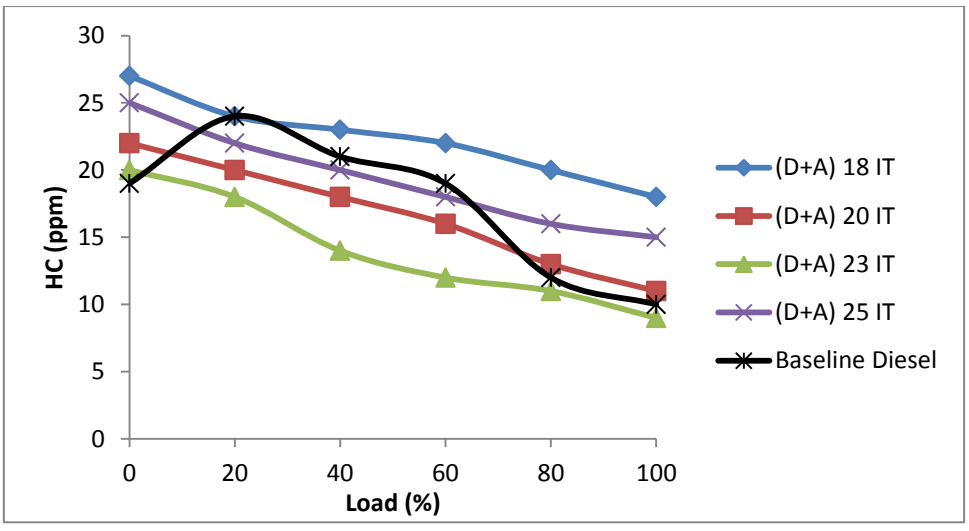

Fig. 4.41 Variation of HC with load in dual fuel mode at different injection timings

Fig. 4.41 shows the variation of HC emission in dual fuel mode with load for all ITs. HC emission decreased as the IT was advanced from 18° to 23° bTDC since combustion started earlier while advancing the IT which led to complete combustion and lower HC emission. Minimum HC emission of 9 ppm was obtained at 23° bTDC IT at full load which was 10% lower than baseline diesel. HC emission further increased on advancing IT to 25° bTDC which could be due to incomplete combustion.

4.4.8.3 Oxides of Nitrogen (NO_x)

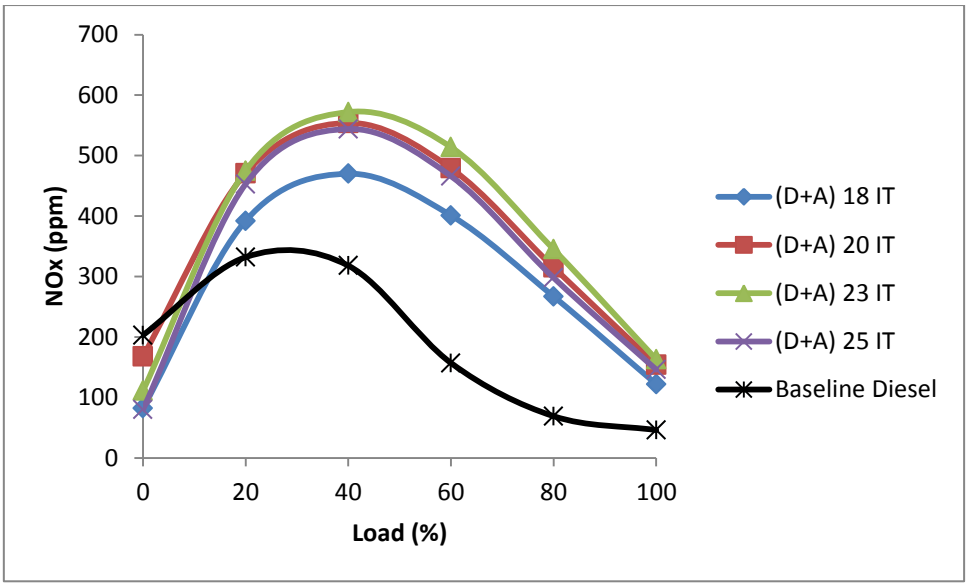

Fig. 4.42 Variation of NO_x with load in dual fuel mode at different injection timings

NO_x emission was higher in dual fuel mode as compared to the diesel mode, as can be seen in Fig. 4.42, because in dual-fuel mode the combustion chamber temperature was higher than diesel due to higher calorific value of acetylene compared to that of diesel. NO_x emission increased as the IT was advanced from 18° to 23° bTDC due to high peak cylinder pressure resulting in high temperature and increase in NO_x. The NO_x emission at full load in dual fuel mode was 122, 154, 163 and 146 ppm which was much higher than 46 ppm in baseline diesel. The reason for this was that the increased ignition delay during advanced timing had promoted premixed combustion phase, leading to higher cylinder temperature which increased the NO_x emissions consequently. NO_x emission decreased with advancing IT to 25° bTDC due to decrease in cylinder pressure and temperature.

4.4.8.4 Smoke

Fig. 4.43 shows the variation of smoke density with load in dual fuel mode for all ITs. Smoke density at full load in dual fuel mode was 2%, 10.8%, 15.2% and 6.8% lower than baseline diesel. Smoke density decreased with advanced IT from 18° to 23° bTDC since advancing the IT led to early injection which caused better combustion as more time was available for oxidation. On further advancement of IT to 25° bTDC, smoke density increased. The highest smoke density was observed in the case of baseline diesel.

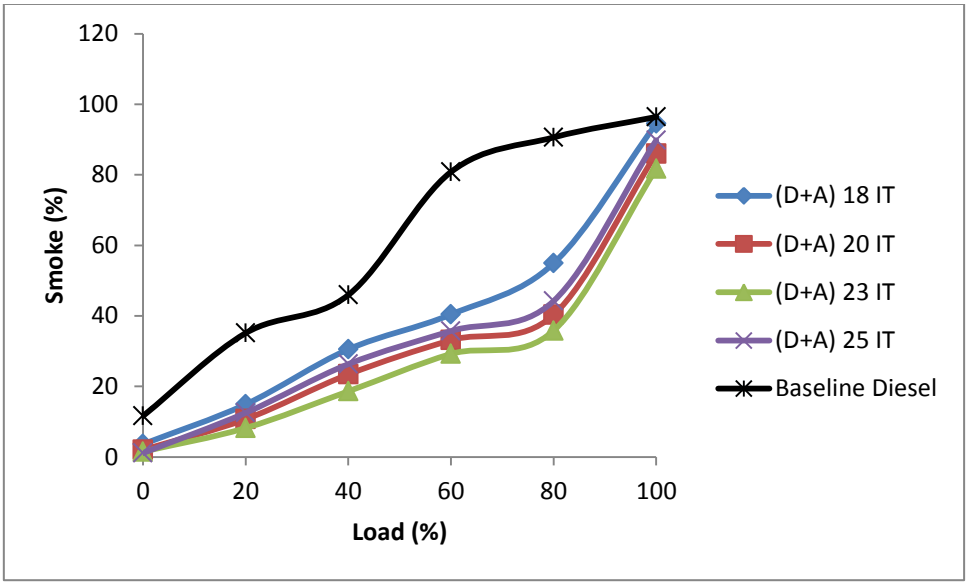

Fig. 4.43 Variation of smoke density (opacity) with load in dual fuel mode at different injection timings

4.4.9 Effect of injection timing on combustion characteristics for dual fuel mode

4.4.9.1 Pressure-Crank Angle

Fig. 4.44 shows the variation of cylinder pressure with respect to crank angle at full load for different ITs. Maximum cylinder pressure was found to be 77.11, 80.89, 83.99 and 80.48 bar for 18°, 20°, 23° and 25° bTDC respectively in comparison to 71.88 bar for baseline diesel. As IT is advanced from 18° to 23° the maximum cylinder pressure increased. This was because of faster burning rate in the premixed combustion phase with the advancement of IT. The maximum cylinder pressure was obtained at 23° bTDC for dual fuel mode.

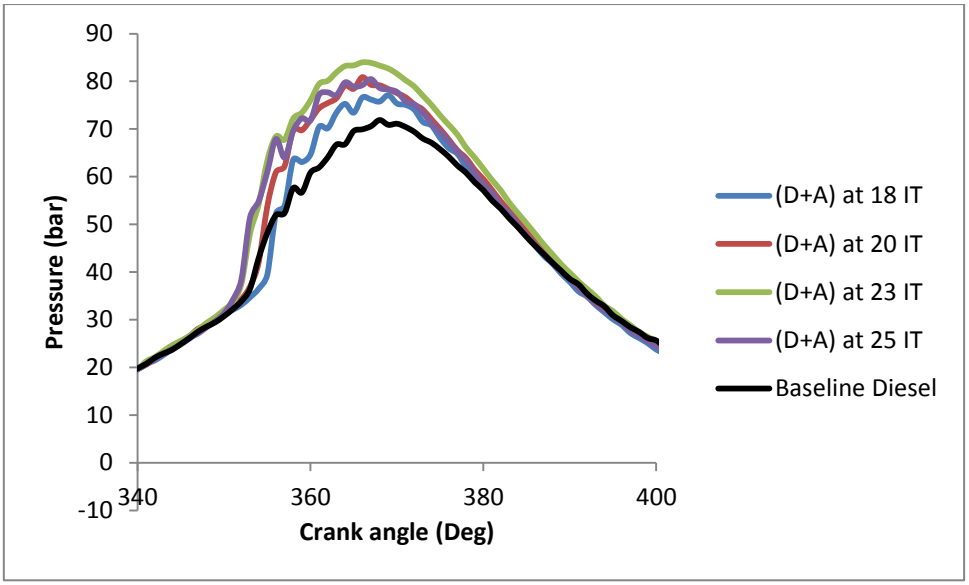

Fig. 4.44 Variation of cylinder pressure with crank angle at full load in dual fuel mode at different injection timings

4.4.9.2 Net Heat Release Rate (NHRR)

Fig. 4.45 shows the variation of net heat release rate (NHRR) with respect to crank angle at full load for dual fuel mode at different ITs. The net heat release rate (NHRR) increased with increase in IT due to increase in cylinder pressure and combustion temperature. In case of dual-fuel mode at full load, the maximum NHRR was 60.80, 66.49, 68.45 and 62.97 J/°CA at 18°, 20°, 23° and 25° bTDC IT respectively. Maximum NHRR for baseline diesel was 40.81 J/°CA. Higher energy density of acetylene diesel air mixture resulted in higher NHRR when compared to baseline diesel operation. NHRR increased from 18° to 23° bTDC IT because of burning of more fuel air mixture accumulated during long delay period as the IT was advanced. On further advancement of IT to 25° bTDC NHRR decreased due to decrease cylinder pressure.

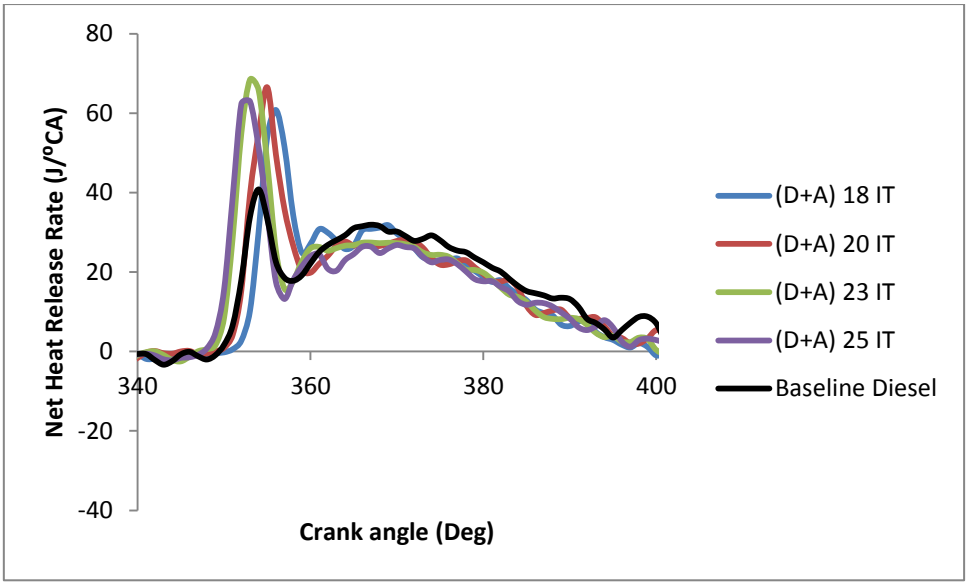

Fig. 4.45 Variation of net heat release rate with crank angle at full load in dual fuel mode at different injection timings

4.4.9.3 Rate of Pressure Rise (RPR)

Fig. 4.46 illustrates the trends for the rate of pressure-rise (RPR) with respect to crank angle for dual fuel mode at full load for different ITs. At full load, the maximum rate of pressure rise for dual fuel mode was found to be 6.80, 7.51, 7.71 and 7.30 bar /°CA for 18°, 20°, 23° and 25° bTDC IT respectively while for baseline diesel the maximum rate of pressure rise was 4.92 bar/°CA. The maximum rate of pressure rise in case of dual fuel mode increased consistently with increase in injection timing up to 23° bTDC beyond which it decreased.

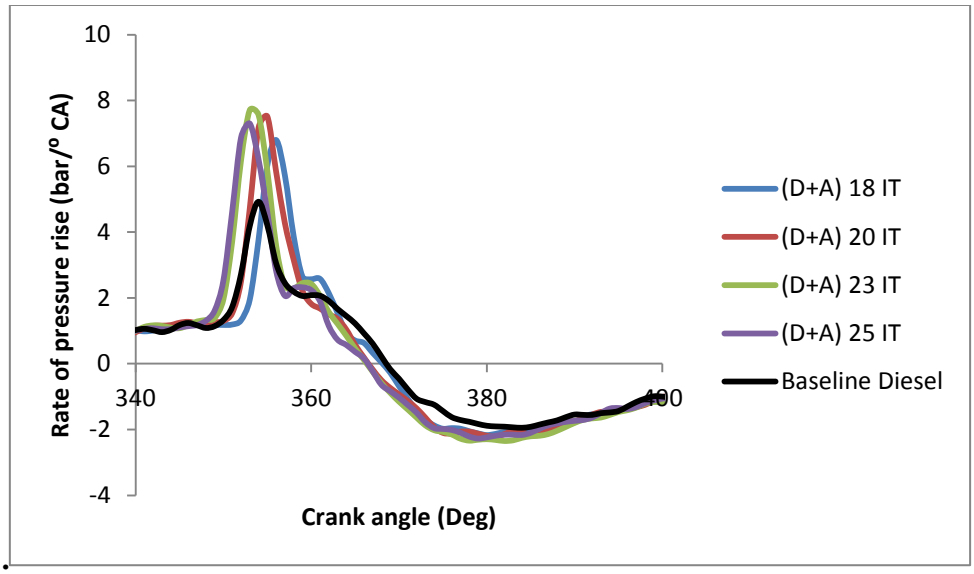

Fig. 4.46 Variation of rate of pressure rise with crank angle at full load in dual fuel mode at different injection timings

The rate of pressure rise was found to be higher with advanced injection timings because of faster combustion.

Hence, from the above results, it was found that for dual fuel mode, the optimum condition in view of engine performance was CR 21, IP 200 bar and IT 23° bTDC with flow rate of 120 LPH of acetylene.

4.5 Mass percentage of acetylene and diesel at the optimized condition

Fig. 4.47 shows the percentage mass fraction of acetylene and diesel in total fuel supplied in case of optimized condition (CR 21, IP 200 bar and IT 23° bTDC) in dual fuel mode when the highest BTE of 27.57% was obtained. The percentage mass of acetylene varied from 53.3% at no load to 11.6% at full load on mass basis while the percentage of diesel varied accordingly to make the total fuel mass to 100% i.e., at no load, when acetylene mass % was 53.3%, diesel mass% was 46.7% and at full load, when acetylene mass % was 11.6%, diesel mass% was 88.4%.

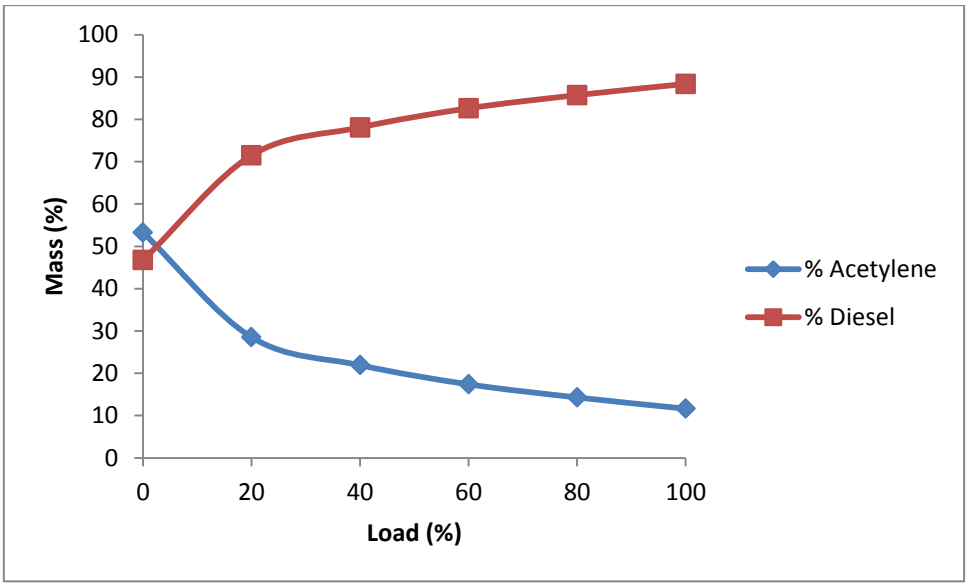

Fig. 4.47 Mass % of Acetylene and Diesel for the optimized condition in dual fuel mode

CHAPTER 5

MODELLING AND SIMULATION

5.1 Computational Fluid Dynamics

Computational Fluid Dynamics (CFD) is a technique used for analysis of heat transfer, fluid flow and chemical reaction with computer-based simulation. There are different numerical methods and algorithms used in CFD to solve and analyze problems of fluids and heat transfer. Computational fluid dynamics involves the creation of large numbers of grids that hopefully provide a realistic result of real life system. In this, the physical characteristic of fluid flow and heat transfer can easily be simulated through numerical method techniques. There is no necessity of physical model to predict or analyze the system properties because CFD involves the well-developed methodologies within the codes. CFD technique has become very effective and strong technique for pure or applied research or industrial applications. To solve any problem, CFD uses the algorithm and numerical methods and involves fluid flow flowing over a domain for simulation.

Three main processes used in CFD techniques are given as:

1. Pre-processing
2. Solver
3. Post-processing

Pre-processing deals with the geometry creation and import of the desired geometry. In ANSYS, there is a facility to create geometry in Design Modeller or design may be imported from other types of 3- d designing software with particular file extension which may allow in ANSYS. After creating the geometry of given problem, it is discretized into very small element or discrete cell which is called mesh. Depending on geometry, mesh is either structured or unstructured. After mesh generation, the name selection with physical modelling and boundary condition is defined which defines the fluid behaviour within the domain. The steady-state and transient problem can be studied in the Fluent and the final solution is generated with the use of different governing equations.

Solver includes the different numerical technique to solve the problem by an iterative approach. There are various types of solver assembled in the Fluent like PISO, COUPLE, SIMPLE and SIMPLEC.

Post process includes the visualization of the results in a different manner like colour contour, vertex, plane and streamline etc. In post processor results like velocity, temperature and pressure etc. can easily visible.

5.2 Governing equations

There are mainly three types of governing equations used for fluid dynamics which includes conservation equations for mass, momentum, and energy. The Governing Equations have been known for over 155 years. In the middle of the 19th century two scientists, Navier and Stokes has described the equations for a viscous flow, compressible fluid, which are now known as the Navier-Stokes Equations. These equations are in the form of differential equations. The generic form of these relationships follows the advection-diffusion equation given by equation 17.

$$\frac{\partial}{\partial t}(\rho\phi) + div\left(\rho\nabla\phi - \Gamma_{\phi} grad\phi\right) = S \tag{5.1}$$

Transient + advection - diffusion = source

The variable ϕ represents any of the physical quantities such as air velocity, temperature or species concentration at any point in the 3-D. This equationis derived by considering a small volume of fluid. The change in time of that quantity within the elemental volume added to that adverted into it, minus the amount diffused out is equal to the amount either created or destroyed. Though deceptively simple, only the emergence of ever faster computers over the past two decades has made it possible to solve the real world problems governed by this equation.

5.2.1 Governing equation for mass conservation

This equation is originated from the Navier-Stokes equation. Conservation of mass represents that the time-rate-of-change of the mass of the fluid element is zero as the element moves along with the flow in equation 18 to 20.

Conservation of mass state that:

{**Net mass flow out of control volume through surface S**}

$=$ {**time rate of decrease of mass inside control volume**}

$$\frac{D(\partial m)}{Dt} = 0 \tag{5.2}$$

And in Cartesian form

$$\frac{\partial \rho}{\partial t} + \frac{\partial(\rho u)}{\partial x} + \frac{\partial(\rho v)}{\partial y} + \frac{\partial(\rho w)}{\partial z} = 0 \tag{5.3}$$

Or in more compact vector notation

$$\frac{\partial \rho}{\partial t} + div(\rho u) = 0 \tag{5.4}$$

For an incompressible fluid (i.e. a liquid) the density ρ is constant and equation 5.5 & 5.6 becomes

$$div(u) = 0 \tag{5.5}$$

Or in long hand notation

$$\frac{\partial(u)}{\partial x} + \frac{\partial(v)}{\partial y} + \frac{\partial(w)}{\partial z} = 0 \tag{5.6}$$

5.2.2 Governing equation for momentum

Governing equation for momentum is based upon the Newton's second law, which states that the rate of change of momentum of a fluid particle equals the sum of the forces on the particle and given by equation 5.7 and 5.8.

$$f = ma \tag{5.7}$$

The rate of increase of momentum per unit volume of a fluid particle are given by

$$\rho \frac{Du}{Dt} + \rho \frac{Dv}{Dt} + \rho \frac{Dw}{Dt} = 0 \tag{5.8}$$

In above equation f, stands for force and a, stands for acceleration, Source of force on the body is of two types, which are mentioned below-

• Body forces - These forces are directly acting on the volume of the domain like gravitational force, magnetic and electric force etc.

• Surface forces – These forces act on the surface of the domain. They are just like pressure distribution along the surface of domain and shear and normal force distribution along the surface of a domain like viscous forces.

It is common practice to highlight the contributions due to the surface forces as separate terms in the momentum equation and to include the effects of body forces as source terms.

The x-component of the momentum equation is found by setting the rate of change of x-momentum of the fluid particle equal to the total force in the x-direction on the element due to surface stresses plus the rate of increase of x-momentum due to sources is given by equation 5.9 and for Y and Z component are given by equation 5.10 and 5.11 respectively.

$$\rho \frac{Du}{Dt} = \frac{\partial(-p+\tau_{xx})}{\partial x} + \frac{\partial \tau_{yx}}{\partial y} + \frac{\partial \tau_{zx}}{\partial z} + S_{Mx} \tag{5.9}$$

Y and Z component of momentum equations are given by

$$\rho \frac{Dv}{Dt} = \frac{\partial \tau_{xy}}{\partial x} + \frac{\partial(-p+\tau_{yy})}{\partial y} + \frac{\partial \tau_{zy}}{\partial z} + S_{My} \tag{5.10}$$

$$\rho \frac{Dw}{Dt} = \frac{\partial \tau_{xz}}{\partial x} + \frac{\partial \tau_{yz}}{\partial y} + \frac{\partial(-p+\tau_{zz})}{\partial z} + S_{Mz} \tag{5.11}$$

5.2.3 Governing equation for energy

The energy equation is derived from the first law of thermodynamics which states that the rate of change of energy of a fluid particle is equal to the rate of heat flux addition to the fluid particle plus the rate of work done on the particle due to surface force.

{Rate of change of energy inside the fluid element}
= {Net flux of heat into the element}
+ {Rate of working done on the element due to body and surface forces}

The energy equations are given by equation no. 28 and 29:

$$\rho \frac{DE}{Dt} = -div(pu) + \left[\frac{\partial(u\tau_{xx})}{\partial x} + \frac{\partial(u\tau_{xy})}{\partial y} + \frac{\partial(u\tau_{xz})}{\partial z} + \frac{\partial(v\tau_{xy})}{\partial x} + \frac{\partial(v\tau_{yy})}{\partial y} + \frac{\partial(v\tau_{zy})}{\partial z} + \frac{\partial(w\tau_{xz})}{\partial x} + \frac{\partial(w\tau_{yz})}{\partial y} + \frac{\partial(w\tau_{zz})}{\partial z}\right] + div(K\ grad\ T) + S_E \quad (5.12)$$

In this equation

$$E = i + \frac{1}{2}(u^2 + v^2 + w^2)$$

5.3 Background

Numerous numerical studies including CFD analysis have been done to predict the combustion and emission parameters in CI engines. Mattarelli et al. performed combustion simulations for natural gas-diesel dual fuel mode at full load and different rpms' (2000, 3000 and 4000 rpm) and found that there was a good agreement of simulated results with the experimental data [133]. Manimaran et al. performed CFD analysis of combustion and pollutant formation in a DI diesel engine at varying EGR, the predicted model showed reduction in flame temperature, NO_x while increase in soot with increase in EGR [134]. Hiwase et al. conducted multidimensional modeling with split multiple stage fuel injections in DI diesel engine. Strong effects on combustion characteristics with controlled pressure and temperature and reduction in NO_x was found using the split multiple stage fuel injection in comparison to that of the continuous fuel injection [135]. Huang et al. performed CFD simulations for diesel engine to study the influence of fuel variability on ignition delay. CFD simulations showed good agreement with experimental result for ignition timing and the influence of fuel variability on ignition timing [136]. Chintala et al. carried out CFD analysis in CI engine for hydrogen-diesel dual-fuel mode to study the effect of localized in-cylinder temperature on nitric oxide (NO) emission and concluded that the simulation results were confirming to the experimental results [137]. Soni et al. performed CFD analysis for methanol powered diesel engine using three different methods (initial swirl ratio, EGR and water addition). As per the numerical analysis the water addition method was found to be more efficient than other methods [138]. Lee et al. used CFD simulating diesel spray tip penetration with multiple injections and CR up to 100:1 using 'KIVA-3V Standard spray model' and the NGJBL model. Simulations results were found to be in good agreement with the experimental one [139]. Stylianidis et al. carried out CFD analysis of combustion of syngas in supercharged micro-pilot ignited dual-fuel engine. Results predicted for Ignition

delay time and laminar flame speed using the new mechanism were in agreement with those obtained by using other validated syngas mechanisms [140]. Neshat et al. performed simulation based on chemical kinetics mechanism for diesel engine using multi-zone model and found that the predicted results for the start of the combustion time, in-cylinder pressure, emissions and combustion duration were in good agreement with experimental data [141].

Numerical modeling of continuous and discrete phase fuel using commercial software Ansys fluent was carried out for diesel engine. Real time "in cylinder dynamic motion" simulation methodology was used in this study. All cases are validated with experimental results for diesel and duel fuel mode. The term duel fuel mode means, primary fuel was diesel and secondary fuel acetylene, which was mixed with air.

5.4 Diesel engine cylinder modeling

5.4.1 Pre processing

Cylinder geometry was created in Design modeler as per the original dimensions of the engine. In dynamic motion numerical modeling, different type of meshing is required because of motion of cell zones. Multi-zone mesh with face element sizing was used and total 2730 mesh elements were generated at TDC position. Discretized domain are present in figure 5.1 (a) and (b) respectively.

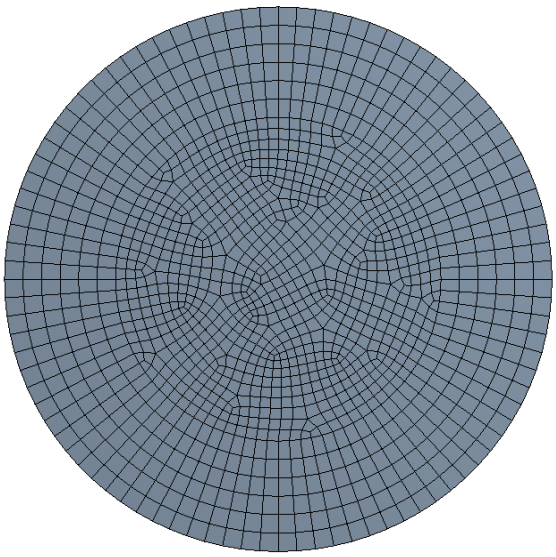

Top View

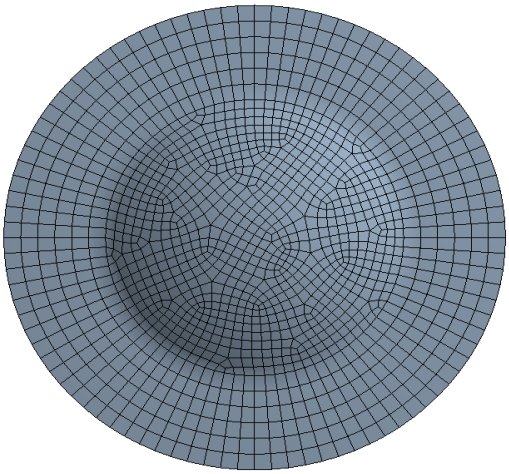

Bottom View

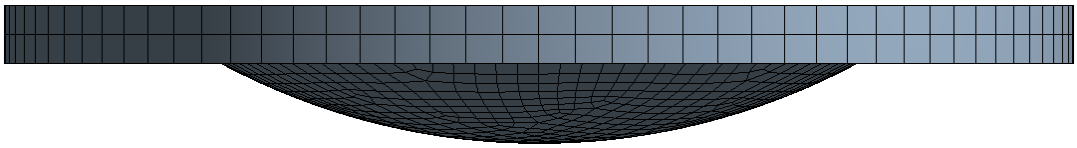

Front View

Fig. 5.1 (a) Meshed Domain for cylinder at TDC

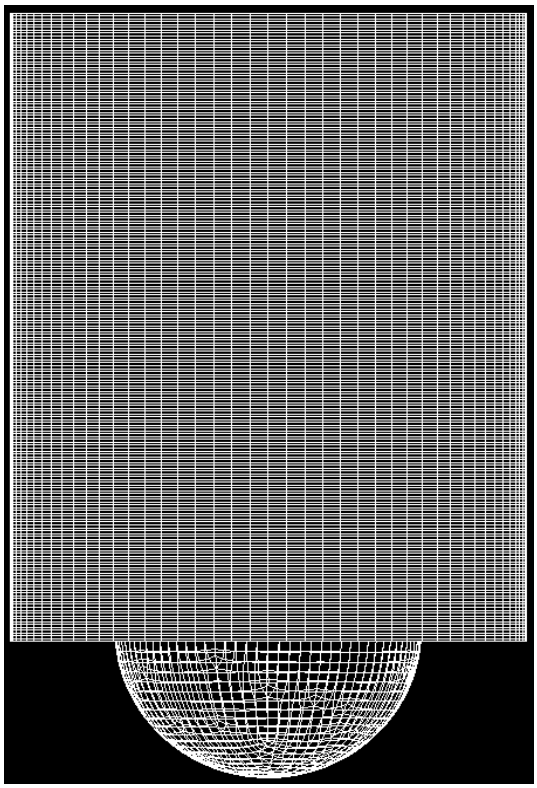

Fig.5.1 (b) Meshed Domain for cylinder at BDC

In this study, mechanisms of valves were not included in simulation, only compression and power stroke were simulated, so no inflow and out flow boundary conditions were applied.Fig.5.2 shows the boundary named selection for cylinder.

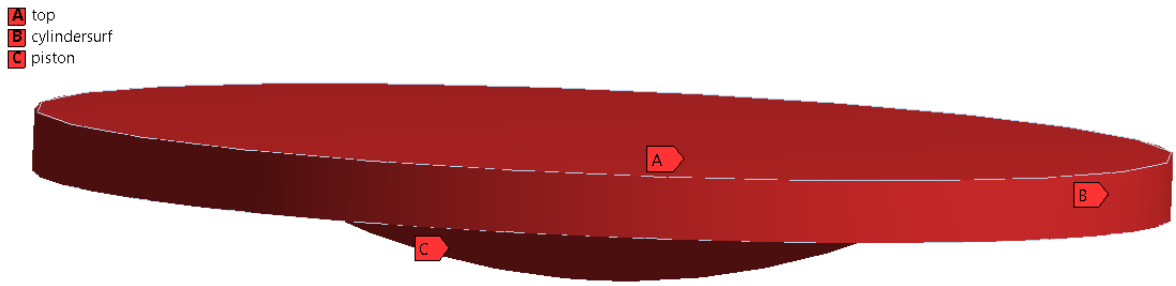

Fig.5.2 Boundaries named selection of Cylinder

5.4.2 Boundary conditions and solution techniques

Total 11 type of injectors are available in Ansys fluent, but for "in cylinder simulation" cone type injector was selected having droplet distribution in the form of cone shaped. In present study injection timing was set to 23° CA bTDC. All required technical specifications of injector are presented in table 5.1.

Table 5.1. Technical specifications of injector

Fuel Injection Pressure	210 bar
Injector	Three hole, centre conical spray
Nozzle Type	Pintle
Diameter	0.5 mm
Cone Angle	12
Fuel type	Diesel Liquid (Droplet)

Total nine equations are solved for unknown variables by converting them into discritize algebraic equations by finite volume method.

Energy and viscous models are used for CFD simulation, but for combustion modeling, species transport model is required to activate chemical modeling. For I.C engine numerical modeling, Auto ignition and discrete phase models are mandatory. Discrete phase models are

required to make injector. The two equation turbulence model k-e (RNG) was used in this study. The reason behind to use this model was its robustness and having the facility for swirl dominated flows in I.C engine.

Species transport models were used to simulate combustion in I.C engine. In this case, volumetric reaction mechanism was used for combustion. Inlet and thermal diffusion options were activated to improve the volumetric reaction in fuel and air. Coupling among chemistry during combustion and turbulence was selected for eddy-dissipation interaction mechanism available in Ansys fluent solver. Total five species participated in chemical mechanism which are following, diesel ($C_{10}H_{22}$), oxygen (O_2), carbon dioxide (CO_2), nitrogen (N_2), water droplet (H_2O). Two reactants and two products are simulated in this volumetric mechanism, with constant mixing rate of chemical reactions. Auto ignition model was also activated for combustion. In auto ignition model, ignition delay model made by **Hardenberg** was activated for fuel species diesel with constant activation energy and cetane number.

5.4.3 Dynamic Meshing

In the present study, transient simulation was performed therefore dynamic meshing was activated for real time simulation of diesel engine. As flow time increased, mesh decomposition in positive or reverse direction continuously changed. So, dynamic meshing with height based layering was used. **"In cylinder"** method was required to toggle on to complete body dynamics of engine movement. In "In cylinder" settings, some important data required to fulfill for dynamics of engine movement is presented in table 5.2.

Table 5.2"In-cylinder" data required for engine dynamics movement

Property	**Value**
Crank shaft speed (RPM)	1500
Starting crank angle (^{o})	360
Crank Period (^{o})	720
Crank Angle Step Size (^{o})	0.2
Crank Radius (mm)	40
Connecting Rod Length	234

Cylinder top was treated as stationary body (DOF was zero) and cylinder surface and piston head was assumed to be a rigid body, having movement in normal direction only and remaining DOF was zero.

5.4.4 Solution techniques

Fluent offers five methods for pressure-velocity coupling: SIMPLE, SIPMLEC, SIMPLER, PISO and Fractional Step Method (FSM) which make use of the segregated algorithm; while the Coupled scheme is based on the coupled solver. In the present study PISO algorithm with Skewness-Neighbour coupling are used to obtain the solution. The main idea of the PISO algorithm is to move the repeated calculations required by SIMPLE and SIMPLEC inside the solution stage of the pressure-correction equation. This process (momentum or "neighbor" correction) allows the corrected velocities to satisfy the continuity and momentum equations more accurately. While the PISO algorithm takes a little more CPU time per solver iteration, it dramatically decreases the number of iterations required for convergence, especially for transient problems.

5.5 Experimental validation of baseline diesel

Experimental validation was conducted for 100% load condition. Validation of p-Θ diagram was done for pressure data from 300º CA to 390º CA obtained from experiment. Fig. 5.3 shows the good agreement between experimental and simulation results.

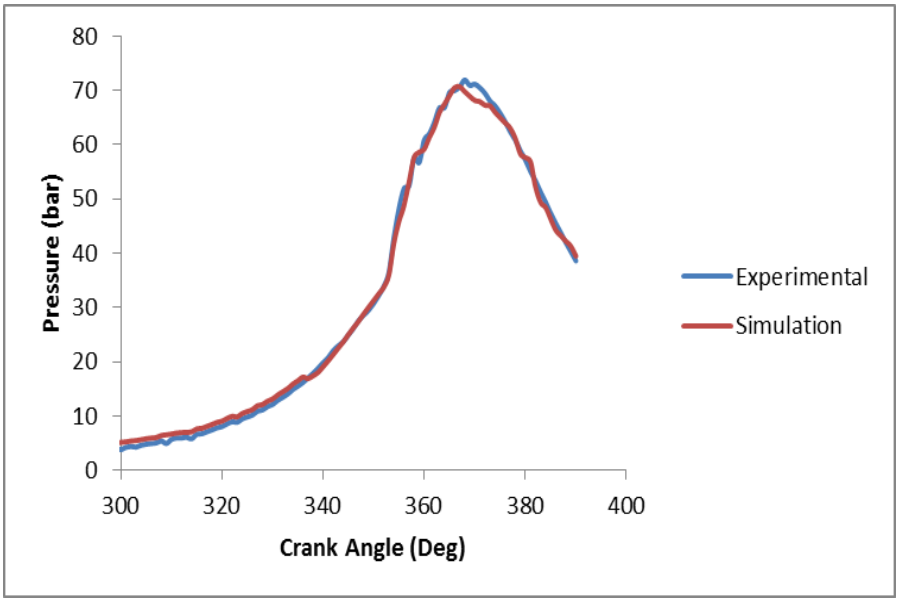

Fig. 5.3 Validation of pressure-crank angle diagram for baseline diesel at 100% load

5.5.1 Variation of temperature at different crank angle

Contours of temperature at different crank angle from 345° to 365° CA are shown in Fig. 5.4

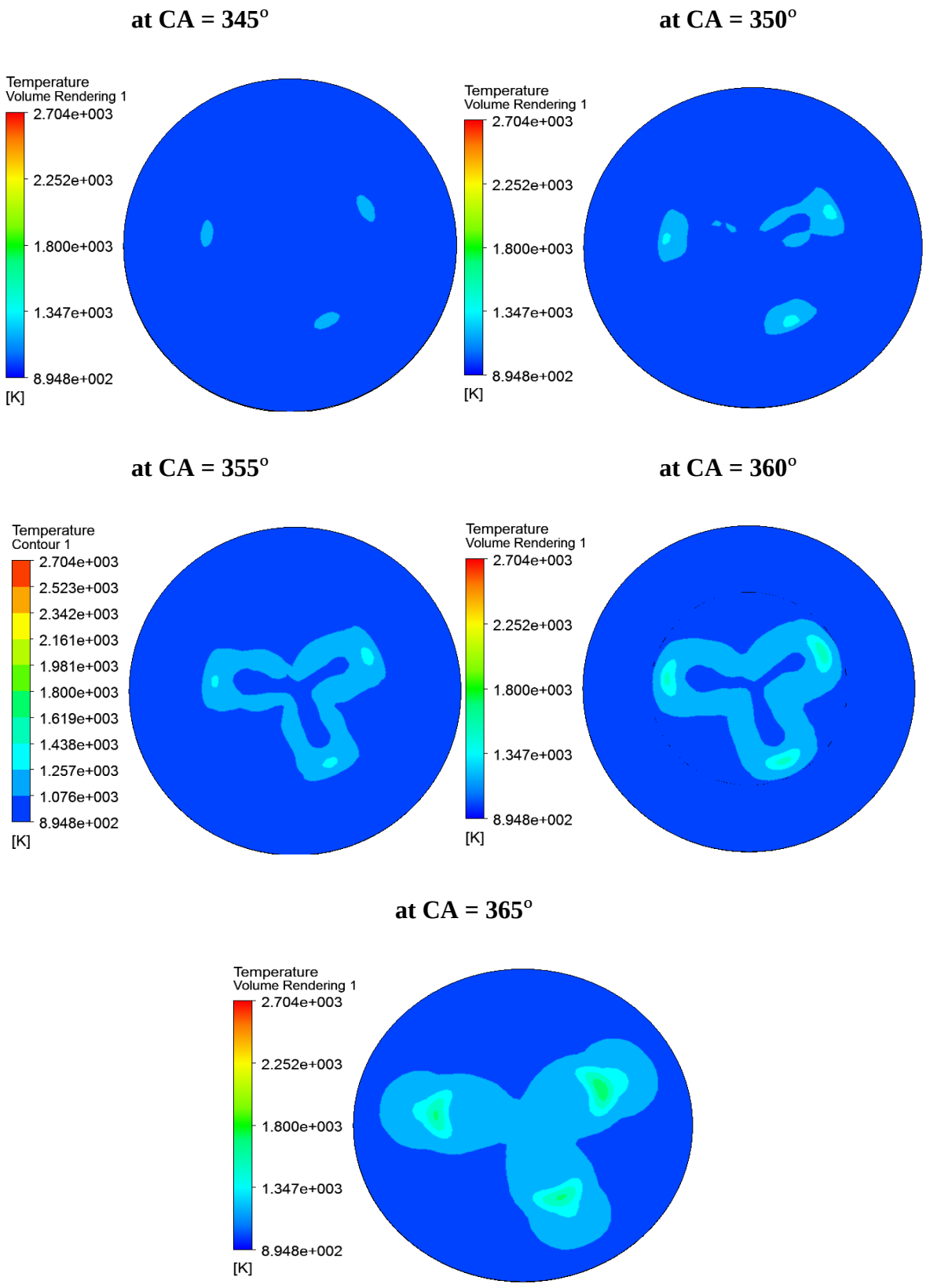

Fig.5.4 Contours of temperature at different crank angle for baseline diesel

5.5.2 NO_x mass fraction

Contours of NO_x mass fraction at different crank angle from 345° to 365° CA are shown in Fig. 5.5

at CA = 345° **at CA = 350°**

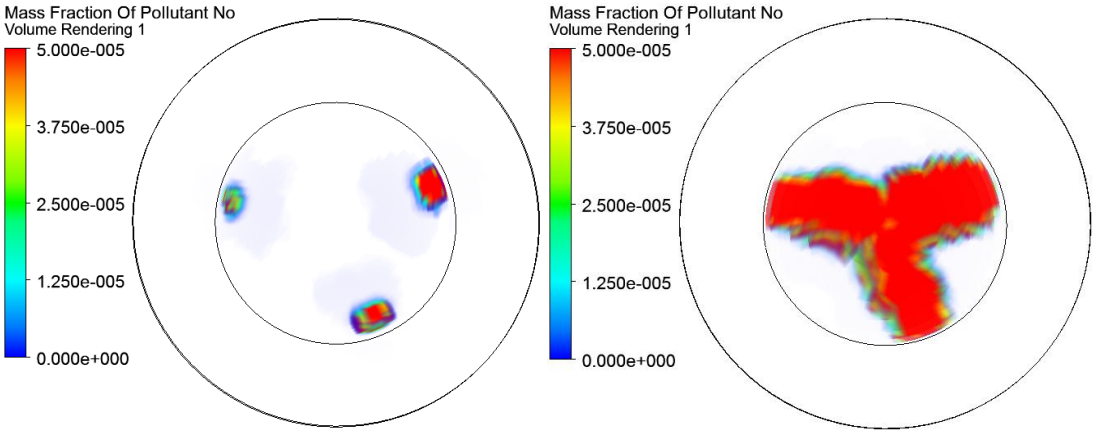

at CA = 355° **at CA = 360°**

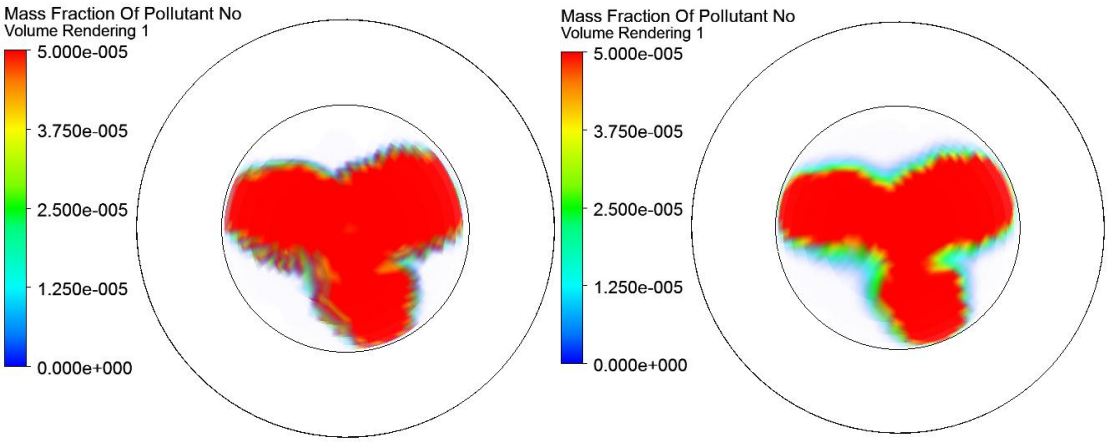

at CA = 365°

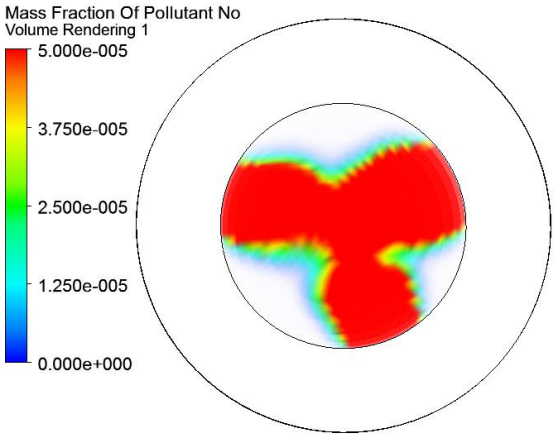

Fig.5.5 Contours for NO_x mass fraction at different crank angle for baseline diesel

5.6 Experimental validation for optimized dual fuel mode at 100% Load

In case of dual fuel mode fixed quantity of acetylene is mixed with air and then supplied into the combustion chamber. Diesel fuel is injected conventionally from injector. Two reactions are occurring in this CFD simulation so material and its species were changed as they were different in this case. Chemical reactions for both fuels are presented here.

Like diesel + air, acetylene + air reaction also occurred in engine cylinder, for this purpose a new species, acetylene was selected from fluid material list available in Ansys fluid data base in vapor phase. Factors involved in reactions are presented in table 3.

Experimental validation was conducted for 100% load condition for optimized dual fuel mode. Validation of p-Ɵ diagram was done for pressure data from 300º CA to 390º CA obtained from experiment. Fig. 5.6 shows the good agreement between experimental and simulation results. Though the peak pressure varies, the computational results are very close to the experimental. The computational model does not account for the pressure losses which are inevitable in mechanical systems. Moreover, it does not consider for limitations of pressure sensors that are used to measure the pressure inside the chamber. Considering the mechanical difficulties in measuring the pressure and limitations of numerical calculation to predict the exact behavior of real systems, the results obtained are considered to be very acceptable.

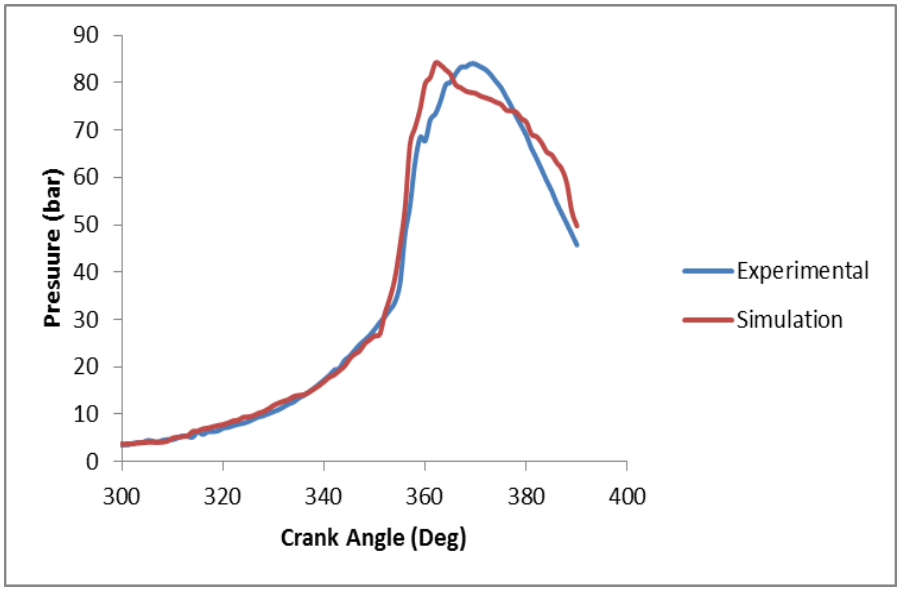

Fig. 5.6 Validation of pressure-crank angle diagram for dual fuel mode at 100% load

Table5.3 Species co-efficient for reactions

Reactants			**Products**		
Species	**Stoichiometric Coefficient**	**Rate Exponent**	**Species**	**Stoichiometric Coefficient**	**Rate Exponent**
Diesel Air (Reaction 1)					
$C_{10}H_{22}$	1	1	CO_2	10	0
O_2	15.5	1	H_2O	11	0
Acetylene Air (Reaction 2)					
C_2H_2	1	0.5	CO_2	2	0
O_2	2.5	1.25	H_2O	1	0

5.6.1 Variation of temperature at different crank angle

Contours of temperature at different crank angle from 345° to 365° CA are shown in Fig. 5.7

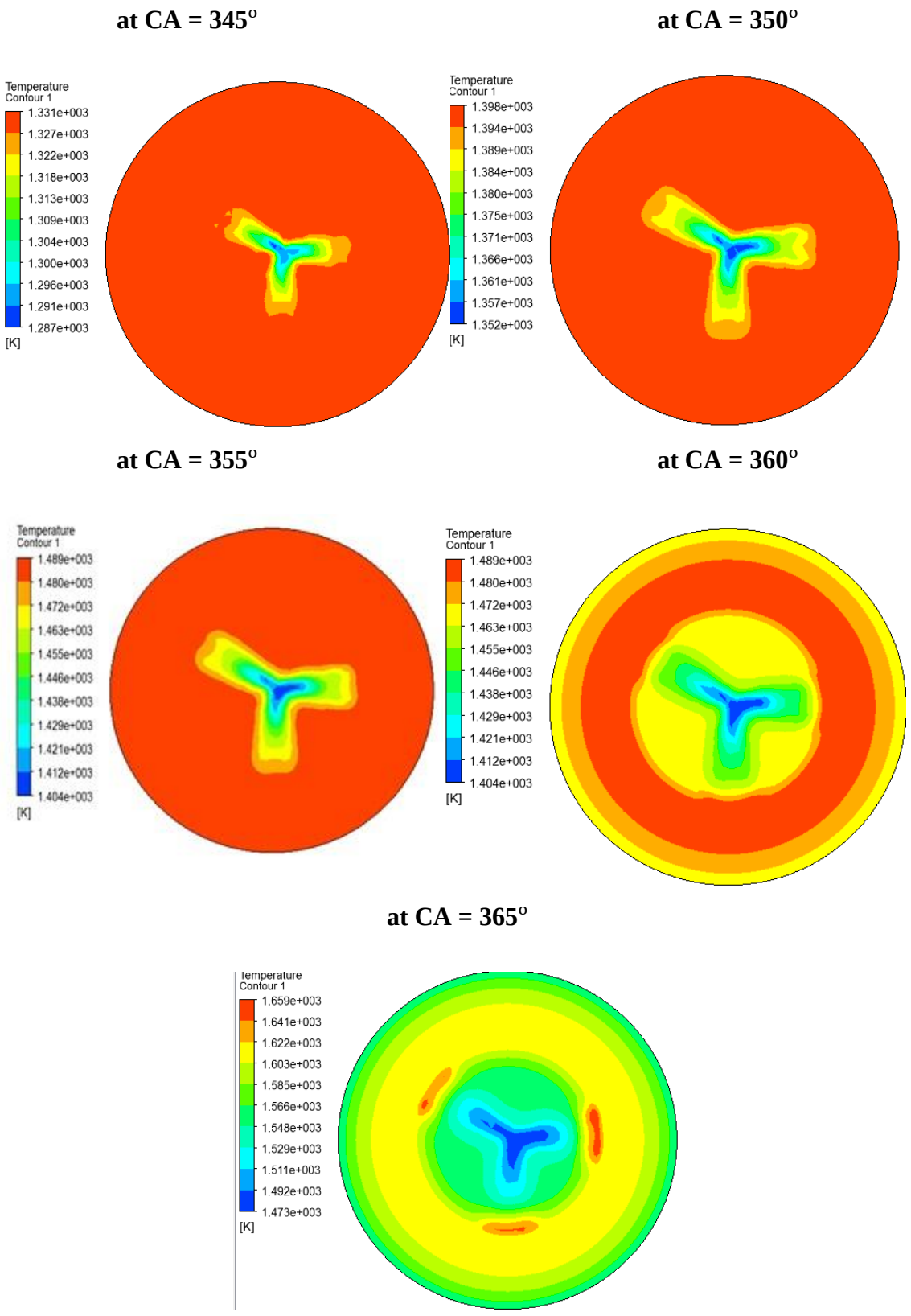

Fig.5.7 Contours of temperature at different crank angle for dual fuel mode

5.6.2 NO_x mass fraction

Contours of NO_x mass fraction at different crank angle from 345° to 365° CA are shown in Fig. 5.8

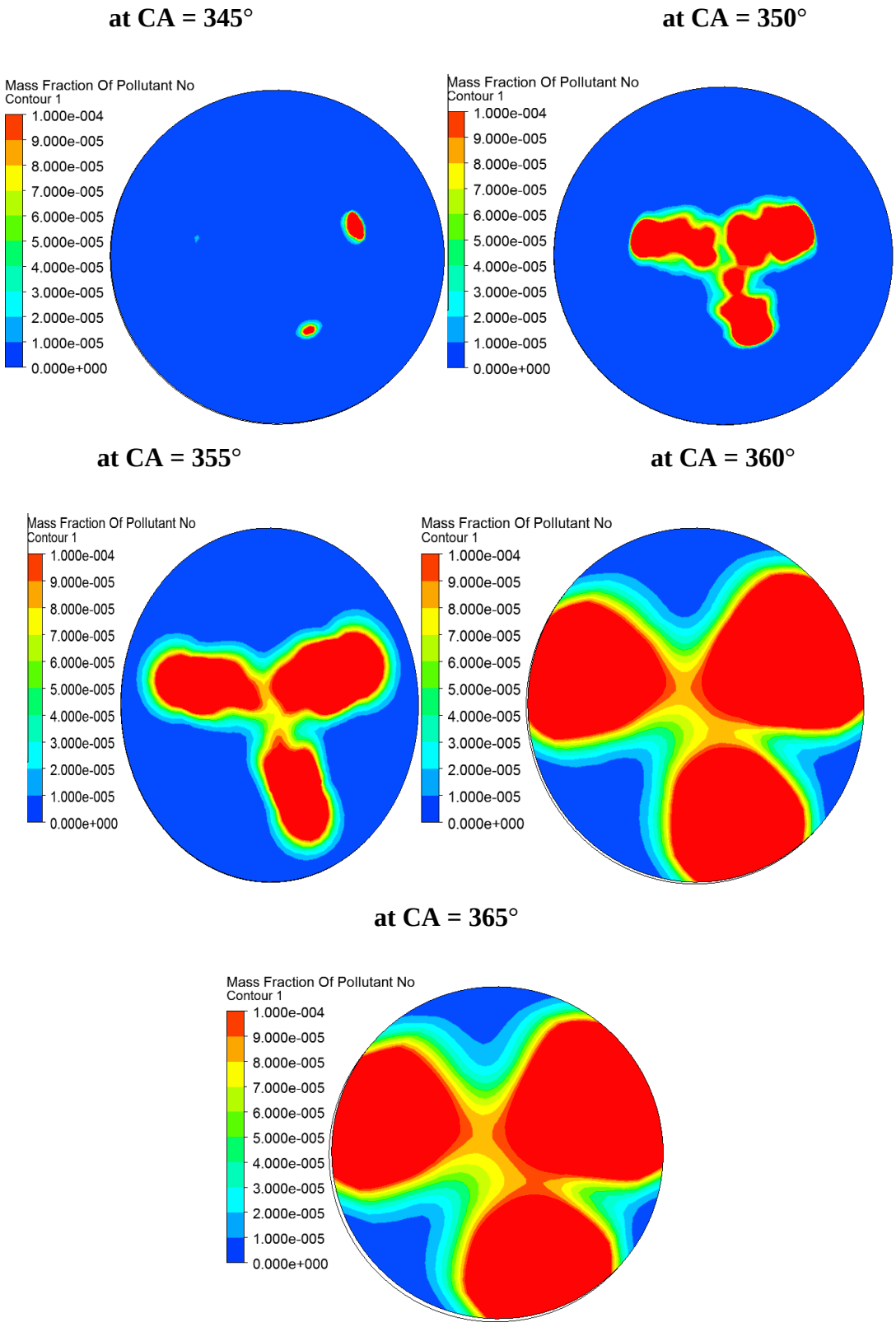

Fig.5.8 Contours for NO_x mass fraction at different crank angle for dual fuel mode

CHAPTER 6

CONCLUSIONS

6.1 Conclusions

The purpose of the current study was to test the feasibility of acetylene as a fuel in a stationary, single cylinder CI engine in dual fuel mode along with diesel using a constant flow rate acetylene generator. Hence, in the present research work, the experimental investigation of the performance, emission and combustion characteristics for a diesel-acetylene fuelled, stationary, water-cooled, constant speed, single cylinder, 4-stroke, compression ignition engine was carried out at varying (i) flow rates of acetylene, (ii) compression ratio (CR), (iii) injection pressure (IP) and (iv) injection timing (IT). To establish the baseline, the engine was operated with diesel alone. Optimum performance was obtained at CR 20 with IP 210 bar and IT 23^{o} bTDC. Investigations were carried out at these operating conditions in dual fuel mode with 60, 120, 180 and 240 LPH flow rate of acetylene. At these operating conditions best results were obtained with 120 LPH flow rate of acetylene and hence, all further investigations in dual fuel mode were done with 120 LPH of acetylene and the results were compared with those of baseline. From the experimental studies, the following conclusions have been drawn:

(a) Engine performance improved substantially in dual fuel mode mainly because of higher energy content of acetylene compared to that of diesel. BTE increased by around 2% in dual fuel mode both at CR20 and CR21 as compared to pure diesel mode. Brake thermal efficiency increased with increase in IP up to 200 bar beyond which it decreased. The highest BTE of 27.57% was found in dual fuel mode at 200 IP in comparison to BTE of 23.34% for baseline diesel. Brake thermal efficiency increased with advancing IT from 18^{o} to 23^{o} bTDC beyond which it decreased. The highest BTE of 27.57% was found in dual fuel mode at 23^{o} bTDC in comparison to BTE of 23.34% for baseline diesel.

(b) BSEC decreased in dual fuel mode. BSEC in dual fuel mode decreased with increase CR up to CR 21. BSEC decreased with increase in IP up to 200 bar beyond which it increased with increase in IP. Lowest BSEC in dual fuel mode was obtained at CR 21, 200 bar IP while the highest BSEC was in the case of baseline diesel. BSEC in dual fuel mode decreased with advancement of IT from 18^{o} to 23^{o} bTDC beyond which it increased with

further advancement in IT. Lowest BSEC in dual fuel mode was obtained at 23° bTDC while the highest BSEC was in the case of baseline diesel.

(c) EGT was found to decrease on increasing CR in dual fuel mode. The EGT in dual fuel mode decreased with increase in IP upto 200 bar. The lowest EGT was found at 200 bar IP in dual fuel mode. The EGT was found to decrease as the IT was advanced from 18° to 23° bTDC and the lowest EGT was obtained at 23° bTDC in dual fuel mode.

(d) Smoke emission in dual fuel mode was lower compared to diesel mode. Smoke decreased with increase in CR in dual fuel mode. Smoke in dual fuel mode was found decreasing with increase in IP up to 200 bar and on further increment of IP, smoke increased. Smoke in dual fuel mode was found decreasing with advancement of IT up to 23° bTDC and on further advancement of IT, smoke increased.

(e) NO_x emission was higher in dual fuel mode compared to diesel mode. In dual fuel mode NO_x emission increased with increase in CR. NO_x emission in dual fuel mode increased with increase in injection pressure up to 200 bar beyond which it decreased. NO_x emission in dual fuel mode increased with advancement of IT up to 23° bTDC beyond which it decreased.

(f) CO emission was found to be lower at high loads and higher at low loads in dual fuel mode compared to diesel mode. CO emission decreased with increase in CR in case of dual fuel mode. It was found that CO emission beyond 60% load was lower in case of dual fuel mode at CR21 than in baseline diesel mode. The CO emissions in dual fuel mode decreased with increase in IP up to 200 bar and hence, minimum CO emission was obtained at 200 bar for dual fuel mode. The CO emission in dual fuel mode decreased with advancement of IT from 18° to 23° bTDC and thus, minimum CO emission was obtained at 23° bTDC IT for dual fuel mode.

(g) HC in dual fuel mode was lower than diesel. In this case HC emission decreased with increase in CR until CR 20 above which it increased with increase in CR. The HC emissions in dual fuel mode decreased with increase in IP up to 200 bar and therefore, minimum HC emissions were obtained at 200 bar for dual fuel mode. The HC emissions in dual fuel mode decreased with advancement of IT from 18° to 23° bTDC hence, minimum HC emission was obtained at 23° bTDC IT for dual fuel mode.

(h) Maximum cylinder pressure in case of dual fuel mode was higher than that in diesel mode at different CRs. Cylinder pressure increased with increase in CR. The maximum cylinder pressure in dual fuel mode was observed at 200 bar and it was higher than that for

baseline diesel mode. The maximum cylinder pressure in dual fuel mode was also observed at 23º bTDC IT and it was higher than that for baseline diesel mode.

(i) Net Heat Release Rate (NHRR) in case of dual fuel mode was higher compared to that in diesel mode. Heat release rate increased with increase in CR. The highest net heat release rate in dual fuel mode was observed at 200 bar. The highest net heat release rate in dual fuel mode was observed at 23º bTDC IT and it was higher than that for baseline diesel mode.

(j) The rate of pressure rise increased with increase in CR in dual fuel mode. The maximum rate of pressure rise in dual fuel mode was observed at 200 bar. The maximum rate of pressure rise in dual fuel mode was observed at 23º bTDC IT and it was higher than that for baseline diesel mode.

(k) Numerical modeling of continuous and discrete phase fuel was carried out using software Ansys Fluent for diesel engine. Real time "in cylinder dynamic motion" simulation methodology was used in this study. Pressure-crank angle diagrams of optimized diesel and optimized dual fuel mode for 100% load were validated with experimental results. As per the validation of experimental data with CFD tool the results obtained were within limits.

It was therefore concluded that acetylene can be easily operated in dual fuel mode with improved performance and low CO, HC and smoke emissions at CR 21, IP of 200 bar and IT of 23º bTDC without any major modifications in engine. However, there was an increment in NO_x emissions in dual fuel mode as compared to that in diesel mode.

6.2 Scope for future work

1. Since everything was found to be favorable in dual fuel mode except for NO_x emissions, further research can be done to integrate a NO_x reduction technology e.g., EGR, SCR, LNT, etc. with this kind of set-up to improve final results.
2. The shape of the acetylene injector and its location can be varied to obtain improved induction in the cylinder to further enhance the performance.
3. Long term durability test (endurance test) and engine component wear analysis can be performed on acetylene operated engine for which an acetylene generator of much larger capacity might be required.
4. Since acetylene proved to be economical as compared to diesel, a detailed economic analysis can be performed to compare results of acetylene with those of diesel.
5. Though acetylene is highly inflammable and explosive in nature, still its feasibility on a multi-cylinder, variable speed, automobile engine can be done with on-board generation of acetylene.

APPENDIX-A: UNCERTAINITY ANALYSIS

Uncertainties in measurements may occur because of several reasons like instruments used and its calibration, experimental methods, the type of working conditions and environment, etc. In this way, uncertainty analysis becomes necessary to discover the exactness of the measured quantity.

The uncertainty associated in this experimental investigation with the measured parameters has been calculated as per the equipment manuals and the standard procedure proposed in theGuide to the expression of uncertainty in measurement (GUM)—JCGM 2008.Uncertainties in measurements were calculated using standard analytical and statistical techniques. Root-sum-square method was adopted, which is as given below.

Let X_1, X_2, X_3….. X_N, are the number of input measured parameters andx_1, x_2,x_3… x_N are their measured values. Let Y be the resulting parameter determined from the input quantities. The functional relationship between Y and X_1, X_2, X_3….. X_N, is denoted by f. If y is the estimation of measure, the combined standard uncertainty u(y) is because of the propagation of uncertainty in individual parameters associated to a measured value and Y. u(y) is given by the following relation,

$$u(y) = \sqrt{\sum_{i=1}^{N} \left(\frac{\partial f}{\partial x_i}\right)^2 * u(x_i)^2}$$

Uncertainty of main parameters in dual fuel mode at engine full load condition was determined using the above equation. All uncertainties of measurements were evaluated for a confidence level of 95 %. Uncertainties in properties like density, specific heat, etc. were neglected.

The maximum uncertainties in the measured and calculated results are given in Table A.1.

Table A.1 The accuracies of the measurements and the maximum uncertainties in the calculated results

Instrument	Parameter	Measuring range	Resolution	Accuracy	Max. Uncertainity
AVL Digas 444	CO (% vol)	0-10 % vol	0.01 % vol	< 0.6 % vol: ± 0.03 % vol ≥ 0.6 % vol: ± 5 % of indicated value	± 2.6%
	HC (ppm)	0- 20000 ppm vol	≤2000:1 ppm vol, > 2000:10 ppm vol	< 200 ppm vol: ±10 ppm vol ≥200 ppm vol: ± 5 % of indicated value	± 2.3%
	NO_X (ppm)	0- 5000 ppm vol	1 ppm vol	< 500 ppm vol:±50 ppm vol ≥ 500 ppm vol: ± 10 % of indicated value	± 2.1%
AVL DiSmoke 480 BT	Smoke (%)	0-100%	0.10%	-	± 1.5%
Calculated Parameters	BTE (%)	-	-	-	± 0.5%
	BSEC (kJ/kWh)	-	-	-	± 0.5%

APPENDIX-B: CFD CONTOURS

Diesel mass fraction in diesel mode

at CA = 345° **at CA = 350°**

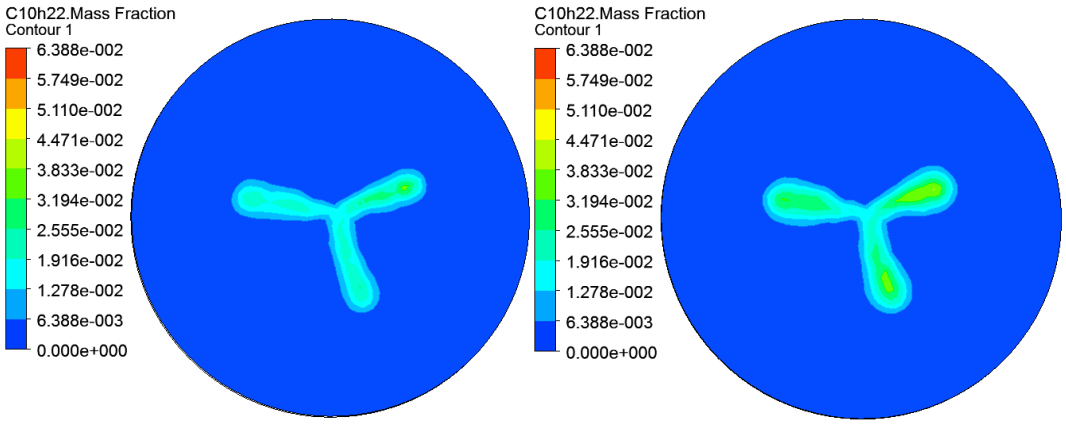

at CA = 355° **at CA = 360°**

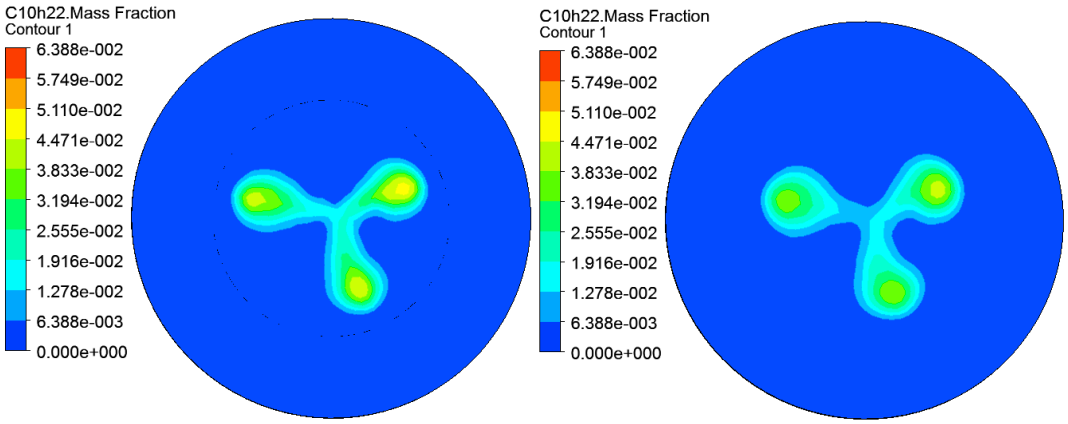

at CA = 365°

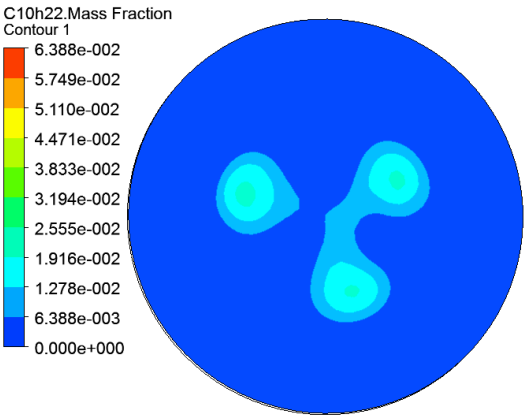

A.1 Contours for diesel mass fraction for diesel mode

Turbulence kinetic energy in diesel mode

at CA = 345° **at CA = 350°**

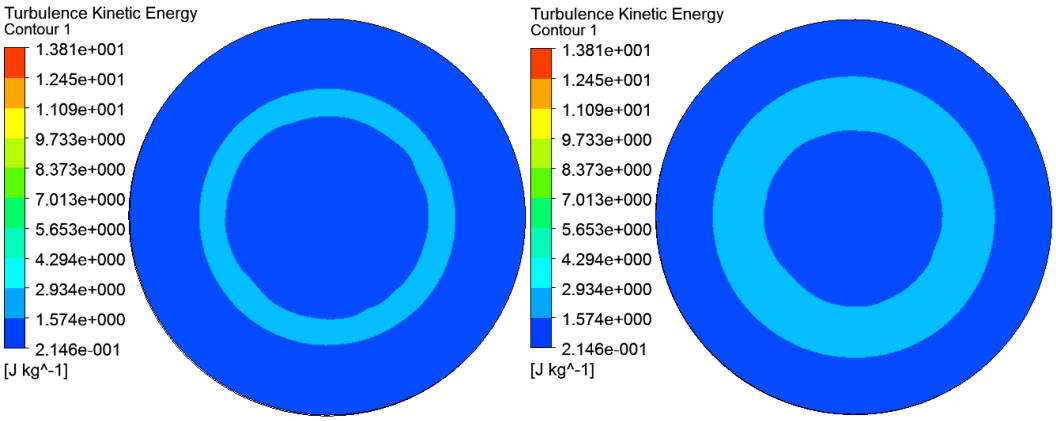

at CA = 355° **at CA = 360°**

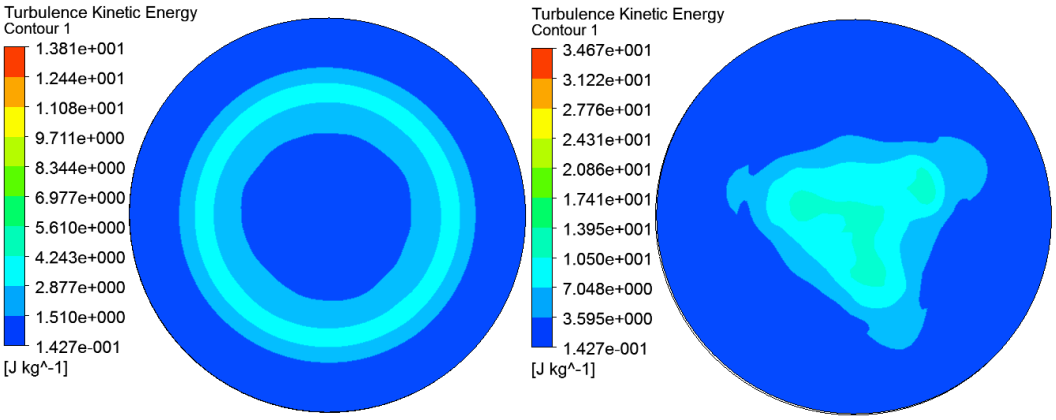

at CA = 365°

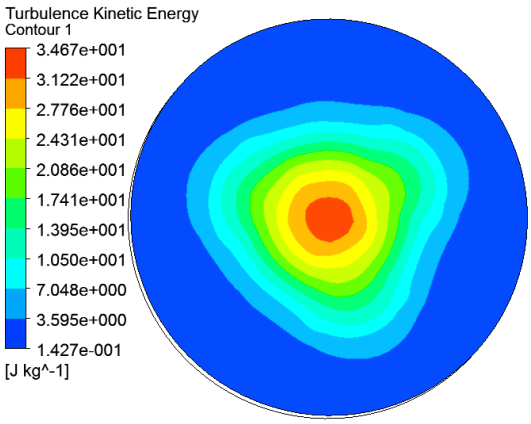

A.2 Contours for Turbulence kinetic energy for diesel mode

Acetylene mass fraction in dual fuel mode

at CA = 345° **at CA = 350°**

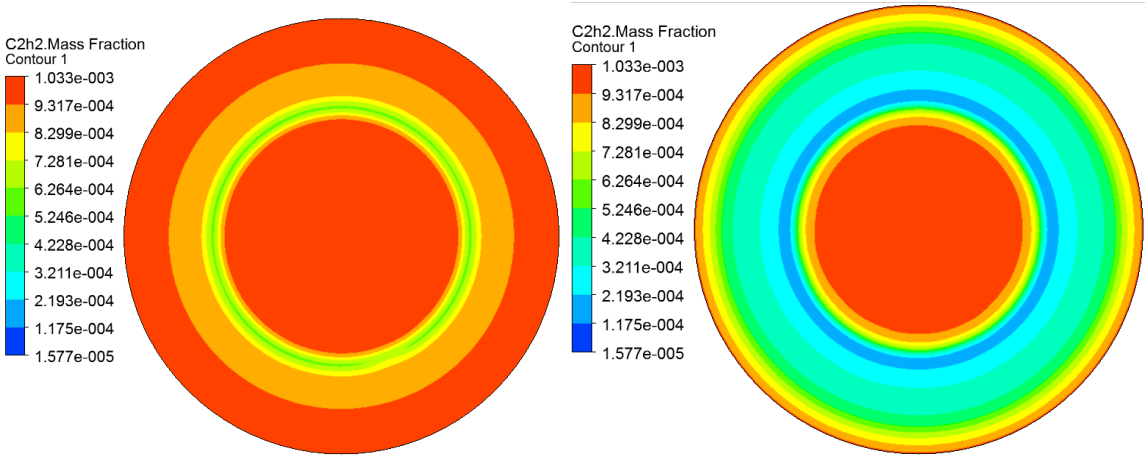

at CA = 355° **at CA = 360°**

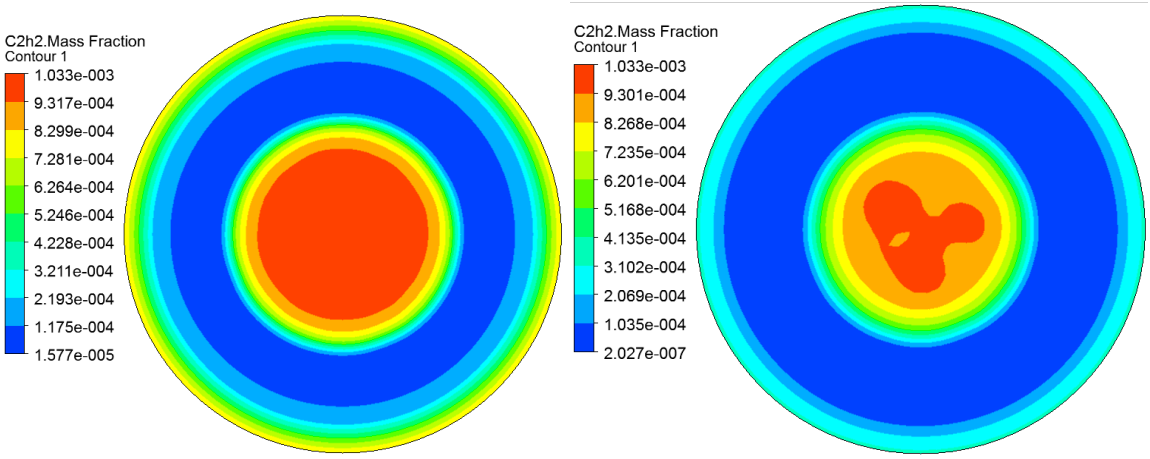

at CA = 365°

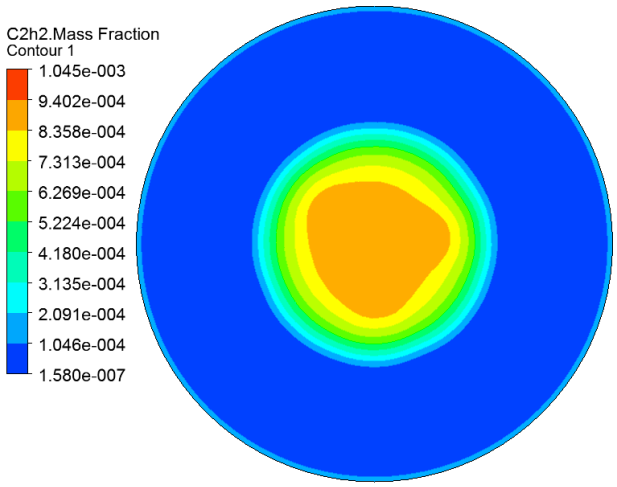

A.3 Contours for acetylene mass fraction in dual fuel mode

Diesel mass fraction in dual fuel mode

at CA = 345° **at CA = 350°**

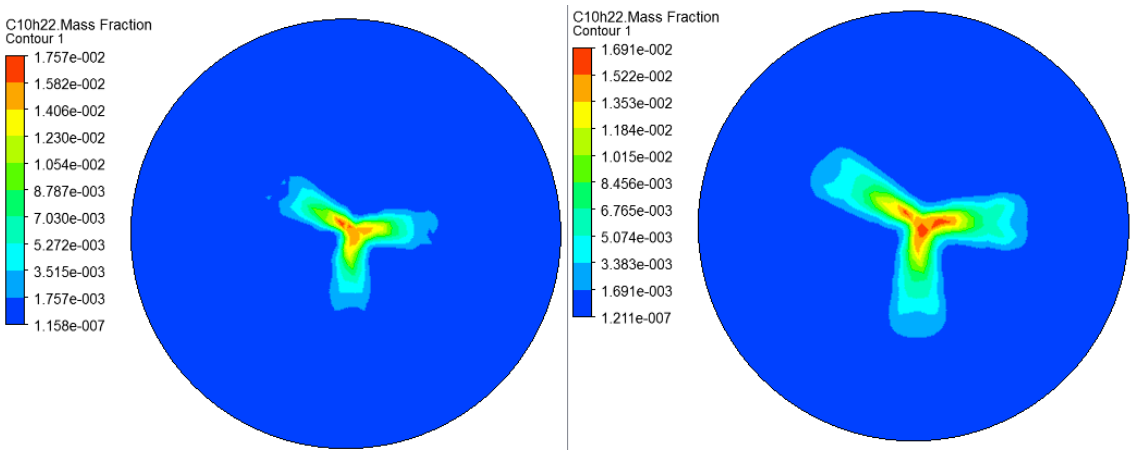

at CA = 355° **at CA = 360°**

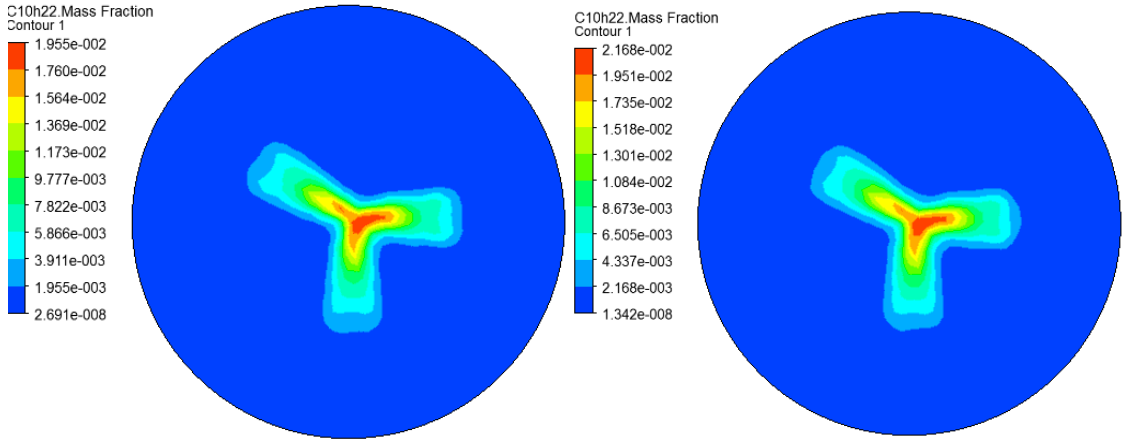

at CA = 365°

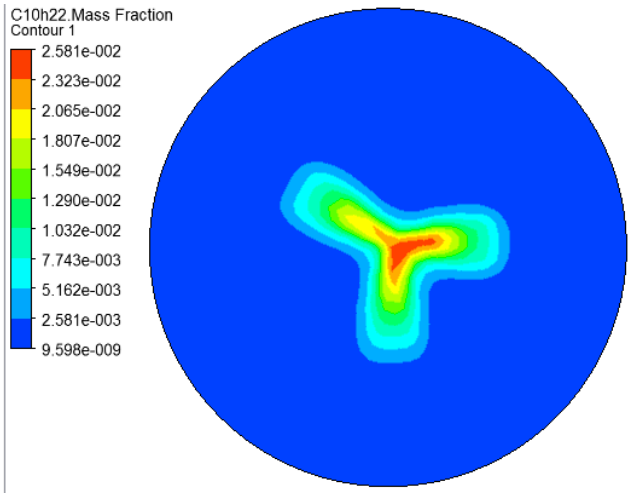

A.4 Contours for diesel mass fraction in dual fuel mode

Turbulence kinetic energy

at CA = 345° **at CA = 350°**

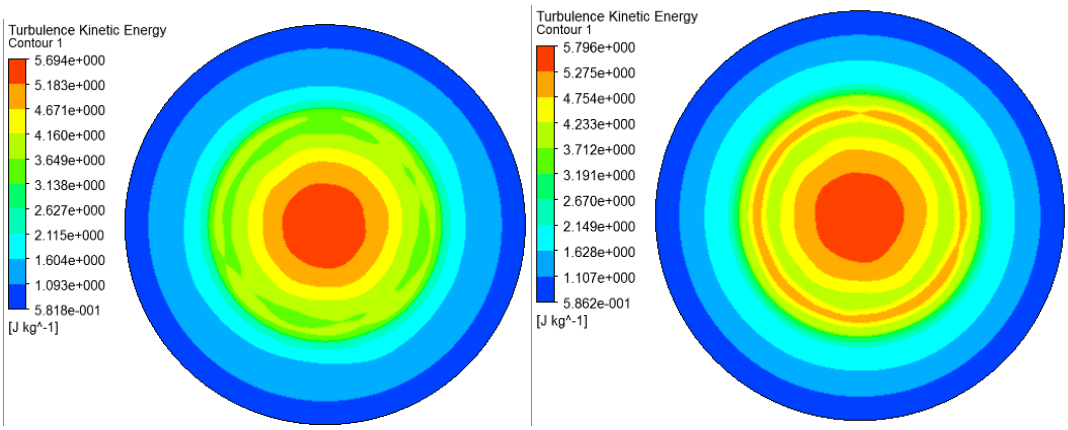

at CA = 355° **at CA = 360°**

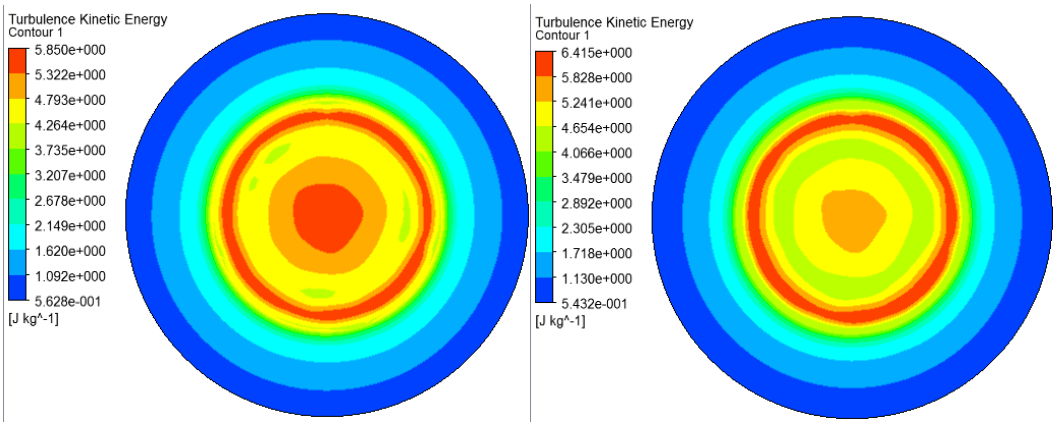

at CA = 365°

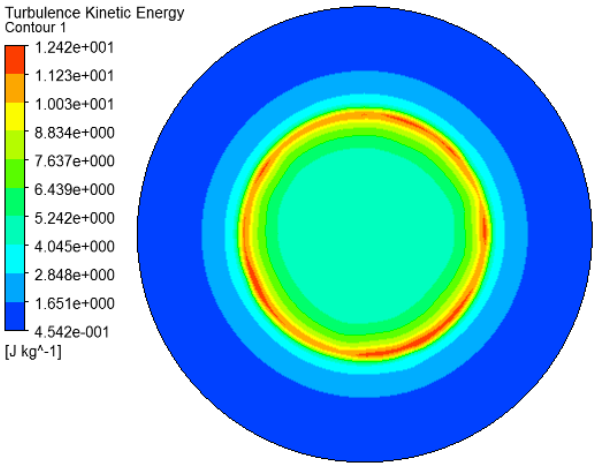

A.5 Contours for Turbulence kinetic energy for dual fuel mode

REFERENCES

1. EIA, International Energy Outlook 2016, 2016. doi:www.eia.gov/forecasts/ieo/pdf/0484(2016).pdf.
2. IEA, India Energy Outlook, World Energy Outlook Spec. Rep. (2015) 1–191. doi: https://www.iea.org/publications/freepublications/publication/IndiaEnergyOutlook_WEO2015.pdf.
3. Bansal N.K., 'BS VI fuel supply and quality up-gradation', Proceedings of ECMA's 9th International Conference on 'Emission Control Technology for Sustainable Growth' (ECT 2016), New Delhi, India, November 9-10, 2016, pp 199-20
4. Sugimoto K., 'Diesel emission controls utilizing advanced ceramic filter technologies', SAEINDIA Symposium on 'Fuels, Lubricants, Emission and After-Treatment Devices - The Road Ahead', Delhi, April 24-25, 2015.
5. Kumar S., 'PCRA – An integrated energy solution provider', SAEINDIA Symposium on 'Fuels, Lubricants, Emission and After-Treatment Devices - The Road Ahead', Delhi, April 24-25, 2015.
6. Dincer I, Zamfirescu C (2014) Chapter 3: Fossil Fuels and Alternatives. Adv Power Gener Syst 95–141. doi: http://dx.doi.org/10.1016/B978-0-12-383860-5.00003-1
7. Demirbas A (2007) Fuel Alternatives to Gasoline. Energy Sources, Part B 2:311–320. doi: 10.1080/15567240600629492
8. Sengupta B., 'Air pollution control from diesel based stationary engines (off road engines) – Inspection and monitoring issues', Proceedings of ECMA's 9th International Conference on 'Emission Control Technology for Sustainable Growth' (ECT 2016), New Delhi, India, November 9-10, 2016, pp 263-283.
9. Marathe N.V., 'Overview – Retrofitment of heavy duty diesel vehicles', Proceedings of ECMA's 9th International Conference on 'Emission Control Technology for Sustainable Growth' (ECT 2016), New Delhi, India, November 9-10, 2016, pp 315
10. H. Yu, The Design , Testing and Analysis of a Biofuel Micro-Trigeneration System Thesis by Hongdong Yu Doctor of Philosophy Sir Joseph Swan Centre for October 2012, (2012).
11. Klass D (2003) A critical assessment of renewable energy usage in the USA. Energy Policy 31:353–367. doi: 10.1016/S0301-4215(02)00069-1
12. Reitz RD (2013) Directions in internal combustion engine research. Combust Flame 160:1–8. doi: 10.1016/j.combustflame.2012.11.002

13. Choi CY, Reitz RD (1999) An experimental study on the effects of oxygenated fuel blends and multiple injection strategies on DI diesel engine emissions. Fuel 78:1303–1317. doi: 10.1016/S0016-2361(99)00058-7
14. Sonar D, Soni SL, Sharma D, Goyal R, Srivastava AK (2014) Performance and emission characteristics of a diesel engine with varying injection pressure and fuelled with raw mahua oil (preheated and blends) and mahua oil methyl ester. Clean Technol Environ Policy 17:1499–1511. doi: 10.1007/s10098-014-0874-9
15. http://www.araiindia.com/services_RnD_services_powertrain_alternative_fuel.asp (website of Automotive Research Association of India, ARAI)
16. Dorer V, Weber R, Weber A (2005) Performance assessment of fuel cell micro-cogeneration systems for residential buildings. Energy Build 37:1132–1146. doi: 10.1016/j.enbuild.2005.06.016
17. Onovwiona HI, Ugursal VI (2006) Residential cogeneration systems: Review of the current technology. Renew Sustain Energy Rev 10:389–431. doi: 10.1016/j.rser.2004.07.005
18. F.Rodica, D.Andrei, "Small scale cogeneration – a viable alternative for Romania", 4th IASME/WSEAS International conference on Energy, Environment, and Sustainable Development (EEESD 08), Algarve, Portugal, June 11- 13, 2008, pp 60-66. http://www.wseas.us/e-library/conferences/2008/algarve/EEESD/008-588-176.pdf
19. "Micro CHP Systems for Residential Applications", 2006, Final Report, United Technologies Research Center. http://nechpi.org/wp-content/uploads/2012/06/MICRO-CHP-UTC.pdf
20. B. Aoun, "Micro Combined Heat and Power Operating on Renewable Energy for Residential Building", Doctoral Thesis, Ecole Nationale Superieure des mines de Paris, 2008.https://tel.archives-ouvertes.fr/pastel-00005092/document
21. Onion G, Bodo LB (1983) Oxygenate fuels for diesel engines: A survey of world-wide activities. Biomass 3:77–133. doi: 10.1016/0144-4565(83)90001-X
22. Purushothaman K, Nagarajan G (2009) Performance, emission and combustion characteristics of a compression ignition engine operating on neat orange oil. Renew Energy 34:242–245. doi: 10.1016/j.renene.2008.03.012
23. Hossain AK, Davies PA (2010) Plant oils as fuels for compression ignition engines: A technical review and life-cycle analysis. Renew Energy 35:1–13. doi: 10.1016/j.renene.2009.05.009

24. Oner C, Altun Sehmus (2009) Biodiesel production from inedible animal tallow and an experimental investigation of its use as alternative fuel in a direct injection diesel engine. Appl Energy 86:2114–2120. doi: 10.1016/j.apenergy.2009.01.005
25. Pradhan P, Raheman H, Padhee D (2014) Combustion and performance of a diesel engine with preheated Jatropha curcas oil using waste heat from exhaust gas. Fuel 115:527–533. doi: 10.1016/j.fuel.2013.07.067
26. http://www.ethanolindia.net/ethanol.html
27. Jamuwa DK, Sharma D, Soni SL (2016) Experimental investigation of performance, exhaust emission and combustion parameters of stationary compression ignition engine using ethanol fumigation in dual fuel mode. Energy Convers Manag 115:221–231. doi: 10.1016/j.enconman.2016.02.055
28. Wang X, Cheung CS, Di Y, Huang Z (2012) Diesel engine gaseous and particle emissions fueled with diesel-oxygenate blends. Fuel 94:317–323. doi: 10.1016/j.fuel.2011.09.016
29. Padala S, Woo C, Kook S, Hawkes ER (2013) Ethanol utilisation in a diesel engine using dual-fuelling technology. Fuel 109:597–607. doi: 10.1016/j.fuel.2013.03.049
30. Aydin H, Ilkilic C (2010) Effect of ethanol blending with biodiesel on engine performance and exhaust emissions in a CI engine. Appl Therm Eng 30:1199–1204. doi: 10.1016/j.applthermaleng.2010.01.037
31. Lei J, Shen L, Bi Y, Chen H (2012) A novel emulsifier for ethanol-diesel blends and its effect on performance and emissions of diesel engine. Fuel 93:305–311. doi: 10.1016/j.fuel.2011.06.013
32. Boretti A (2012) Advantages of converting Diesel engines to run as dual fuel ethanol-Diesel. Appl Therm Eng 47:1–9. doi: 10.1016/j.applthermaleng.2012.04.037
33. Bayraktar H (2008) An experimental study on the performance parameters of an experimental CI engine fueled with diesel-methanol-dodecanol blends. Fuel 87:158–164. doi: 10.1016/j.fuel.2007.04.021
34. Wei L, Yao C, Han G, Pan W (2016) Effects of methanol to diesel ratio and diesel injection timing on combustion, performance and emissions of a methanol port premixed diesel engine. Energy 95:223–232. doi: 10.1016/j.energy.2015.12.020
35. Wang Q, Wei L, Pan W, Yao C (2015) Investigation of operating range in a methanol fumigated diesel engine. Fuel 140:164–170. doi: 10.1016/j.fuel.2014.09.067

36. Wei H, Yao C, Pan W, et al (2017) Experimental investigations of the effects of pilot injection on combustion and gaseous emission characteristics of diesel/methanol dual fuel engine. Fuel 188:427–441. doi: 10.1016/j.fuel.2016.10.056
37. Zhang ZH, Cheung CS, Yao CD (2013) Influence of fumigation methanol on the combustion and particulate emissions of a diesel engine. Fuel 111:442–448. doi: 10.1016/j.fuel.2013.05.014
38. http://www.daviddarling.info/encyclopedia/H/AE_hydrogen.html
39. Sukjit E, Herreros JM, Dearn KD, et al (2013) Effect of hydrogen on butanol-biodiesel blends in compression ignition engines. Int J Hydrogen Energy 38:1624–1635. doi: 10.1016/j.ijhydene.2012.11.061
40. Yadav VS, Sharma D, Soni SL (2015) Performance and combustion analysis of hydrogen-fuelled C.I. engine with EGR. Int J Hydrogen Energy 40:4382–4391. doi: 10.1016/j.ijhydene.2015.01.162
41. Yadav VS, Soni SL, Sharma D (2014) Engine performance of optimized hydrogen-fueled direct injection engine. Energy 65:116–122. doi: 10.1016/j.energy.2013.12.007
42. Santoso WB, Bakar RA, Nur A (2013) Combustion characteristics of diesel-hydrogen dual fuel engine at low load. Energy Procedia 32:3–10. doi: 10.1016/j.egypro.2013.05.002
43. Ashok B, Denis Ashok S, Ramesh Kumar C (2015) LPG diesel dual fuel engine - A critical review. Alexandria Eng J 54:105–126. doi: 10.1016/j.aej.2015.03.002
44. Cernat A, Pana C, Negurescu N, Nutu C (2016) On Combustion of Diesel Fuel Drops at LPG Fuelling by Diesel Gas Method. Procedia Technol 22:705–712. doi: 10.1016/j.protcy.2016.01.146
45. Tira HS, Herreros JM, Tsolakis A, Wyszynski ML (2012) Characteristics of LPG-diesel dual fuelled engine operated with rapeseed methyl ester and gas-to-liquid diesel fuels. Energy 47:620–629. doi: 10.1016/j.energy.2012.09.046
46. Elnajjar E, Hamdan MO, Selim MYE (2013) Experimental investigation of dual engine performance using variable LPG composition fuel. Renew Energy 56:110–116. doi: 10.1016/j.renene.2012.09.048
47. Saleh HE (2008) Effect of variation in LPG composition on emissions and performance in a dual fuel diesel engine. Fuel 87:3031–3039. doi: 10.1016/j.fuel.2008.04.007

48. Ambarita H (2017) Performance and emission characteristics of a small diesel engine run in dual-fuel (diesel-biogas) mode. Case Stud Therm Eng 10:179–191. doi: 10.1016/j.csite.2017.06.003
49. Chandra R, Vijay VK, Subbarao PM V, Khura TK (2011) Performance evaluation of a constant speed IC engine on CNG, methane enriched biogas and biogas. Appl Energy 88:3969–3977. doi: 10.1016/j.apenergy.2011.04.032
50. Bora BJ, Saha UK, Chatterjee S, Veer V (2014) Effect of compression ratio on performance, combustion and emission characteristics of a dual fuel diesel engine run on raw biogas. Energy Convers Manag 87:1000–1009. doi: 10.1016/j.enconman.2014.07.080
51. Barik D, Murugan S (2014) Investigation on combustion performance and emission characteristics of a DI (direct injection) diesel engine fueled with biogas-diesel in dual fuel mode. Energy 72:760–771. doi: 10.1016/j.energy.2014.05.106
52. Yilmaz IT, Gumus M (2017) Investigation of the effect of biogas on combustion and emissions of TBC diesel engine. Fuel 188:69–78. doi: 10.1016/j.fuel.2016.10.034
53. Liu J, Yang F, Wang H, et al (2013) Effects of pilot fuel quantity on the emissions characteristics of a CNG/diesel dual fuel engine with optimized pilot injection timing. Appl Energy 110:201–206. doi: 10.1016/j.apenergy.2013.03.024
54. Wang Z, Zhao Z, Wang D, et al (2016) Impact of pilot diesel ignition mode on combustion and emissions characteristics of a diesel/natural gas dual fuel heavy-duty engine. Fuel 167:248–256. doi: 10.1016/j.fuel.2015.11.077
55. Hilden DL, Stebar RF (1979) Evaluation of acetylene as a Spark Ignition engine fuel, Energy Res Soc Sci. 3:59–71.
56. Lakshmanan T, Nagarajan G (2010) Experimental investigation on dual fuel operation of acetylene in a DI diesel engine. Fuel Process Technol 91:496–503. doi: 10.1016/j.fuproc.2009.12.010
57. Price JWH (2006) An acetylene cylinder explosion: A most probable cause analysis. Eng Fail Anal 13:705–715. doi: 10.1016/j.engfailanal.2005.04.014
58. Lakshmanan T, Nagarajan G (2009) Performance and Emission of Acetylene-Aspirated Diesel Engine. Jordan Journal of Mechanical and Industrial Engineering 3:125–130.
59. Lakshmanan T, Nagarajan G (2010) Experimental investigation of timed manifold injection of acetylene in direct injection diesel engine in dual fuel mode. Energy 35:3172–3178. doi: 10.1016/j.energy.2010.03.055

60. Lakshmanan T, Nagarajan G (2011) Study on using acetylene in dual fuel mode with exhaust gas recirculation. Energy 36:3547–3553. doi: 10.1016/j.energy.2011.03.061
61. Lakshmanan T, Nagarajan G (2011) Experimental investigation of port injection of acetylene in di diesel engine in dual fuel mode. Fuel 90:2571–2577. doi: 10.1016/j.fuel.2011.03.039
62. Swami Nathan S, Mallikarjuna JM, Ramesh A (2010) Effects of charge temperature and exhaust gas re-circulation on combustion and emission characteristics of an acetylene fuelled HCCI engine. Fuel 89:515–521. doi: 10.1016/j.fuel.2009.08.032
63. Wulff J, Hulett.W, Sunggyu L, Internal combustion system using acetylene fuel. United States Patent No 6076487. June 20, 2000
64. Wulff J. et al, Dual Fuel composition including acetylene for use with diesel and other internal combustion engines,patent no: US 6,287,351 B1,patent date:Sep11,2001.
65. Sudheesh K, Mallikarjuna JM (2010) Effect of cooling water flow direction on performance of an acetylene fuelled HCCI engine.Indian Journal of Engineering & Materials Sciences 17:79–85 pp. 79-85
66. Sharma PK, Kuinkel H, Shrestha P, & Poudel S (2012) Use of Acetylene as an Alternative fuel in IC Engine, Rentech Symposium Compendium,19-22.
67. Mahla SK, Kumar S, Shergill H, Kumar A (2012)Study the Performance Characteristics of Acetylene Gas In Dual FuelEngine With Diethyl Ether Blends, International Journal on Emerging Technologies 3(1),80-83
68. Srivastava AK, Sharma D, Soni SL (2013), Experimental Investigation of Acetylene as an Alternative Fuel for C.I Engine.International Conference on Alternative Fuels for I.C.Engines 2013 MNIT Jaipur. ISBN 978-81-924029-8-7
69. Brusca S, Lanzafame R, Marino Cugno Garrano A, Messina M (2014) On the possibility to run an internal combustion engine on acetylene and alcohol. Energy Procedia 45:889–898. doi: 10.1016/j.egypro.2014.01.094
70. Behera P, Murugan S, Nagarajan G (2014) Dual fuel operation of used transformer oil with acetylene in a di diesel engine. Energy Convers Manag 87:840–847. doi: 10.1016/j.enconman.2014.07.034
71. Sudheesh K, Mallikarjuna JM (2010) Diethyl ether as an ignition improver for biogas homogeneous charge compression ignition (HCCI) operation - An experimental investigation. Energy 35:3614–3622. doi: 10.1016/j.energy.2010.04.052

72. Rao GA, Raju AVS, Rajulu KG, Rao CVM (2010) Performance evaluation of a dual fuel engine (diesel +LPG). Indian journal of science and technology Vol. 3 No. 3 pp 235-237. ISSN: 0974- 6846.
73. Galal MG, Aal MMA, El Kady M a. (2002) A comparative study between diesel and dual-fuel engines: Performance and emissions. Combust Sci Technol 174:241–256. doi: 10.1080/713712964
74. Sahoo BB, Sahoo N, Saha UK (2009) Effect of engine parameters and type of gaseous fuel on the performance of dual-fuel gas diesel engines-A critical review. Renew Sustain Energy Rev 13:1151–1184. doi: 10.1016/j.rser.2008.08.003
75. Mustafi NN, Raine RR, Verhelst S (2013) Combustion and emissions characteristics of a dual fuel engine operated on alternative gaseous fuels. Fuel 109:669–678. doi: 10.1016/j.fuel.2013.03.007
76. Muralidharan K, Vasudevan D (2011) Performance, emission and combustion characteristics of a variable compression ratio engine using methyl esters of waste cooking oil and diesel blends. Appl Energy 88:3959–3968. doi: 10.1016/j.apenergy.2011.04.014
77. Sivaramakrishnan K (2017) Investigation on performance and emission characteristics of a variable compression multi fuel engine fuelled with Karanja biodiesel – diesel blend. Egypt J Pet 1–10. doi: 10.1016/j.ejpe.2017.03.001
78. Hariram V, Vagesh Shangar R (2015) Influence of compression ratio on combustion and performance characteristics of direct injection compression ignition engine. Alexandria Eng J 54:807–814. doi: 10.1016/j.aej.2015.06.007
79. Nagaraja S, Sooryaprakash K, Sudhakaran R (2015) Investigate the Effect of Compression Ratio Over the Performance and Emission Characteristics of Variable Compression Ratio Engine Fueled with Preheated Palm Oil - Diesel Blends. Procedia Earth Planet Sci 11:393–401. doi: 10.1016/j.proeps.2015.06.038
80. De B, Panua RS (2014) An experimental study on performance and emission characteristics of vegetable oil blends with diesel in a direct injection variable compression ignition engine. Procedia Eng 90:431–438. doi: 10.1016/j.proeng.2014.11.873
81. Senthil R, Silambarasan R, Ravichandiran N (2015) Influence of injection timing and compression ratio on performance, emission and combustion characteristics of Annona methyl ester operated diesel engine. Alexandria Eng J 54:295–302. doi: 10.1016/j.aej.2015.05.008

82. Lal S, Mohapatra SK (2017) The effect of compression ratio on the performance and emission characteristics of a dual fuel diesel engine using biomass derived producer gas. Appl Therm Eng 119:63–72. doi: 10.1016/j.applthermaleng.2017.03.038
83. Tangoz S, Akansu SO, Kahraman N, Malkoc Y (2015) Effects of compression ratio on performance and emissions of a modified diesel engine fueled by HCNG. Int J Hydrogen Energy 40:15374–15380. doi: 10.1016/j.ijhydene.2015.02.058
84. Hirkude J, Padalkar AS (2014) Experimental investigation of the effect of compression ratio on performance and emissions of CI engine operated with waste fried oil methyl ester blend. Fuel Process Technol 128:367–375. doi: 10.1016/j.fuproc.2014.07.026
85. El-Kassaby M, Nemit-Allah MA (2013) Studying the effect of compression ratio on an engine fueled with waste oil produced biodiesel/diesel fuel. Alexandria Eng J 52:1–11. doi: 10.1016/j.aej.2012.11.007
86. Jindal S, Nandwana BP, Rathore NS, Vashistha V (2010) Experimental investigation of the effect of compression ratio and injection pressure in a direct injection diesel engine running on Jatropha methyl ester. Appl Therm Eng 30:442–448. doi: 10.1016/j.applthermaleng.2009.10.004
87. Sastry GRK, Deb M, Panda JK (2015) Effect of Fuel Injection Pressure, Isobutanol and Ethanol Addition on Performance of Diesel-biodiesel Fuelled D.I. Diesel Engine. Phys Procedia 66:81–84. doi: 10.1016/j.egypro.2015.02.043
88. Aalam CS, Saravanan CG, Anand BP (2016) Impact of high fuel injection pressure on the characteristics of CRDI diesel engine powered by mahua methyl ester blend. Appl Therm Eng 106:702–711. doi: 10.1016/j.applthermaleng.2016.05.176
89. Quadri SAP, Masood M, Ravi Kumar P (2015) Effect of pilot fuel injection operating pressure in hydrogen blended compression ignition engine: An experimental analysis. Fuel 157:279–284. doi: 10.1016/j.fuel.2015.04.068
90. Liu J, Yao A, Yao C (2015) Effects of diesel injection pressure on the performance and emissions of a HD common-rail diesel engine fueled with diesel/methanol dual fuel. Fuel 140:192–200. doi: 10.1016/j.fuel.2014.09.109
91. Gumus M, Sayin C, Canakci M (2012) The impact of fuel injection pressure on the exhaust emissions of a direct injection diesel engine fueled with biodiesel-diesel fuel blends. Fuel 95:486–494. doi: 10.1016/j.fuel.2011.11.020

92. Ryu K (2013) Effects of pilot injection pressure on the combustion and emissions characteristics in a diesel engine using biodiesel-CNG dual fuel. Energy Convers Manag 76:506–516. doi: 10.1016/j.enconman.2013.07.085
93. Nanthagopal K, Ashok B, Raj RTK (2016) Influence of fuel injection pressures on Calophyllum inophyllum methyl ester fuelled direct injection diesel engine. Energy Convers Manag 116:165–173. doi: 10.1016/j.enconman.2016.03.002
94. Shehata MS, Attia AMA, Abdel Razek SM (2015) Corn and soybean biodiesel blends as alternative fuels for diesel engine at different injection pressures. Fuel 161:49–58. doi: 10.1016/j.fuel.2015.08.037
95. Sayin C (2011) An Experimental Investigation on the Effect of Injection Pressure on the Exhaust Emissions of a Diesel Engine Fueled with Methanol-diesel Blends. Energy Sources, Part A Recover Util Environ Eff 33:2206–2217. doi: 10.1080/15567030903419471
96. Purushothaman K, Nagarajan G (2009) Effect of injection pressure on heat release rate and emissions in CI engine using orange skin powder diesel solution. Energy Convers Manag 50:962–969. doi: 10.1016/j.enconman.2008.12.030
97. Behera P, Murugan S (2012) Studies on a Diesel Engine Fueled with Used Transformer Oil at Different Fuel Injection Nozzle Opening Pressures. Int J Ambient Energy 750:121119094216005. doi: 10.1080/01430750.2012.740421
98. Channapattana S V., Pawar AA, Kamble PG (2015) Effect of Injection Pressure on the Performance and Emission Characteristics of VCR engine using Honne Biodiesel as a Fuel. Mater Today Proc 2:1316–1325. doi: 10.1016/j.matpr.2015.07.049
99. Syed A, Quadri SAP, Rao GAP, Mohd W (2017) Experimental investigations on DI (direct injection) diesel engine operated on dual fuel mode with hydrogen and mahua oil methyl ester (MOME) as injected fuels and effects of injection opening pressure. Appl Therm Eng 114:118–129. doi: 10.1016/j.applthermaleng.2016.11.152
100. Anbarasu A, Karthikeyan A (2015) Effect of injection pressure on the performance and emission characteristics of CI engine using canola emulsion fuel. Int J Ambient Energy 7269:1–6. doi: 10.1080/01430750.2015.1092472 1.
101. Balusamy T, Marappan R (2010) Effect of Injection Time and Injection Pressure on CI Engine Fuelled with Methyl Ester of Thevetia Peruviana Seed Oil. Int J Green Energy 7:397–409. doi: 10.1080/15435075.2010.493811
102. Belagur VK, Chitimini VR (2010) Effect of injector opening pressures on the performance, emission and combustion characteristics of di diesel engine running on

honne oil and diesel fuel blend. Therm Sci 14:1051–1061. doi: 10.2298/TSCI1004051B

103. Sayin C, Gumus M, Canakci M (2012) Effect of fuel injection pressure on the injection, combustion and performance characteristics of a DI diesel engine fueled with canola oil methyl esters-diesel fuel blends. Biomass and Bioenergy 46:435–446. doi: 10.1016/j.biombioe.2012.07.016

104. Yang B, Wang L, Ning L, Zeng K (2016) Effects of pilot injection timing on the combustion noise and particle emissions of a diesel/natural gas dual-fuel engine at low load. Appl Therm Eng 102:822–828. doi: 10.1016/j.applthermaleng.2016.03.126

105. Mani M, Nagarajan G (2009) Influence of injection timing on performance, emission and combustion characteristics of a DI diesel engine running on waste plastic oil. Energy 34:1617–1623. doi: 10.1016/j.energy.2009.07.010

106. Kannan GR, Anand R (2012) Effect of injection pressure and injection timing on DI diesel engine fuelled with biodiesel from waste cooking oil. Biomass and Bioenergy 46:343–352. doi: 10.1016/j.biombioe.2012.08.006

107. Liu J, Yao A, Yao C (2014) Effects of injection timing on performance and emissions of a HD diesel engine with DMCC. Fuel 134:107–113. doi: 10.1016/j.fuel.2014.05.075

108. Suresh G, Kamath HC, Banapurmath NR (2014) Effects of injection timing, injector opening pressure and nozzle geometry on the performance of cottonseed oil methyl ester-fuelled diesel engine. Int. J. Sustain. Eng. 7:82–92. doi:10.1080/19397038.2013.811703

109. Saravanan S (2015) Effect of EGR at advanced injection timing on combustion characteristics of diesel engine. Alexandria Eng J 54:339–342. doi: 10.1016/j.aej.2015.05.001

110. Aljamali S, Abdullah S, Wan Mahmood WMF, Ali Y (2016) Effect of fuel injection timings on performance and emissions of stratified combustion CNGDI engine. Appl Therm Eng 109:619–629. doi: 10.1016/j.applthermaleng.2016.08.127

111. Ayetor GK, Sunnu AK, Gyamfi GB (2016) Idling effect of injection pressure and timing and their effects on performance and emissions of a compression ignition engine fuelled with biodiesel. Biofuels 7269:1–6. doi: 10.1080/17597269.2016.1231950

112. Bora BJ, Saha UK. On the attainment of optimum injection timing of pilot fuel in a dual fuel diesel engine run on biogas, Proceedings of the ASME 2014 12th Biennial Conference on Engineering Systems Design and Analysis, ESDA2014, June 25-27, 2014, Copenhagen, Denmark, ESDA2014-20162 2017:1–10
113. Sayin C, Canakci M. Effects of injection timing on the engine performance and exhaust emissions of a dual-fuel diesel engine. Energy Convers Manag 2009; 50:203–13. doi:10.1016/j.enconman.2008.06.007
114. Sayin C, Uslu K, Canakci M. Influence of injection timing on the exhaust emissions of a dual-fuel CI engine. Renew Energy 2008; 33:1314–23. doi:10.1016/j.renene.2007.07.007
115. Sayin C, Ilhan M, Canakci M, Gumus M. Effect of injection timing on the exhaust emissions of a diesel engine using diesel-methanol blends. Renew Energy 2009;34:1261–9. doi:10.1016/j.renene.2008.10.010
116. Datta A, Mandal BK. Effect of injection timing on the performance and emission characteristics of a CI engine using diesel and methyl soyate, Biofuels 2015, DOI: 10.1080/17597269.2015.1100039
117. Barik D, Murugan S, Sivaram NM , Baburaj E, Sundaram PS. Experimental investigation on the behavior of a direct injection diesel engine fueled with Karanja methyl ester-biogas dual fuel at different injection timings. Energy 2017, 118:127-138. doi:10.1016/j.energy.2016.12.025
118. Balusamy T, Marappan R (2010) Effect of Injection Time and Injection Pressure on CI Engine Fuelled with Methyl Ester of Thevetia Peruviana Seed Oil. Int J Green Energy 7:397–409. doi: 10.1080/15435075.2010.493811
119. Sakthivel G (2016) Prediction of CI engine performance, emission and combustion characteristics using fish oil as a biodiesel at different injection timing using fuzzy logic. Fuel 183:214–229. doi: 10.1016/j.fuel.2016.06.063
120. Ryu K (2013) Effects of pilot injection timing on the combustion and emissions characteristics in a diesel engine using biodiesel-CNG dual fuel. Appl Energy 111:721–730. doi: 10.1016/j.apenergy.2013.05.046
121. Yadav SPR, Saravanan CG, Kannan M (2015) Influence of injection timing on DI diesel engine characteristics fueled with waste transformer oil. Alexandria Eng J 54:881–888. doi: 10.1016/j.aej.2015.07.008

122. Ganapathy T, Gakkhar RP, Murugesan K (2011) Influence of injection timing on performance, combustion and emission characteristics of Jatropha biodiesel engine. Appl Energy 88:4376–4386. doi: 10.1016/j.apenergy.2011.05.016
123. Hwang J, Qi D, Jung Y, Bae C. Effect of injection parameters on the combustion and emission characteristics in a common-rail direct injection diesel engine fueled with waste cooking oil biodiesel. Renew Energy 2014;63:9–17. doi:10.1016/j.renene.2013.08.051
124. Park SH, Youn IM, Lee CS. Influence of ethanol blends on the combustion performance and exhaust emission characteristics of a four-cylinder diesel engine at various engine loads and injection timings. Fuel 2011;90:748–55. doi:10.1016/j.fuel.2010.08.029
125. Instruction Manual research engine test set up 1 cylinder, 4 stroke, multi-fuel, VCR with Open ECU (Computerized) Product code 240PE, Apex Innovations Pvt. Ltd, www.apexinnovations.co.in
126. Operating Manual of "B" type acetylene generator, IIGAS Ltd. Howrah (India), http://www.iigas.com
127. Operating manual of 'AVL DIGAS 444 Gas Analyser', AVL, Austria
128. Operating manual of 'AVL DI Smoke 480BT', AVL, Austria
129. Bedoya ID, Saxena S, Cadavid FJ, Dibble RW (2012) Exploring Strategies for Reducing High Intake Temperature Requirements and Allowing Optimal Operational Conditions in a Biogas Fueled HCCI Engine for Power Generation. J Eng Gas Turbines Power 134:72806. doi: 10.1115/1.4006075
130. Heywood JB, Internal Combustion Engines Fundamentals, Tata McGraw-Hill Education Private Limited, New Delhi, India, 2013, pp. 509–511.
131. Bora BJ, Saha UK (2016) Optimisation of injection timing and compression ratio of a raw biogas powered dual fuel diesel engine. Appl Therm Eng 92:111–121. doi: 10.1016/j.applthermaleng.2015.08.111
132. Srivastava AK, Soni SL, Sharma D, et al (2017) Effect of compression ratio on performance, emission and combustion characteristics of diesel–acetylene-fuelled single-cylinder stationary CI engine. Clean Technol Environ Policy. doi: 10.1007/s10098-017-1334-0
133. Mattarelli E, Rinaldini CA, Golovitchev VI (2014) CFD-3D analysis of a light duty Dual Fuel (Diesel/Natural Gas) combustion engine. Energy Procedia 45:929–937. doi: 10.1016/j.egypro.2014.01.098

134. Manimaran R, Raj RTK (2013) CFD analysis of combustion and pollutant formation phenomena in a direct injection diesel engine at different EGR conditions. In: Procedia Engineering. pp 497–506
135. Hiwase SD, Moorthy S, Prasad H, et al (2013) Multidimensional modeling of direct injection diesel engine with split multiple stage fuel injections. Procedia Eng 51:670–675. doi: 10.1016/j.proeng.2013.01.095
136. Huang M, Gowdagiri S, Cesari XM, Oehlschlaeger MA (2016) Diesel engine CFD simulations: Influence of fuel variability on ignition delay. Fuel 181:170–177. doi: 10.1016/j.fuel.2016.04.137
137. Chintala V, Subramanian KA (2016) CFD analysis on effect of localized in-cylinder temperature on nitric oxide (NO) emission in a compression ignition engine under hydrogen-diesel dual-fuel mode. Energy 116:470–488. doi: 10.1016/j.energy.2016.09.133
138. Soni DK, Gupta R (2016) Optimization of methanol powered diesel engine: A CFD approach. Appl Therm Eng 106:390–398. doi: 10.1016/j.applthermaleng.2016.06.026
139. Lee CH, Reitz RD (2013) CFD simulations of diesel spray tip penetration with multiple injections and with engine compression ratios up to 100:1. Fuel 111:289–297. doi: 10.1016/j.fuel.2013.04.058
140. Stylianidis N, Azimov U, Maheri A, et al (2017) Chemical kinetics and CFD analysis of supercharged micro-pilot ignited dual-fuel engine combustion of syngas. Fuel 203:591–606. doi: 10.1016/j.fuel.2017.04.125
141. Neshat E, Honnery D, Saray RK (2017) Multi-zone model for diesel engine simulation based on chemical kinetics mechanism. Appl Therm Eng 121:351–360. doi: 10.1016/j.applthermaleng.2017.04.090

PUBLICATIONS

Paper published in international journal

1. Anmesh Kumar Srivastava, Shyam Lal Soni, Dilip Sharma, Deepesh Sonar, Narayan Lal Jain, "Effect of compression ratio on performance, emission and combustion characteristics of diesel–acetylene-fuelled single-cylinder stationary CI engine", Clean Technologies and Environmental Policy, Springer Berlin Heidelberg, pp-1361- 1372, Vol. 19, July 2017, doi: 10.1007/s10098-017-1334-0.[**SCI, Impact Factor: 3.331**]
2. Anmesh Kumar Srivastava, Shyam Lal Soni, Dilip Sharma, Narayan Lal Jain, "Experimental investigation on the effect of injection pressure on performance, emission and combustion characteristics of diesel-acetylene fuelled single cylinder stationary CI engine", Environmental Science and Pollution Research, Springer Berlin Heidelberg, pp 7767–7775, Vol. 25, March 2018, doi: 10.1007/s11356-017-1070-3.[**SCI, Impact Factor: 2.741**]

Papers communicated in international journals

1. Anmesh Kumar Srivastava, S.L.Soni, Dilip Sharma, "Effect of injection timing on performance, emission and combustion characteristics of diesel-acetylene fuelled single cylinder stationary CI engine"

Papers presented/published in international conferences:

1. Anmesh Kumar Srivastava, S.L.Soni, Dilip Sharma, 'Viability of Acetylene as an Alternative Fuel for I.C.Engines', International Conference on Environment and Energy, Jawaharlal Nehru Technological University Hyderabad (JNTUH), December 15-17, 2014, ISBN: 978-93- 81212-96- 7.
2. Anmesh Kumar Srivastava, S.L. Soni, Dilip Sharma, "Performance and emission analysis of diesel-acetylene fuelled single cylinder, CI engine", First International Conference on Recent Innovation in Engineering and Technology (ICRIEAT-2016), Aurora's Scientific, Technological and Research Academy, Chandrayangutta, Hyderabad-500005, 22-23, December 2016. ISBN: 978-1- 5396-2645- 9.

OTHER PUBLICATIONS DURING RESEARCH PERIOD

Publication as corresponding author

Papers presented/published in international conferences:

1. Anmesh Kumar Srivastava, S.L.Soni, Dilip Sharma, 'Alternative Fuels for I.C.Engines : A Review', International Conference on Futuristic Trends in Mechanical and Industrial Engineering, January 18-19,2013, JECRC UDML College of Engineering, Kukas, Jaipur. Page- 239-247, ISBN: 978-81-926383-0-0.
2. Anmesh Kumar Srivastava, S.L.Soni, Dilip Sharma, 'Experimental Investigation of Acetylene as an Alternative Fuel for I.C. Engine', International Conference on Alternative Fuels for I.C. Engines, Department of Mechanical Engineering, Malaviya National Institute of Technology Jaipur, February 6-8, 2013, Page 351-357, ISBN: 978-81-924029-8-7.
3. Anmesh Kumar Srivastava, S.L.Soni, Dilip Sharma, Deepesh Sonar, 'Biogas Generation from Waste Water Treatment', International Conference on Water Desalination, Treatment and Management & Indian Desalination Association Annual Congress-2013 (InDACON 2013), February 21-22,2013 at Ramada Hotel, Govind Marg, Rajapark, Jaipur-302004.
4. Anmesh Kumar Srivastava, S.L. Soni, Dilip Sharma, 'Emerging New Alternate Fuels for I.C. Engines: A Review', 1st ISEES International Conference on Sustainable Energy and Environment Challenges (SEEC-2017), at Centre of Innovative and Applied Bioprocessing, Mohali, India, 26-28, February, 2017.

Publications as co-author

Papers published / accepted in international journals

1. Deepesh Sonar, S. L. Soni, Dilip Sharma, Anmesh Srivastava, Rahul Goyal, 'Performance and emission characteristics of a diesel engine with varying injection pressure and fuelled with raw mahua oil (preheated and blends) and mahua oil methyl ester', Clean Technologies and Environmental Policy, Springer Berlin Heidelberg, ISSN1618-9558(Online). Vol. 17, Issue 6, pp 1499–1511. August 2015 **[SCI, Impact Factor: 3.331]** doi: 10.1007/s10098-014-0874-9.

2. Narender Kumar, Shyam Lal Soni, Dilip Sharma, Anmesh Kumar Srivastava, 'Performance evaluation and emission analysis of variable compression ratio direct injection diesel engine', International Journal of Science and Technology, Vol. 2, Issue 2, pp-32-47, ISSN 2454-5880, doi: http://dx.doi.org/10.20319/mijst.2016.22.3247.
3. Narayan Lal Jain, S.L. Soni, M.P. Poonia, Dilip Sharma, Anmesh K. Srivastava, Hardik Jain, 'Performance and emission characteristics of preheated and blended thumba vegetable oil in a compression ignition engine', Applied Thermal Engineering, Vol. 113 pp 970–979, February 2017, doi: https://doi.org/10.1016/j.applthermaleng.2016.10.186. **[SCI, Impact Factor: 3.356]**